PROCEEDINGS
OF THE
NATIONAL ACADEMY OF SCIENCES,
INDIA
1991

VOL. LXI SECTION–A PART II

Synthesis and structural investigation of some mixed-ligand cyanonitrosyl $\{CrNO\}^5$ complexes of chromium with some tertiary alkylanilines

(Key words : I.R./E.S.R./mixed ligand cyanonitrosyl complexes/chromium/tertiary alkylanilines/ molar conductance)

R. C. MAURYA, D.D. MISHRA, S. AWASTHI and I.B. KHAN

Department of P.G. Studies and Research in Chemistry, Rani Durgavati Vishwavidyalaya, Jabalpur -482 001, India.

Received December 12, 1989; Accepted May 19, 1990.

Abstract

Six Novel mixed-ligand cyanonitrosyl complexes of chromium (I) of composition, $[Cr(NO)(CN)_2(L)_2(H_2O)]$ (where L = N, N-dimethylaniline, N, N-diethylaniline, N-ethyl-N-methylaniline, N,N-dimethyl-p-toluidine, N,N-dimethyl-m-toluidine or N,N-dimethyl-m-anisidine) have been prepared by the interaction of potassium pentacyanonitrosylchromate (I) monohydrate, $K_3[Cr(NO)(CN)_5].H_2O$ with the said tertiary amines. The complexes, which have been characterized by elemental analyses, magnetic measurements, conductance studies, electron spin resonance and infrared spectral studies, contain chromium (I) in a low-spin $\{CrNO\}^5$ electron configuration.

Introduction

A literature survey[1-14] of neutral mixed-ligand nitrosyl complexes of monovalent chromium reveals few reports on such complexes. Although in recent years there has been a great interst in preparation and characterization of neutral mixed-ligand cyanonitrosyl complexes of chromium(I), there is no report on cyanonitrosyl complexes of monovalent chromium with tertiary alkylanilines. It was, therefore, thought worth-while to synthesize and characterize some neutral mixed-ligand cyanonitrosyl complexes of chromium involving $\{CrNO\}^5$ electron configuration with tertiary alkylanilines like N, N-dimethylaniline, N, N-diethylaniline, N-ethyl-N-methylaniline, N,N-dimethyl-p-toluidine, N,N-dimethyl-m-toluidine and N,N-dimethyl-m-anisidine.

Materials and Methods

N,N-dimethylaniline (Thomas Baker & Company, London), N, N-diethylaniline (The British Drug House Ltd., Poole, England), and N-ethyl-N-methylaniline, N,N-dimethyl-p-toluidine and N,N-dimethyl-m-toluidine (Aldrich Chemical Company, Inc., Wisconsion, U.S.A.) and N,N-dimethyl-m-anisidine (Tokyo Chemical Company Ltd., Japan) were used as supplied.

Preparation of the parent compound : The parent compound, potassium pentacyanonitrosyl-chromate(I) monohydrare, $K_3[Cr(NO)(CN)_5].H_2O$ was prepared by following the procedure of Grifith and Wilkinson[9].

Analysis of the constituent elements : Carbon, hydrogen and nitrogen present in the investigated complexes were estimated microanalytically. Chromium was estimated by the method reported[10] elsewhere.

Physical methods : The magnetic susceptibility measurements were made at room temperature by the Gouy method. The apparatus was calibrated using cobalt mercury thiocyanate, $Hg[Co(NCS)]_4$. The diamagnetic corrections were computed using Pascal's constant[15,16]. I.R. spectra (4000-600 cm^{-1}) of the complexes were recorded in Nujol mulls supported between NaCl plates on a Beckman IR-20 spectrophotometer. Conductances were measured in analytical grade ethanol (EtOH) and dimethylformamide (DMF) using dip type cell on Toshniwal conductivity bridge, Japan. E.S.R. spectra of the complexes were recorded at room temperature on a Varian E-3 spectrometer using powdered sample at the microwave frequency of 9.53 GHz.

General method of preparation of the complexes : To a filtered aqueous solution of the parent compound, potassium pentacyanonitrosylchromate (I) monohydrate (0.01 M, 50 ml), an aqueous acetic acid solution 10 ml (1:1) of the corresponding tertiary amine (0.02 M) was added with shaking and a coloured solid was precipitated on warming for 15-20 min. over a hot plate at 80°C. The resulting mixture was freed from the liberated HCN by passing a current of CO_2 through the mixture for a few hours. The precipitate was suction filtered and washed several times with dilute acetic acid solution and finally with H_2O and dried *in vacuo* over anhydrous $CaCl_2$ at room temperature to a constant weight. The analytical data are given in Table 1.

Results and Discussion

All the complexes were air stable coloured solids. They were soluble in DMF, DMSO, ethanol, and insoluble in nitrobenzene. The complexes were thermally stable and did not melt or decompose up to 280C. They decomposed in dilute acids and alkalis only on heating. All the compounds after decomposition in KOH followed by acidifying with acetic acid gave a pink colour with few drops of Griess Reagent[15]. This reaction indicates the presence of NO group in the complexes. The probable reaction scheme for the Griess reaction is given in scheme 1.

The mixed-ligand cyanonitrosyl complexes (see Table 1 for ligand names) were synthesized according to the following equation :

$$K_3[Cr(NO)(CN)_5].H_2O + 2L \xrightarrow[H_2O]{CH_3COOH} [Cr(NO)(CN)_2(L)_2(H_2O)] + 3CH_3COOK + 3HCN(g) + H_2O$$

(where L = NNdman, NNdean, NeNman, NNdmpt, NNdmmt, NNdmma).

The partial replacement of the cyano groups in the hexa-coordinated complex, $K_3[Cr(NO)(CN)_5].H_2O$ by two molecules of ligand arises from the *trans* effect of the NO group. The work of Burgess *et al.*[17] on the stepwise aquation of the pentacyanonitrosylchromate (I) anion, $[Cr(NO)(CN)_5]^{3-}$ to attain $[Cr(NO)(CN)_2(H_2O)_3]$, favours the reaction scheme.

$$[Cr(NO)(CN)_2(L)_2(H_2O)] \xrightarrow[\text{Decomposition}]{KOH, H_2O} NO_2^- + \text{Chromium oxide}$$

$$NO_2^- + H^+ \longrightarrow HNO_2$$

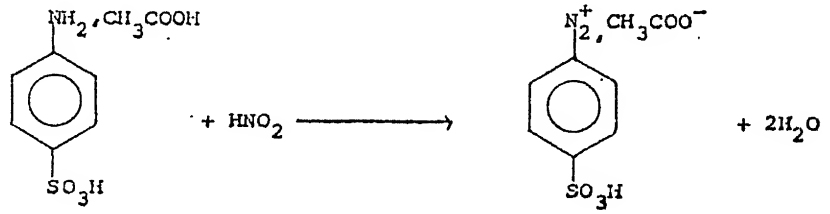

Sulphanilic acid
(A component of Griess Reagent)

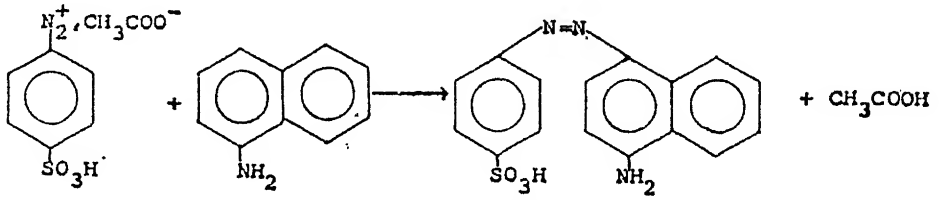

α-Naphthylamine
(Another component of Griess reagent)

Pink coloured dye

Scheme 1- Probable reaction scheme for the Griess reaction.

Table 1 - % yield, analytical, magnetic and E.S.R. data of complexes.

Compound	% Yield	% Cr Found (Calc.)	% C Found (Calc.)	% H Found (Calc.)	% N Found (Calc.)	μ_{eff}	'g'	Decomposition Temp. (°C)
$[Cr(NO)(CN)_2(NNdman)_2(H_2O)]$	50	12.95 (13.20)	54.20 (54.80)	5.90 (6.09)	17.20 (17.76)	1.71	1.981	>300
$[Cr(NO)(CN)_2(NNdean)_2(H_2O)]$	51	11.45 (11.57)	58.35 (58.65)	7.10 (7.40)	15.32 (15.55)	1.70	1.980	>300
$[Cr(NO)(CN)_2(NeNman)_2(H_2O)]$	50	12.00 (12.34)	56.20 (56.86)	6.38 (6.63)	16.00 (16.58)	1.72	1.983	>300
$[Cr(NO)(CN)_2(NNdmpt)_2(H_2O)]$	49	11.90 (12.34)	56.45 (56.86)	6.09 (6.63)	16.32 (16.58)	1.74	1.982	>300
$[Cr(NO)(CN)_2(NNdmmt)_2(H_2O)]$	49	12.10 (12.34)	55.98 (56.86)	5.97 (6.63)	15.89 (16.58)	1.70	1.985	>300
$[Cr(NO)(CN)_2(NNdmma)_2(H_2O)]$	50	11.00 (11.47)	52.10 (52.85)	5.99 (6.17)	14.90 (15.40)	1.72	1.982	>300

NNdan = N,N–dimethylaniline; NNdean = N,N-diethylaniline; NeNman = N-ethyl-N-methylaniline; NNdmpt = N,N-dimethyl-p-toluidine; NNdmmt = N,N-dimethyl-m-toluidine; NNmma = N,N-dimethyl-m-anisidine.

Table 2 - Important I.R. spectral bands (cm^{-1}) and their assignments.

Compound	υ(NO)	υ(C≡N)	υ(C–N)	υ(OH)
$[Cr(NO)(CN)_2(NNdman)_2(H_2O)]$	1710 (VS)	2160 (S)	1380 (S)	3580 (br) 3380 (br)
$[Cr(NO)(CN)_2(NNdean)_2(H_2O)]$	1705 (VS)	2160 (S)	1385 (S)	3580 (br) 3400 (br)
$[Cr(NO)(CN)_2(NeN\text{-}man)_2(H_2O)]$	1710 (VS)	2155 (S)	1380 (S)	3575 (br) 3400 (br)
$[Cr(NO)(CN)_2(NNdmpt)_2(H_2O)]$	1705 (VS)	2150 (S)	1385 (S)	3580 (br) 3380 (br)
$[Cr(NO)(CN)_2(NNdmmt)_2(H_2O)]$	1705 (VS)	2160 (S)	1380 (S)	3570 (br) 3380 (br)
$[Cr(NO)(CN)_2(NNdmma)_2(H_2O)]$	1705 (VS)	2160 (S)	1375 (S)	3580 (br) 3400 (br)

Compounds were characterized on the basis of the following results :

Magnetic and E.S.R. studies : The magnetic and E.S.R. data of the complexes are reported in Table 1. The magnetic moments, 1.70 to 1.74 B.M., at room temperature and g values, 1.980-1.985 of powdered compounds, which are comparable to the literature[16,18] values, are consistent with a low-spin $\{CrNO\}^5$ electron configuration of chromium (I).

I.R. spectra : The important I.R. spectral bands for the synthesized complexes are reported in Table 2. The appearance of a very strong band at 1705 to 1710 cm^{-1} and a strong band at 2150-2160 cm^{-1} are assigned to $\upsilon(NO)^+$ and $\upsilon(C\equiv N)$, respectively, in agreement with the result reported[5] elsewhere. The broad bands in the 3570-3580 cm^{-1} and 3380-3400 cm^{-1} regions are due to $\upsilon(OH)$ of coordinated water[19] in all the complexes. The absorption bands in 1590-1600 cm^{-1} and 830-850 cm^{-1} regions are assigned to the coordinated water molecule. A comparison of the I.R. spectral bands of the free tertiary anilines and their complexes show that the $\upsilon(C-N)$ observed at 1350, 1360, 1355, 1355, 1350, 1345 cm^{-1} in free NNdman, Nndean, NeNman, NNdmpt, NNdmmt and NNdmma, respectively, is shifted to 1380, 1385, 1380, 1385, 1380, 1375 cm^{-1} in their respective complexes. This indicates the bonding of the tertiary nitrogen[20] to chromium.

Conductance measurements : The molar conductances in the range 6.8 to 10.0 ohm^{-1}-cm^2 $mole^{-1}$ in ethanol and 10.4 to 11.5 ohm^{-1} cm^2 $mole^{-1}$ in DMF are in agreement with the non-electrolytic nature of these complexes[10].

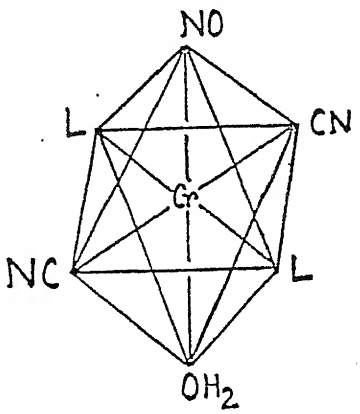

Fig. 1 · Proposed octahedral structure of $[Cr(NO)(CN)_2(L)_2(H_2O)]$ where L = NNdman, NNdean, NeNman, NNdmpt, NNdmmt or NNdmma.

The analytical data and physico-chemical studies presented above suggest that the complexes may be formulated as $[Cr(NO)(CN)_2(L)_2(H_2O)]$. Since these complexes show one CN stretching band and one NO stretching band, it is reasonable to propose an octahedral structure with CN *trans* to CN, L *trans* to L, and NO *trans* to water molecule (Fig. 1).

References

1. Lukerhart, C.M. & Troup, J.N. (1977) *Inorg. Chim. Acta* **22** : 81.
2. Sarkar, S., Maurya, R.C. & Chaurasia, S.C. (1976) *Indian J. Chem.* **14A** : 285.

3. Maurya, R.C. & Shukla, R.K. (1982) *J. Indian Chem. Soc.* **59** : 340.
4. Maurya, R.C. (1983) *Indian J. Chem.* **22A** : 529.
5. Maurya, R.C., Shukla, R.K., Maurya, M.R. & Anandam, N. (1985) *J. Indian Chem. Soc.* **62** : 63.
6. Maurya, R.C., Shukla, R., Shukla, R.K., Anandam, N., Maurya, M.R. & Malik, W.U. (1986) *Proc. INSA, Physical Science* **52A** : 1428.
7. Maurya, R.C., Shukla, R., Anandam, N., Srivastava, S.K. & Malik, W.U., *Transition Met. Chem.* (In press).
8. Maurya, R.C., Shukla, R., Gupta, D.C., Shukla, R.K., Anandam, N. & Malik, Wahid U. (1986) *Synth. React. Inorg. Met. -Org. Chem.* **16** : 1243.
9. Griffith, W.P. & Wilkinson, G. (1959) *J. Chem. Soc.* 872.
10. Maurya, R.C., Shukla, R., Shukla, R.K., Anandam, N., Gupta, D.C. & Maurya, M.R. (1986) *Synth. React. Inorg. Met-Org. Chem.* **16** : 1059.
11. Maurya, R.C., Shukla, R., Shukla, R.K. & Anandam, N. (1986) *Proceedings* XXIV–ICCC, A-6, 402, Athens, Greece.
12. Maurya, R.C. & Mishra, D.D. (1988) *Synth. React. Inorg. Met.–Org. Chem.* **18** : 133.
13. Maurya, R.C. & Mishra, D.D. (1987) *Transition Met. Chem.* **12** : 551.
14. Maurya, R.C. & Mishra, D.D. *Synth. React. Inorg. Met.-Org. Chem.* (In press).
15. Griess, P. (1979) *Chem. Ber.* **12** : 427.
16. Manoharan, P.T. & Gray, H.B.(1966) *Inorg. Chem.* **5** : 823.
17. Burgess, J., Goodman, B.A. & Raynor, J.B. (1968) *J. Chem. Soc.* (A) 501.
18. Meriwether, L.S., Robinson, S.D. & Wilkinson, G. (1966) *J. Chem. Soc.* 1488.
19. Nakanoto, K. (1978) *"Infrared and Raman spectra of Inorganic and coordination compounds,"* 3rd. Ed., John Wiley and Sons, New Delhi.
20. Cross, A.D. (1960) *An Introduction to Practical Infrared Spectroscopy*, Butterworth Scientific Publications, London, P-65.

PROC. NAT. ACAD. SCI. INDIA, 61 (A), II, 1991

Polarographic study of the complexes of Ni(II) with some plant auxins

(Key words : polarography/Ni(II)/3-indoleacetate/3-indolebutyrate/1-naphthaleneacetate)

RAM PARKASH, ANJU D. MASSEY and S. K. REHANI

Department of Chemistry, Panjab University, Chandigarh-160 014, India.

Received October 28, 1989; Revised May 12, 1990; Accepted June 16, 1990.

Abstract

Interaction of Ni(II) with 3-indoleacetate, 3-indolebutyrate and 1-naphthaleneacetate ions was studied at DME in aqueous and 50% methanol media at μ = 1.0M(KCl) at 25±0.1°C. The metal undergoes reversible diffusion-controlled two electron reduction. The overall stability constants of 1:1 and 1:2 complexes were determined using DeFord and Hume method. Percentage distribution of metal ion in various forms in equilibrium as a function of ligand concentration was calculated.

Introduction

In continuation of the polarographic determination of the stability constants of the complexes of certain plant auxins and fungicides with trace elements[1-4] we report herein the quantitative evaluation of the binding affinity of 3-indoleacetate, 3-indolebutyrate and 1-naphthaleneacetate ions with Ni(II) in aqueous and 50% methanol media at DME. Percentage distribution of the metal in various forms in equilibrium as a function of ligand concentration has also been calculated.

Materials and Methods

All the chemicals used were of AR grade. Triple-distilled mercury and double distilled water were used. Methanol was purified and distilled before use by the literature method[5].

Stock solution (10^{-2}M) of Ni(II) was prepared in water and standardized[6]. Sodium salts of 3-indoleacetic, 3-indolebutyric and 1-naphthaleneacetic acids were prepared in aqueous and/or 50% methanol media and pH of these solutions was maintained with sodium hydroxide. Solutions containing metal ions (4×10^{-4}M) and varying concentrations of the ligand (0.00-0.25M) were prepared in water and 50% methanol media at ionic strength 1.0M maintained with potassium chloride.

The capillary characteristics measured in 0.1M potassium chloride (open circuit) and at a mercury height of 25.5 cm were m=1.07 mg s^{-1} and t = 2.06 s. Purified N_2 gas, presaturated with the background solution to be polarographed, was used for deaeration and an inert atmosphere was maintained over the solution during electrolysis. Electrolysis was carried out using a thermostated H-cell in conjunction with saturated calomel electrode. Polarograms of 4×10^{-4}M of Ni(II) were obtained in the presence of different concentrations of the ligand at pH 10.2 ± 0.1 in aqueous medium and pH 7 ± 0.1 in 50% methanol at 25 ± 0.1°C using EG & G Princeton Applied Research Model 174A Polarographic Analyser and Model RE 0089 *X-Y* recorder. While working in aqueous-methanol mixture medium, I.R. compensation was used. Gelatin was used as the maxima suppressor. Necessary corrections were made in processing the diffusion current data. The resulting polarographic data as a function of ligand concentration (C_x) which was calculated from the pK value of the auxin are given in Tables (1-3).

Table 1- $E_{1/2}$ and $F_j([X])$ function for Ni (II)-1-naphthaleneacetate system in 50% methanol at 25±0.1°C.

C_x (M)	$E_{1/2}$ $-V$(*vs.* S C E)	I_d (μA)	$F_0([X])$	$F_1([X])$	$F_2([X])$
0.00	1.097	2.850	–	–	–
0.02	1.098	2.934	1.11	5.65	32.50
0.04	1.099	2.844	1.24	6.01	25.25
0.05	1.100	2.839	1.32	6.50	30.00
0.09	1.103	2.835	1.64	7.20	28.00
0.10	1.103	2.800	1.75	7.50	25.00
0.12	1.105	2.785	1.96	8.00	25.00
0.15	1.107	2.750	2.35	9.00	26.06
0.16	1.107	2.700	2.46	9.15	25.93
0.18	1.108	2.645	2.71	9.50	25.00
0.20	1.109	2.600	3.00	10.00	25.06
0.25	1.112	2.550	3.81	11.25	25.00
				β_1= 5.00;	β_2 = 25.00

Ni^{2+} = 5x10^{-4}M; μ = 0.01M (KCl); pH = 7 ± 0.1

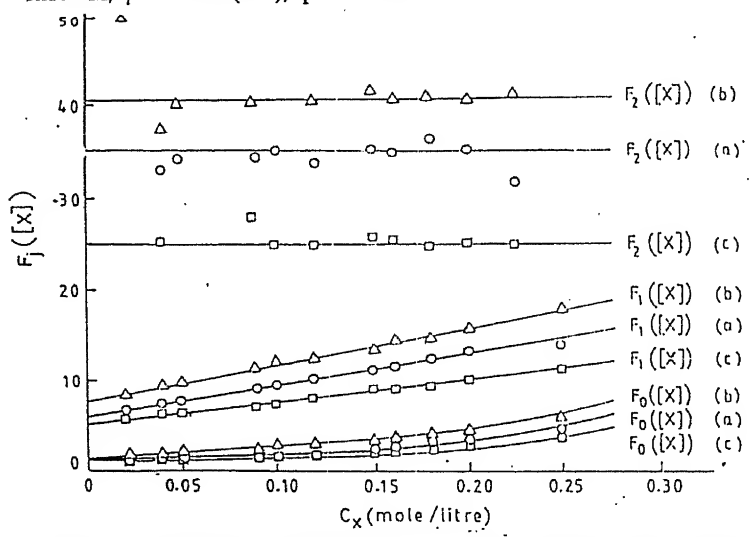

Fig. 1- Plot of C_x and $F_j([X])$ functions for (a) nickel (II) - 3-indolebutyrate system (-o-o-), (b) nickel (II)-3-indole acetate system (-Δ-Δ-), and (c) nickel (II)-1-naphthalene acetate system (-□-□-) in 50% methanol medium.

Results and Discussion

The polarographic reduction of Ni(II) gives a single well defined reversible wave. Current

Table 2 - $E_{1/2}$ and F_j ([X]) function for Ni(II)-3-indolebutyrate system in aqueous and 50% methanol media at 25 ± 0.1°C.

C_x (M)	$E_{1/2}$ $-V$(*vs.* S C E)		i_d (μA)		F_0([X])		F_1([X])		F_2([X])	
	Aqueous	50% Methanol	Aqueous	50% Methanol	Aqueous	50% Methanol	Aqueous	50% Methanol	Aqueous	50% Methanol
0.00	1.095	1.097	2.950	2.850	–	–	–	–	–	–
0.02	1.098	1.096	2.854	2.760	1.15	1.14	7.75	6.85	37.50	45.00
0.04	1.100	1.097	2.810	2.730	1.34	1.29	8.45	7.25	36.20	32.50
0.05	1.101	1.098	2.794	2.707	1.43	1.38	8.65	7.65	33.00	34.00
0.09	1.104	1.102	2.702	1.682	1.91	1.81	10.15	9.01	35.00	34.05
0.10	1.105	1.103	2.675	2.635	2.05	1.94	10.50	9.45	35.00	35.00
0.12	1.106	1.104	2.582	2.577	2.35	2.20	11.25	10.00	35.40	33.95
0.15	1.108	1.106	2.405	2.498	2.87	2.69	12.50	11.25	36.60	35.33
0.16	1.109	1.107	2.391	2.478	3.07	2.85	12.95	11.55	37.10	35.00
0.18	1.110	1.108	2.345	2.401	3.46	3.26	13.65	12.55	36.90	36.66
0.20	1.112	1.109	2.300	2.359	3.90	3.60	14.50	13.01	37.50	35.32
0.25	1.114	1.111	2.217	2.289	5.04	4.05	16.15	13.80	36.60	31.40
							Aqueous medium		$\beta_1 = 7.0$; $\beta_2 = 36.25$	
							50% Methanol medium		$\beta_1 = 5.95$; $\beta_2 = 34.96$	

$Ni^{2+} = 5x10^{-4}M$; μ = 0.01M (KCl); pH = 10.2 ± 0.1 (aqueous medium) and 7± 0.1 (50% methanol)

$E_{1/2}$ and F_j ([X]) function for Ni(II)-3-idoleacetate system in aqueous and 50% methanol media at 25±0.1°C.

$E_{1/2}$ –V(*vs.* S C E)		i_d (μA)		F_0([X])		F_1([X])		F_2([X])	
Aqueous	50% Methanol	Aqueous	50% Methanol	Aqueous	50% Methanol	Aqueous	50% Methanol	Aqueous	50% Methanol
1.095	1.097	2.925	2.850	–	–	–	–	–	–
1.097	1.091	2.825	2.705	1.19	1.17	9.75	8.50	42.50	50.00
1.099	1.092	2.820	2.693	1.42	1.36	10.50	9.00	40.00	37.50
1.100	1.093	2.816	2.689	1.56	1.48	11.15	9.51	45.00	40.30
1.104	1.097	2.812	2.677	2.14	2.00	12.65	11.15	41.60	40.50
1.105	1.098	2.809	2.671	2.34	2.20	13.45	12.02	45.50	45.20
1.107	1.099	2.805	2.664	2.68	2.48	14.02	12.35	42.60	40.40
1.111	1.101	2.798	2.656	3.29	3.06	15.25	13.76	42.30	41.60
1.111	1.102	2.793	2.648	3.56	3.24	16.00	14.01	44.30	40.70
1.112	1.103	2.739	2.646	3.97	3.67	16.55	14.85	42.50	40.80
1.113	1.104	2.705	2.638	4.50	4.12	17.50	15.62	43.00	41.00
1.116	1.106	2.637	2.630	5.96	5.54	19.50	17.75	42.40	41.00

Aqueous medium $\beta_1 = 8.90$; $\beta_2 = 42.48$
50% Methanol medium $\beta_1 = 7.50$; $\beta_2 = 40.46$

$i^{2+} = 5x10^{-4}$M; μ = 0.01M (KCl); pH = 10.2 ± 0.1 (aqueous medium) and 7± 0.1 (50% methanol)

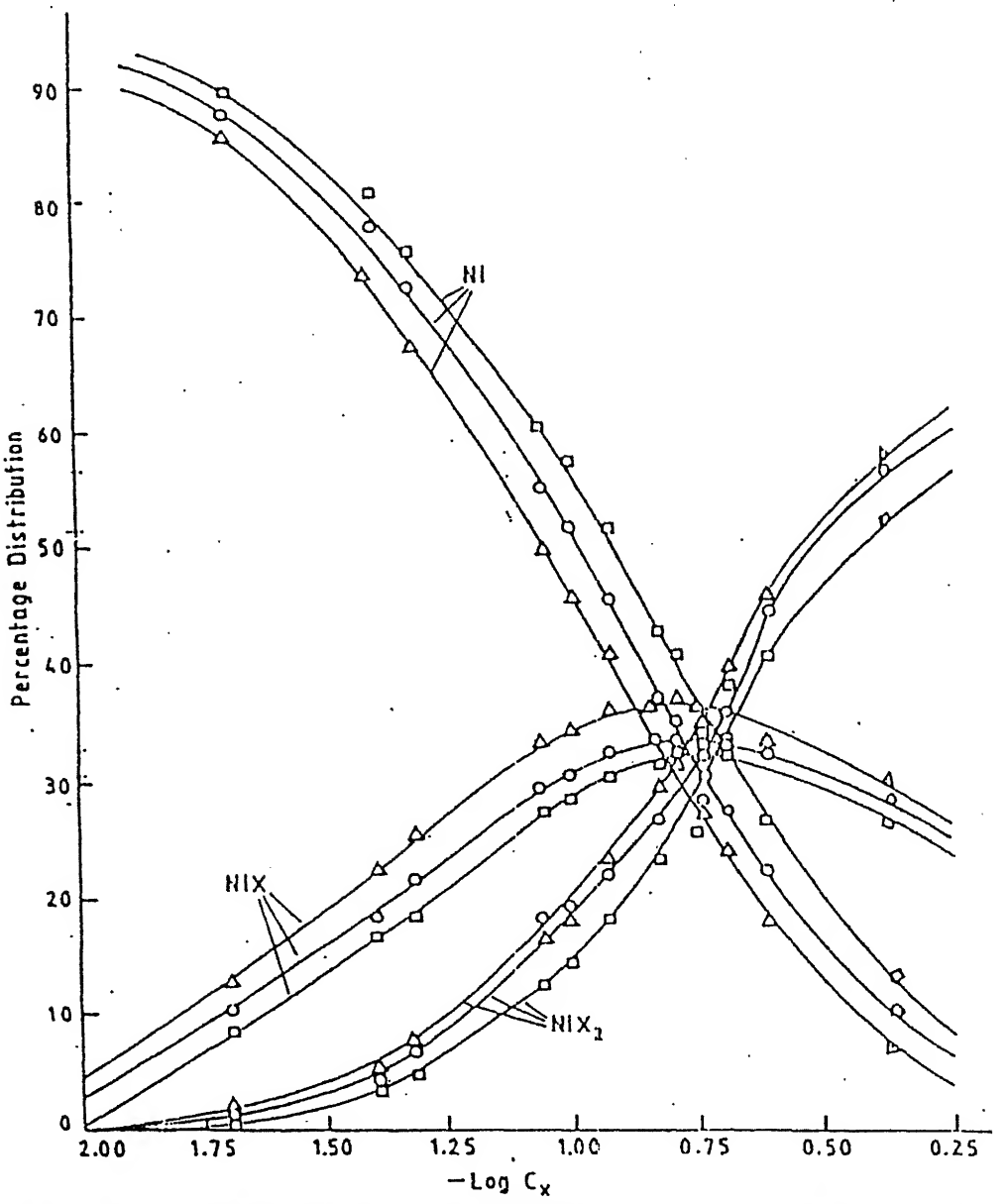

Fig. 2 - Plot of percentage distribution of nickel (II) in various forms *vs.* $-\log C_x$ at 25 ± 0.1°C in 50% methanol. Symbols are the same as in Fig. 1.

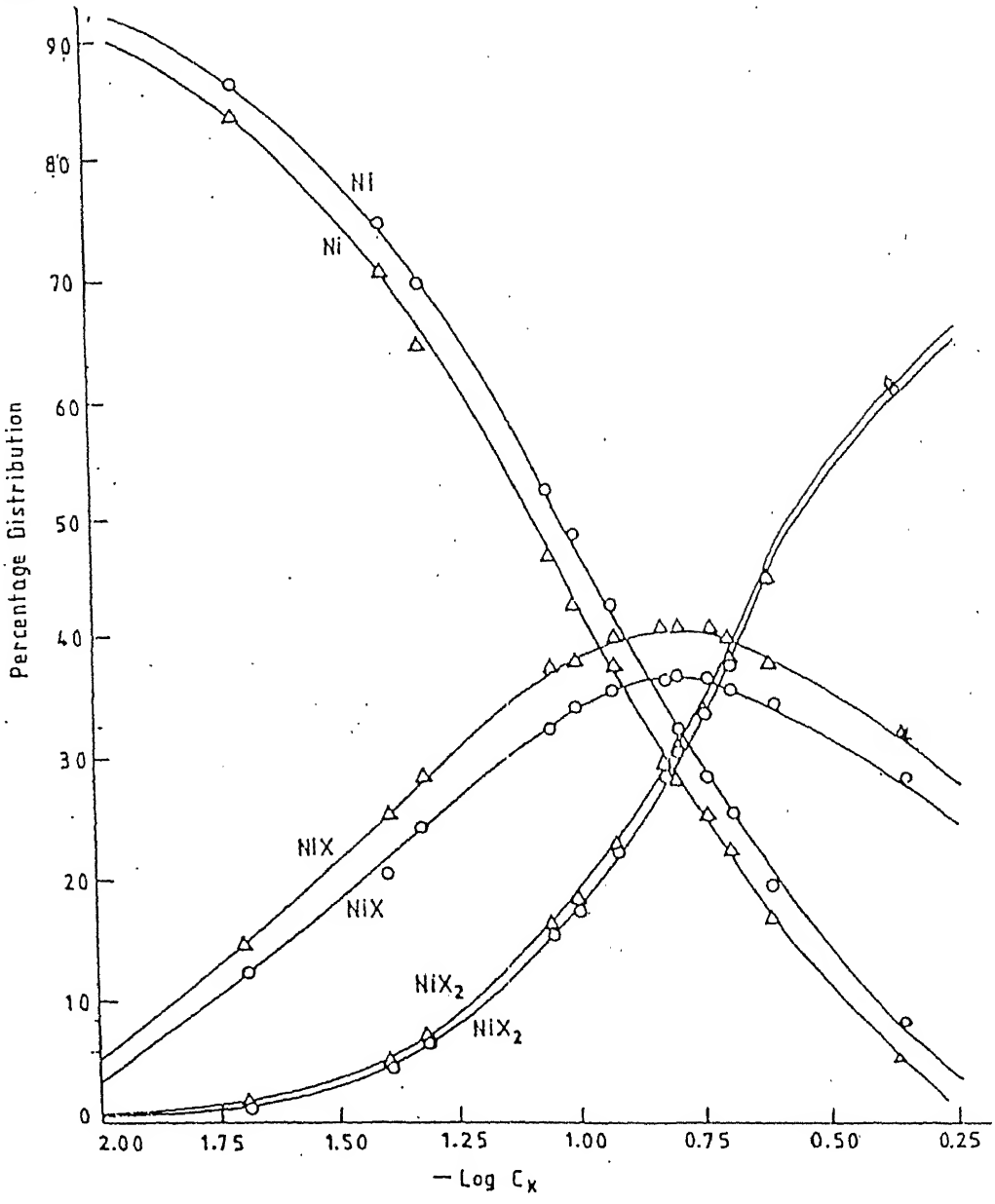

Fig. 3 - Plot of percentage distribution of nickel (II) in various forms *vs.* $-\log C_x$ at 25 ± 0.1°C in aqueous medium. Symbols are the same as in Fig. 1.

is directly proportional to $(h_{eff})^{1/2}$ indicating that the reduction is diffusion-controlled. The study reveals that the cathodic reduction of Ni(II) in 3-indoleacetate, 3-indolebutyrate and 1-naphthaleneacetate involves two electron transfer. Decrease in diffusion current of the metal ion and shift in its half-wave potential to more negative values as a function of ligand concentration suggests complex formation.

$F_j([X])$ functions were calculated at different ligand concentrations[7] and then solved for the stability constants by a graphical procedure. Plot of $F_0([X])$, $F_1([X])$ and $F_2([X])$ against C_x is a smooth curve, a straight line whose slope gives the value of β_1 and a line parallel to the abcissa respectively confirming the formation of 1:1 and 1:2 complexes in all the cases, depicted for nickel(II)-3-indolebutyrate system in 50% methanol medium as an example, in Fig. 1.

The stability constants of 1:1 and 1:2 complexes of Ni(II) with 3-indoleacetate, 3-indolebutyrate and 1-naphthaleneacetate in aqueousmethanol medium at pH 7 ± 0.1 are $\beta_1 = 7.50$, $\beta_2 = 40.46$; $\beta_1 = 5.95$, $\beta_2 = 34.96$ and $\beta_1 = 5.00$, $\beta_2 = 25.00$ respectively. Thus the complexes of 3-indoleacetate are stronger than the corresponding complexes of 3-indolebutyrate which in turn are stronger than the 1-naphthaleneacetate complexes. The low values of stability constant of 3-indolebutyrate complexes may be due to the presence of more methylene groups in the chain having carboxylic group. The basicity of the ligand and the steric effect influence the stability of the complex. It is noted that the complexes in water are stronger than those in methanolic medium. (The values for 3-indoleacetate and 3-indolebutyrate complexes in aqueous medium at pH 10.2 ± 0.1 are $\beta_1 = 8.90$, $\beta_2 = 42.48$, and $\beta_1 = 7.00$ and $\beta_2 = 36.25$ respectively). The stability increases with the increase in pH of the medium.

Percentage distribution of the metal ion present in various forms in equilibrium as a function of the ligand concentration was also calculated and the results are presented in Fig. (2&3).

References

1. Parkash, R., Singh, B. & Bala, R. (1981) *Trans. Soc. Adv. Electrochem. Sci. Technol.* **16** : 141.
2. Parkash, R., Singh, B. & Bala, R. (1983) *J. Ind. Chem. Soc.* **60** : 92.
3. Parkash, R., Rehani, S.K. & Bala, R. (1984) *Proc. Indian Acad. Sci. (Chem. Sci.)* **93** : 69.
4. Prakash, R., Rehani, S.K. & Bala, R. (1984) *J. Ind. Chem. Soc.* **61** : 930.
5. Vogel, A.I. (1959) *A Text Book of Practical Organic Chemistry*, Longmans, London.
6. Vogel A.I. (1961) *A Text Book of Quantitative Inorganic Analysis*, Longmans, London, p. 435.
7. DeFord, D.D. & Hume, D.N. (1951) *J.Am. Chem. Soc.* **73** : 5321.

PROC. NAT. ACAD. SCI. INDIA, 61 (A), II, 1991

Thermal studies on Pr(III) and Dy(III) succinates

(Key words : thermal studies/IR/TG/DTA/kinetic parameters/Pr(III)succinate/Dy(III) succinate)

M. L. KAUL and R. M. SHARMA*

Department of Chemistry, University of Jammu, Jammu-180 001, India.
**Department of Chemistry, Government Degree Cllege, Kathua-184 001 (J&K), India.*

Received April 19, 1989; Revised July 16, 1990; Accepted August 11, 1990.

Abstract

The compounds, $Pr_2C_{12}H_{12}O_{12}.6H_2O$ and $Dy_2C_{12}H_{12}O_{12}.8H_2O$ have been prepared and characterised by elemental analysis and I.R. spectroscopy. TG and DTA studies show that these lose four and six water molecules respectively in the first step, yielding $M_2C_{12}H_{12}O_{12}.2H_2O$ (M = Pr or Dy) and form the anhydrous species, $M_2C_{12}H_{12}O_{12}$ in the second step. There is an indication of formation of $MO(CO_3)_{1/2}$ in the case of Pr compound. M_2O_3 appears as the final stable product in each case. Kinetic parameters like apparent order, energy and entropy of activation for the dehydration process have been arrived at by analysing the data using Piloyan-Novikova, Coats-Redfern and Horowitz-Metzger equations. α *vs.* T curves show that there is no indication of branching or surface nucleation preceding the dehydration process which in both the compounds proceeds with phase boundary mechanism.

Introduction

Tartarates and succinates of rare earths, including those of praseodymium and dysprosium, have assumed considerable importance in view of being good starting materials for oxide catalysts and also due to their use in several electronic devices. Besides being good materials for studying decomposition mechanisms their decomposition products, including intermediates, could be of interest in the search for materials of high electrical conductivity. Hence, in continuation to our work on rare earth tartarates[1-3], it was thought worthwhile to study the thermal decomposition of Pr(III) and Dy(III) succinates.

Materials and Methods

The compounds $Pr_2C_{12}H_{12}O_{12}.6H_2O$ and $Dy_2C_{12}H_{12}O_{12}.8H_2O$ were prepared by mixing aqueous solutions containing equimolar (0.01 mole) amounts of respective rare earth metal chloride (Indian rare earths, 99.9% pure) and succinic acid (LOBA, 99% pure) containing some pyridine (Ranbaxy, A.R. 99.5% pure) at room temperature. Presence of pyridine seems to control the pH of the solution to the required extent (~4-5). The fine crystals of the compounds so obtained were separated by filtration, washed with distilled water and air dried without pressing. The percentage of the metal was estimated gravimetrically by precipitation as $M(OH)_3$ and weighing as M_2O_3 (M = Pr or Dy). The percentage of carbon and hydrogen was found by micro-analytical method.

IR-435 spectrophotometer Shimadzu, (Japan) was used for I.R. spectral studies, using KBr pellets in the range 4000-400 cm^{-1}.

Derivatographic studies of both the compounds were carried out on Paulik-Paulik-Erdey MOM derivatograph (Hungary, Budapest) using α–alumina as the reference material up to a temperature of 1173K. The thermal runs were recorded at constant heating rate of 10° min^{-1} in

static air atmosphere using 200 mg sensitivity. As a further check, TG and DTA curves were also recorded on Stanton Redcroft 780- series instrument (England) for one of the compounds, Pr(III), using alumina as inert material at 5MW sensitivity and 10° min^{-1} heating rate. The results from both the instruments were found wholly compatible.

Reflectance spectra of $Pr_2C_{12}H_{12}O_{12}.6H_2O$ was recorded on Beckmann-DK-2A reflectance spectrophotometer (MgO as reference material, speed = 36 nm/min; scale = 10 nm/cm and sensitivity = 50).

ECIL-TDC-316 computer (India) was used to evaluate the various kinetic parameters *viz.* energy of activation, pre-exponential factor, entropy of activation, apparent order of the reaction and the mechanism involved in the dehydration process in conformation to integral and approximation methods using the Piloyan-Novikova[4], Coats-Redfern[5] and Horowitz-Metzger[6] equations (non-isothermal).

Results and Discussions

On elemental analysis (Table 1) the compounds were found to have the composition $Pr_2C_{12}H_{12}O_{12}.6H_2O$ and $Dy_2C_{12}H_{12}O_{12}.8H_2O$.

Table 1 - Values obtained by elemental analysis.

Sl. no.	Compound	Metal %		C %		H %	
		Found	Calc.	Found	Calc.	Found	Calc.
1.	$Pr_2C_{12}H_{12}O_{12}.6H_2O$	38.07	38.19	19.40	19.52	3.00	3.25
2.	$Dy_2C_{12}H_{12}O_{12}.8H_2O$	39.93	39.78	17.50	17.62	3.50	3.43

The I.R. spectra of the compounds show a strong and broad band at 3400 cm^{-1} due to OH stretching of water. The broadness of the band is expected due to the intra-molecular hydrogen bonding in the compounds. The strong band ~1575 cm^{-1} can be assigned to υ_{asym}(OCO) and the bands ~1425 and 1320 cm^{-1} to υ_{sym}(OCO) of the coordinated carboxylate groups[7].

Thermal decomposition : The thermal decomposition pattern of both the compounds is very similar (Fig. 1-3). The first step of decomposition involves partial dehydration leading to the formation of the same product *viz.* dihydrate in both cases. In the case of the Pr compound, the first decomposition step starts at 315K and continues up to 433K, the weight loss observed (Derivatograph 9.50%; Stanton 9.40%) corresponds to removal of four water molecules (calc. loss 9.70%). In the case of Dy compound this decomposition step starts at 310K and ends at 393K; during this step six molecules of water are removed (observed weight loss 13.30% calc. loss 13.20%). This step can be represented as

$$M_2(C_{12}H_{12}O_{12})_3x\ H_2O \rightarrow M_2(C_{12}H_{12}O_{12})_3 2H_2O + (x-2)H_2O$$

In the second step of decomposition both the compounds loose the remaining two H_2O molecules leading to the formation of the anhydrous salts. In the case of the Pr compound this decomposition step starts at 473K and continues up to 520K showing an observed weight loss of 15.0% (Derivatograph), 14.8% (Stanton) (calc. wt. loss 14.6%). In the case of the Dy

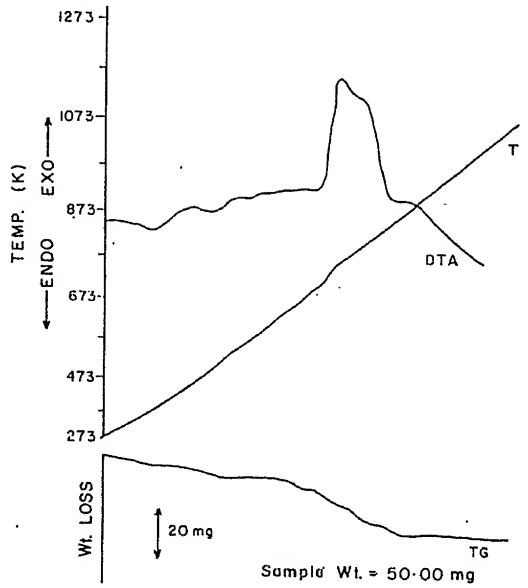

Fig. 1 - TG–DTA curves of $Pr_2C_{12}H_{12}O_{12}.6H_2O$ (Derivatograph).

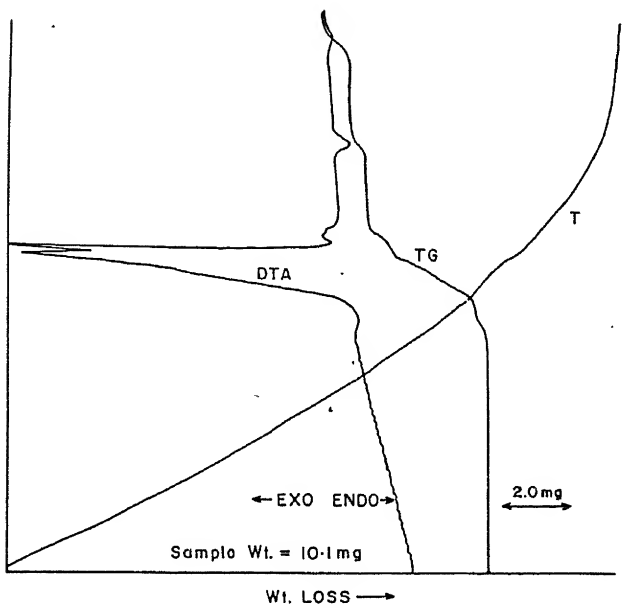

Fig. 2 - TG–DTA curves of $Pr_2C_{12}H_{12}O_{12}.6H_2O$ (Stanton).

compound this step starts at 400K and ends at 516K with an observed weight loss of 18.2% (calc. 17.6%)

$$M_2(C_{12}H_{12}O_{12})_3 2H_2O \rightarrow M_2(C_{12}H_{12}O_{12})_3 + 2H_2O$$

The anhydrous salts show remarkable stability over a range of temperature as evidenced by the corresponding smooth plateaus in the TG curves. The anhydrous Pr salt remains stable between 520 and 698K while the Dy shows stability in a similar temperature range *viz.* 516 to 693K.

In the third step anhydrous praseodymium succinate starts decomposing at 698K. The decomposition continues up to 800K giving basic carbonate[8,9] $PrO(CO_3)_{1/2}$ as indicated by the observed weight loss (Derivatograph 50.0%; Stanton 50.5% calc. 50.6%) up to this stage.

$$M_2(C_{12}H_{12}O_{12})_3 \xrightarrow{+93/2O_2} 2MO(CO_3)_{\frac{1}{2}} + 35CO_2 + 18H_2O$$

This intermediate product remains stable over a relatively small range of temperature (800-820K) and decomposes between (820 and 958K) leading to the formation of the oxide M_2O_3 as the final product as shown by the total observed weight loss 55.8% (Derivatograph); 55.4% (Stanton); (55.8% calc.)

$$2MO(CO_3)_{\frac{1}{2}} \xrightarrow{+O_2} M_2O_3 + 2CO_2$$

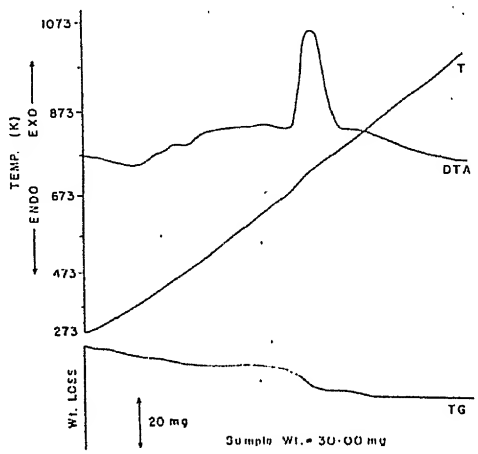

Fig. 3 - TG–DTA curves of $Dy_2C_{12}H_{12}O_{12}.8H_2O$.

In the case of dysprosium succinate the basic carbonate intermediate does not appear to be stable. The decomposition steps involving the formation of the basic carbonate and its subsequent decomposition overlap and the final product formed is the oxide.

$$M_2(C_{12}H_{12}O_{12})_3 \xrightarrow{+57/2O_2} M_2O_3 + 36CO_2 + 18H_2O$$

This overall step of decomposition starts at 693K and ends at 985K beyond which the oxide M_2O_3 remains stable. Total weight loss up to the formation of M_2O_3 is observed to be 54.2% (calc. 54.3%).

DTA curve of praseodymium succinate shows two endotherms with peaks at 368 and 513K and two exotherms with peaks at 763 and 823K. In the case of dysprosium compound, DTA shows two endotherms with peaks at 373 and 493K. The exotherm peak is seen at 763K. Thus the steps of decomposition indicated by TG correspond to those indicated by DTA. The endotherms correspond to decomposition processes while the exotherms represent decomposition accompanied by oxidative processes.

The reflectance spectra of the original compound (praseodymium succinate) and the species got after heating the compound at different temperatures are shown in Fig. 4. Besides room temperature (303K), the reflectance spectra were taken for sample heated to 403, 463 and 523K. A decrease in the intensity of bands is observed near 590, 485, 370 and 445 nm as dehydration proceeds with the rise in temperature.

The I.R. spectrum of the dehydrated product shows all the characteristic bands of the starting material except the band at 3400 cm^{-1} which vanishes completely at 525K (for Dy compound) suggesting the formation of the anhydrous salt.

Kinetics of decomposition : The fractional weight loss (α) at different temperatures was calculated from TG traces and α *vs.* T curves plotted for the first decomposition step in the case of both the compounds (Fig. 5). The curves do not begin with any apparent induction period and thus suggest that the initial stages involved very little or no physical desorption and also indicate that no surface nucleation or branching occurs before the decomposition starts[10]. The beginning of α–T curves with acceleratory period, followed by a region of maximum rate which virtually continues up to the end of process (α=1), is suggestive of there being no significant retention or decay period.

The kinetics of first decomposition step for both the compounds have been studied by non-isothermal method using the following equations :

(i) Coats and Redfern equation

$$(a)\ \log\frac{g(\alpha)}{T^2} = \log\frac{-\ln(1-\alpha)}{T^2} = -\frac{E}{2.303RT} + \log\left[\frac{ZR}{\beta E}\left(1-\frac{2RT}{E}\right)\right] \ldots \text{for } n=1 \qquad (1)$$

$$(b)\ \log\frac{g(\alpha)}{T^2} = \log\frac{\frac{1-(1-\alpha)^{1-n}}{1-n}}{T^2} = -\frac{E}{2.303RT} + \log\left[\frac{ZR}{\beta E}\left(1-\frac{2RT}{E}\right)\right] \ldots \text{for } n \neq 1$$

(ii) Piloyan and Novikova equation :

$$\log\frac{g(\alpha)}{T^2} = \log\frac{\alpha}{T^2} = \log\frac{ZR}{\beta E} - \frac{E}{2.303RT} \ldots (\alpha = 0.05\text{–}.5) \qquad (2)$$

(iii) Horowitz and Metzger equation

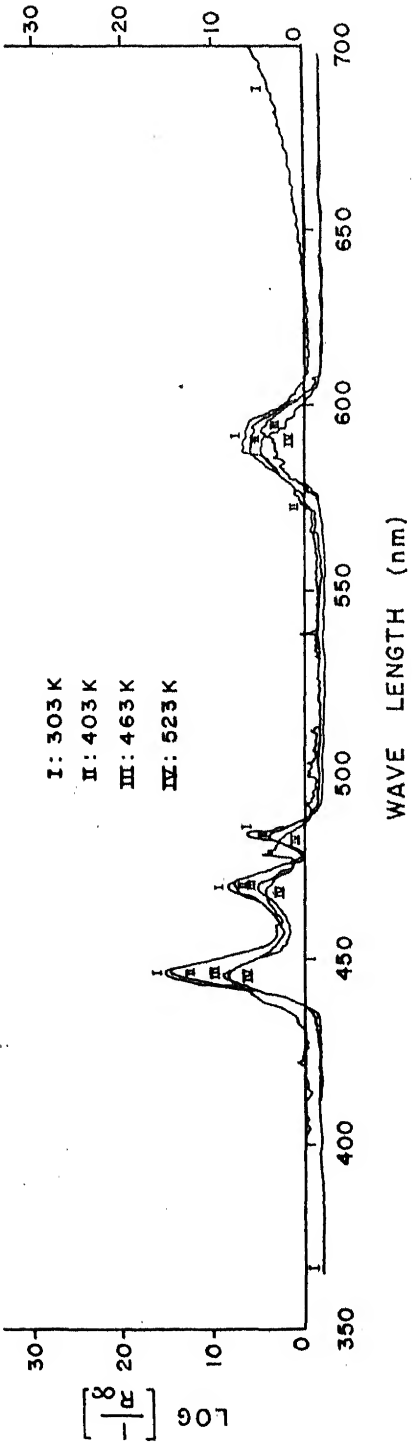

Fig. 4 - Reflectance spectra of $Pr_2C_{12}H_{12}O_{12}\cdot 6H_2O$

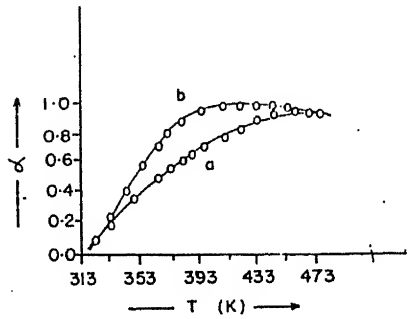

Fig. 5 - α–T curves : a, $Pr_2C_{12}H_{12}O_{12}.6H_2O$, b, $Dy_2C_{12}H_{12}O_{12}.8H_2O$

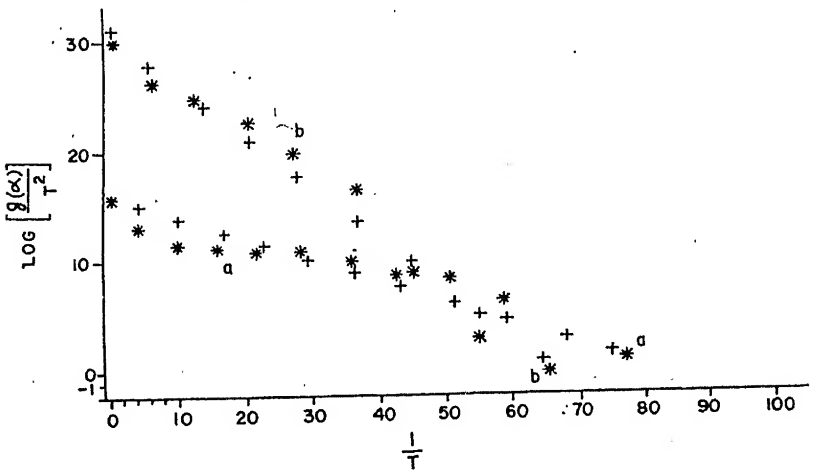

Fig. 6 – Coats-Redfern Plots : a, $Pr_2C_{12}H_{12}O_{12}.6H_2O$, b, $Dy_2C_{12}H_{12}O_{12}.8H_2O$

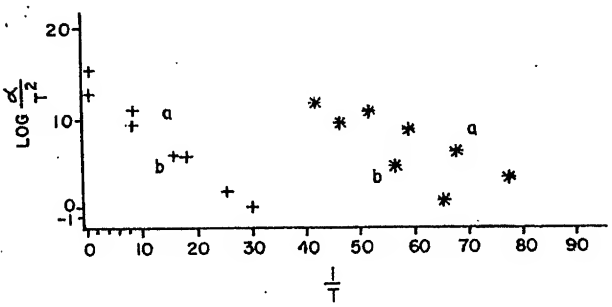

Fig. 7 – Piloyan–Novikova Plots : a, $Pr_2C_{12}H_{12}O_{12}.6H_2O$, b, $Dy_2C_{12}H_{12}O_{12}.8H_2O$

$$(a)\ \log g(\alpha) = \log[-\ln(1-\alpha)] = \frac{E\theta}{2.303RTm^2} \quad \text{for } n = 1$$

$$(b)\ \log g(\alpha) = \log\left[\frac{1-(1-\alpha)^{1-n}}{1-n}\right] = \frac{E\theta}{2.303RTm^2} \quad \text{for } n \neq 1 \tag{3}$$

where T = temperature; R = molar gas constant; E = energy of activation; Tm = peak temperature; $\theta = T - Tm$; Z = pre-exponential factor; β = rate of heating and $g(\alpha) = \int_0^{\alpha} \frac{d\alpha}{f(\alpha)}$; where $f(\alpha)$ is the appropriate function of α depending upon the mechanism involved). $g(\alpha)$ values corresponding to different models were got computerised and the values of $g(\alpha)/T^2$ *vs.* $1/T$ plotted for eqn. (1) and (2). The linear fits for different models were investigated. The best fit linear plot (Fig. 6) with minimum least square error was selected while applying Coats-Redfern equation. The values of slope, intercept, E and Z, were calculated from this very plot as also in the case of Piloyan-Novikova plot (Fig. 7) and the mechanism was decided. The value of entropy of activation ΔS^* was computed from the equation

$$Z = \frac{kTm}{h}\exp(\Delta S^*/R) \tag{4}$$

where K is the Boltzmann constant and h is the Planck constant. * represents the observed values and + the values calculated for ideal linear fits respectively. Plots of $g(\alpha)$ *vs.* T were constructed while applying eqn. (3) and the best fit linear plot (Fig. 8) having minimum least square error was selected to find $g(\alpha)$ and hence the mechanism. E was calculated from the slope of this plot and Z was determined from the equation

$$Z = \frac{E}{RTm^2}\beta\exp(E/RTm)$$

The value of entropy of activation, ΔS^*, was calculated from eqn. (4).

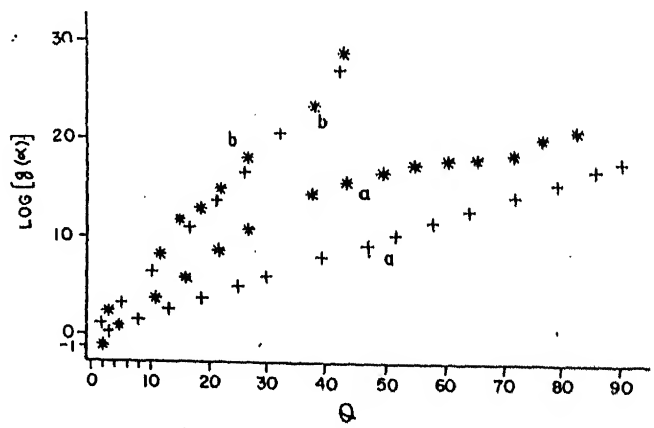

Fig. 8 – Horowitz–Metzger Plots : a, $Pr_2C_{12}H_{12}O_{12}.6H_2O$, b, $Dy_2C_{12}H_{12}O_{12}.8H_2O$

Table 2 presents the computed kinetic results. It is found that the best linear fit for both the compounds is obtained for $n = \frac{1}{2}$ or $g(\alpha) = 2\left[1-(1-\alpha)^{\frac{1}{2}}\right]$ by both Coats-Redfern and Horowitz-Metzger method.

Table 2 – Values of the computed kinetic results.

Sl. no.	Compound		Equation	E (KJ mol^{-1})	Z (S^{-1})	S^* (JK^{-1}mol^{-1})
1.	$Pr_2C_{12}H_{12}O_{12}.6H_2O$	(i)	Coats-Redfern	17.26	0.43 x 10^1	–253.75
		(ii)	Piloyan–Novikova	36.95	1.0 x 10^3	–188.91
		(iii)	Horowitz–Metzger	22.59	0.54 x 10^1	–232.66
2.	$Dy_2C_{12}H_{12}O_{12}.8H_2O$	(i)	Coats-Redfern	41.27	4.4 x 10^3	–177.23
		(ii)	Piloyan–Novikova	53.06	3.9 x 10^5	–139.82
		(iii)	Horowitz–Metzger	55.36	2.7 x 10^5	–143.05

Phase boundary mechanism involves the progress of the decomposition reaction along the reactant product interface and the reaction rate at any stage is proportional to the area of the interface at that stage. If a solid follows "contracting cylinder" mechanism of decomposition, its rate of decomposition is proportional to surface area

$$d\alpha/dT \propto 2\pi rl \quad \text{(for a cylinder)}$$

For a degree of decomposition, α, the volume of the sample is $\frac{M}{d}(1-\alpha)$, (M = mol. wt., d = density), and therefore

$$\frac{M}{d}(1-\alpha) = \pi r^2 l \quad \text{(for a cylinder)}$$

and $r = \frac{M}{d\pi l}(1-\alpha)^{\frac{1}{2}}$; therefore

$$\frac{d\alpha}{dT} \propto 2\pi rl \propto 2\pi\left[\frac{M}{d\pi l}(1-\alpha)\right]^{\frac{1}{2}}$$

$$= K(1-\alpha)^{\frac{1}{2}} = K f(\alpha)$$

$$\text{and } g(\alpha) = \int_0^{\alpha} \frac{d\alpha}{df(\alpha)} = 2\left[1-2(1-\alpha)^{\frac{1}{2}}\right]$$

Since the use of this value of g(α) in Coats-Redfern and Horowitz-Metzger equations gives the best linear fit for both the compounds, phase boundary decomposition model with "contracting cylinder" mechanism is suggested for the first step of their decomposition.

The values of kinetic parameters obtained by the application of different equations are reasonable and in good agreement. The values of ΔS^* suggest that the "transition state" involved in the decomposition process has a more ordered structure.

Acknowledgement

One of the authors (R.M.S.) thanks U.G.C., New Delhi for the award of a teacher fellowship.

References

1. Kaul, M.L. & Sharma, R.M. (1987) *J. Indian Chem. Soc.* **64** : 459.
2. Kaul, M.L., Raina, K.K. & Kotru, P.N. (1987) *Indian J. Pure and Appl. Phys.* **25** : 224.
3. Kaul, M.L., Raina, K.K. & Kotru, P.N. (1986) *J. Mater. Sc.* **21** : 3933.
4. Piloyan, G.O. & Novikova, O.S. (1966) *Russian J. Inorg. Chem.* **12** : 313.
5. Coats, A.W. & Redfern, J.P. (1964) *Nature* **201** : 68.
6. Horowitz, H.M. & Metzger, G. (1963) *Anal. Chem.* **35** : 1464.
7. Nakamoto, K. (1970) *Infra-red spectra of Inorganic and co-ordination compounds*, Wiley Interscience, New York, 2nd Ed. p. 244.
8. Turova, A.I., Shnyp, Z.A. & Serebrennikov, V.V. (1973) *Russ. Tr. Tomsk. Gos Univ.* 27–32 : 237.
9. Brazyska, W. & Ferene, W. (1981) *J. Therm. Anal.* **22** : 53.
10. Young, D.A. (1966) in *The International Encyclopaedia of Physical Chemistry, Solid and Surface Kinetics*, Ed., Tompkins, F.C., Pergamon Press, London, p. 68.

PROC. NAT. ACAD. SCI. INDIA, 61 (A), II, 1991

Electrochemical properties of selected soils in West Bengal

(Key words : electrochemical properties/soil/surface charge/zero point of charge)

A.K. DOLUI and S. DEY

Division of Agricultural Chemistry and Soil Science, Calcutta University, 35 Ballygunge Circular Road, Calcutta-700 019, India.

Received April 26, 1990; Accepted August 11, 1990.

Abstract

A study of the distribution of electric charges of selected soils from West Bengal was made by means of potentiometric titration in the presence of varying concentration of indifferent electrolyte. The electrochemical behaviour of these soils was found to be similar to that of the constant potential systems in which the surface potential is determined by H^+ and OH^- ions in the equilibrium solution, hence charge distribution varied substantially with pH and electrolyte concentration. The pH at the zero point of charge (ZPC) (varying from 2.40 to 2.90) occurred below the natural pH value of the soil indicating that the soils had a net negative charge under natural condition. σ_i(ZPT-ZPC) values indicated that soils had almost same amounts of permanent negative charge.

Introduction

Much of the work in soil has been conducted in temperate regions where, in general, soils are characterized by surfaces bearing a constant surface charge, whereas soils of the humid tropics are characterized by surfaces having a constant surface potential[1]. In such systems, the surface potential remains constant and the surface charge varies with changes in electrolyte concentration and in the activity of the potential determining H^+ and OH^- ions[2].

The most important parameter to describe a reversible surface charge system is its zero point of charge (ZPC). The ZPC is defined as the pH at which the surface charge of the system reduces to zero[3]. On the acid side of the ZPC, the system is positively charged and on its alkaline side it is negatively charged. Information on the electrochemical properties in Tarai and Teesta alluvial regions of West Bengal is rather limited. The aim of this study is to examine the ZPC and change of charges in profiles of two soil series in above regions of West Bengal due to pH and salt concentrations.

Materials and Methods

Nine soil samples from different horizons of two typical pedons located in Tarai and Teesta alluvial regions were collected based on the information of soil survey conducted by All India Soil and Land Use Survey, Calcutta Centre. General characteristics of the soils are reported in Table 1. The soils were air dried under shade, ground and passed through 2 mm sieve. The relevant selected properties of the soils are reported in Table 2. Potentiometric titrations for determination of the ZPC were done in 0.001, 0.1 and 1N sodium chloride solution following the method of Van Raij and Peech[1].

Table 1 - General characteristics of soils.

Soil series	Latitude	Logitude	District	Soil taxonomy	Height above mean sea level (m)	Annual precipitation (mm)	Annual mean temperature (°C)
Anandapur	26°18'N	89°41'E	Cooch Behar	Typic Udifluvent	38	2746.0	25.00
Dalingkote	26°41'N	88°18'E	Darjeeling	Typic Dystropept	131	3483.6	24.45

Table 2 - Selected properties of soils.

Horizon (cm)	pH		specific conductance (dSm^{-1})	Organic carbon (%)	Cation exchange capacity (c $molkg^{-1}$)	Fe_{KCl} (cmol kg^{-1})	Al_{KCl} (cmol kg^{-1})	Particle size distribution (%)			Texural* class
	H_2O	IN KCl						Sand	Silt	Clay	
Typic Udifluvent - Anandapur series (Cooch Behar)											
0-13	6.00	4.80	0.04	0.62	8.1	0.020	0.121	38.3	51.7	10.0	SiL
13-28	6.80	4.90	0.05	0.27	5.5	0.018	0.111	45.5	45.5	9.0	L
28-57	7.75	4.90	0.04	0.42	8.5	0.019	0.097	36.1	43.0	20.9	L
57-79	7.15	4.80	0.05	0.20	7.3	0.019	0.037	51.1	36.0	12.9	L
79-150+	7.60	5.00	0.04	0.17	6.4	0.010	0.038	68.5	23.0	8.5	SL
Typic Dystropept - Dalingkote series (Darjeeling)											
0-11	5.15	3.90	0.03	1.88	8.3	0.072	0.360	63.0	21.5	15.5	SL
11-44	5.30	4.00	0.02	1.69	9.2	0.065	0.356	51.0	27.3	21.7	SCL
44-77	5.30	4.40	0.02	1.31	8.1	0.066	0.269	61.0	12.7	26.3	SCL
77-130+	5.25	4.20	0.01	1.06	6.4	0.054	0.295	64.5	14.7	20.8	SCL

*SCL - Sandy clay loam, SL - Sandy loam, L-Loam, SiL - Silt loam.

Results and Discussion

Net electric charge by potentiometric titration : Potentiometric titration curves at different ionic strengths for two samples one each belonging to Anandapur series and Dalingkote series are shown in Fig. 1. The other samples, in each of these series, behaved in a similar manner. The charge-pH curves measured in the various ionic strengths intersected one another at single point indicating that these soils belong to the constant potential type of colloids with H^+ and OH^- as the potential determining ions. The ZPC values ranged from 2.40 to 2.90 (Table 3). In all cases, the ZPC values occurred below the natural pH values of the soils indicating that soil colloids bear net negative charges under natural conditions. This is also in agreement with the negative delta pH values ($\Delta pH = pH_{KCl} - pH_{H_2O}$) of the soils (Table 3). The ZPC of the charge-pH curves is on the acid side of the zero point of titration (ZPT), whereby indicating

that soils contain appreciable amounts of permanent negative charge[1].

Table 3 - ΔpH and ZPC values for the two soils.

Horizon (cm)	$\Delta pH=pH_{KCl}-pH_{H_2O}$	ZPC	pH_{KCl}–ZPC	σ_i=(ZPT-ZPC) (cmolkg^{-1})	Surface electric potential at soil pH=59(ZPC-pH)mv at 25°C
		Typic Udifluvent - Anandapur series (Cooch Behar)			
0-13	– 1.20	2.40	2.40	4.94	– 212.4
13-28	– 1.90	2.45	2.45	4.95	– 256.6
28-57	– 1.85	2.50	2.40	4.96	– 250.7
59-79	– 2.35	2.55	2.25	4.97	– 211.4
79-150+	– 2.60	2.60	2.40	4.98	– 295.0
		Typic Dystropept - Dalingkote series (Darjeeling)			
0-11	– 1.25	2.45	1.45	4.95	– 159.3
11-44	– 1.30	2.60	1.40	4.96	– 159.3
44-77	– 0.90	2.80	1.60	4.97	– 147.5
77-130+	– 1.05	2.90	1.30	4.98	– 138.6

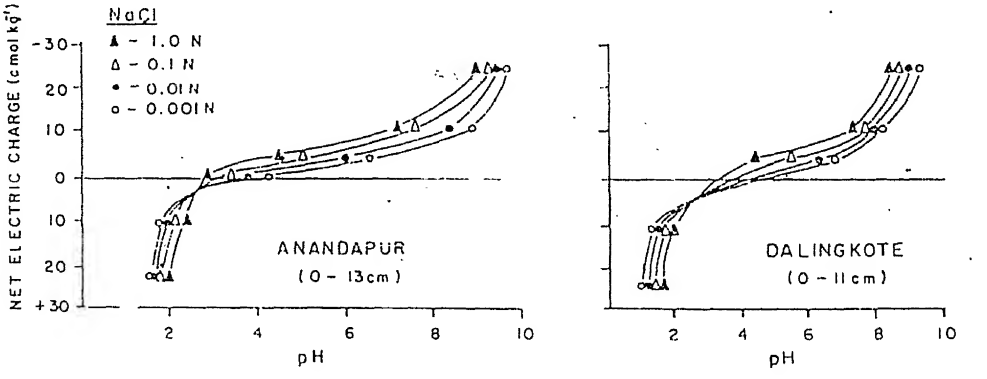

Fig. 1 - The net electric charge *vs.* pH curves of soil as determined by potentiometric titration.

The values of ZPC (Table 3) obtained from the potentiometric titration curves show strikingly the effect of the higher organic matter content of the surface horizon in lowering the ZPC, when compared with the ZPC of the corresponding subsurface horizons. The ZPC of the soils is different for different soils due to the difference in organic matter as well as sesquioxides content in soils.

The distribution of net electric charge on soil colloids (Fig. 1) indicates that the charge is influenced by the pH as well as the concentration of the NaCl. The common point of intersection of potentiometric titration curves of soil samples obtained in the presence of varying cocentration of indifferent electrolyte (NaCl) is not affected by the addition of salt, was

called the 'point of neutrality' by Mattson and Wiklander[4] who interpreted this unique point as the pH of the soil at which the exchange acidity due to displacement of H^+ ions was just balanced by the displacement of OH^- ions by the added salt. Except at ZPC, the net electric charge of the soil colloids has been increased with the increasing concentrations of indifferent electrolyte (NaCl). Above ZPC, the negative charge of the soils increases with increasing pH whereas the positive charge of the soils increases with decreasing pH.

The [pH_{KCl} - ZPC] values (Table 3) of Anandapur series vary from 2.25 to 2.45 and 1.30 to 1.60 in Dalingkote series. It is inferred that Dalingkate soil series is more developed than Anandapur series. Because with increasing pedogenic development, the ZPC approaches the natural pH of the soil[5,6]. The σ_i(ZPT - ZPC) values indicate the presence of 4.94 to 4.98 $cmolkg^{-1}$ of pH-independent negative charge in the soils. σ_i values also reveal that all soil samples bear almost same amount of negative pH-independent permanent charge. Surface potential of the soils at natural pH varies from –138.6 to –256.6 mV at 25°C.

From the present study it may be concluded that the charge distributed on the soil colloid increases with the increase in the concentration of indifferent electrolyte. Hence, both cation exchange capacity and anion exchange capacity measurement of these soil systems would be necessary to determine both positive and negative electrical charges of the soil in a dilute electrolyte with concentration similar to that encountered in the soil solution.

Acknowledgement

The authors express their appreciation to the I.C.A.R., New Delhi for financial assistance.

References

1. Van Raij, B. & Peech, M. (1972) *Soil Sci. Soc. Am. Proc.* **36** : 587.
2. Van Olphen, H. (1963) *Introduction to clay colloid chemistry*, Interscience Publishers, New York.
3. Parks, G.A. & de Bruyn, P.L. (1962) *J. Phys. Chem.* **66** : 967.
4. Mattson, S. & Wiklander, L. (1940) *Soil Sci.* **49** : 109.
5. Hendershot, W.H. & Lavkulich, L.M. (1978) *Soil Sci. Soc. Am. J.* **42** : 468.
6. Dolui, A.K., Dey, S. & Nayek, A.K. (1987) *J. Indian Soc. Soil Sci.* **35** : 353.

PROC. NAT. ACAD. SCI. INDIA, 61 (A), II, 1991

Integral operators involving multivariable *I*-Function

(Key words : integral operators/*I*-function/kernel)

R.K. SAXENA and Y. SINGH

Department of Mathematics and Statistics, University of Jodhpur, Jodhpur-342 00 India.

Received January 24, 1990; Acccepted June 5, 1990.

Abstract

Two fractional integration operators associated with a multivariable *I*-function have been defined. Three theorems are established. Some formal properties of these operators are also given.

Introduction

In the present paper two fractional integration operators with new representations introduced, whose kernels are associated with the multivariable *I*-function due to Prasad[1]. important theorems of these operators are established. Results given earlier by authors[2-13] are the special cases of the results proved here.

The multivariable *I*-function introduced by Prasad[1] will be defined and represented in following manner :

$$I\left[z_1,\ldots,z_r\right] = I^{0,n_2:\ldots:0,n_r:(m',n'):\ldots:\left(m^{(r)},n^{(r)}\right)}_{p_2,q_2:\ldots:p_r,q_r:(p',q'):\ldots:\left(p^{(r)},q^{(r)}\right)}\left[z_1,\ldots,z_r\;\middle|\begin{matrix}\left(a_{2j};\alpha'_{2j},\alpha''_{2j}\right)_{1,p_2}:\ldots:\left(a_{rj};\alpha'_{rj},\ldots,\alpha^{(r)}_{rj}\right)_{1,p_r}:\left(a'_j,\alpha'_j\right)_{1,p'}:\ldots:\left(a_j^{(r)},\alpha_j^{(r)}\right)_{1,p^{(r)}}\\ \left(b_{2j};\beta'_{2j},\beta''_{2j}\right)_{1,q_2}:\ldots:\left(b_{rj};\beta'_{rj},\ldots,\beta^{(r)}_{rj}\right)_{1,q_r}:\left(b'_j,\beta'_j\right)_{1,q'}:\ldots:\left(b_j^{(r)},\beta_j^{(r)}\right)_{1,q^{(r)}}\end{matrix}\right]$$

$$= \frac{1}{(2\pi w)^r}\int_{L_1}\cdots\int_{L_r}\phi_1(s_1)\ldots\phi_r(s_r)\psi(s_1,\ldots,s_r).z_1^{s_1}\ldots z_r^{s_r}\,ds_1\ldots ds_r$$

where $w=\sqrt{-1}$

$$\phi_i(s_i)=\frac{\prod_{j=1}^{m^{(i)}}\Gamma\left(b_j^{(i)}-\beta_j^{(i)}s_i\right)\prod_{j=1}^{n^{(i)}}\Gamma\left(1-a_j^{(i)}+\alpha_j^{(i)}s_i\right)}{\prod_{j=m^{(i)}+1}^{q^{(i)}}\Gamma\left(1-b_j^{(i)}+\beta_j^{(i)}s_i\right)\prod_{j=n^{(i)}+1}^{p^{(i)}}\Gamma\left(a_j^{(i)}-\alpha_j^{(i)}s_i\right)}\quad\forall i\varepsilon\{1,\ldots,r\}$$

$$\psi(s_1,\ldots,s_r)=\frac{\prod_{j=1}^{n_2}\Gamma\left(1-a_{2j}+\sum_{i=1}^{2}\alpha_{2j}^{(i)}s_i\right)\prod_{j=1}^{n_3}\Gamma\left(1-a_{3j}+\sum_{i=1}^{3}\alpha_{3j}^{(i)}s_i\right)}{\prod_{j=n_2+1}^{p_2}\Gamma\left(a_{2j}-\sum_{i=1}^{2}\alpha_{2j}^{(i)}s_i\right)\prod_{j=n_3+1}^{p_3}\Gamma\left(a_{3j}-\sum_{i=1}^{3}\alpha_{3j}^{(i)}s_i\right)}$$

$$\frac{\ldots\prod_{j=1}^{n_r}\Gamma\left(1-a_{rj}+\sum_{i=1}^{r}\alpha_{rj}^{(i)}s_i\right)}{\prod_{j=n_r+1}^{p_r}\Gamma\left(a_{rj}-\sum_{i=1}^{r}\alpha_{rj}^{(i)}s_i\right)\prod_{j=1}^{q_2}\Gamma\left(1-b_{2j}+\sum_{i=1}^{2}\beta_{2j}^{(i)}s_i\right)}$$

$$\frac{1}{\ldots\prod_{j=1}^{q_r}\Gamma\left(1-b_{rj}+\sum_{i=1}^{r}\beta_{rj}^{(i)}s_i\right)} \tag{3}$$

$\alpha_j^{(i)},\beta_j^{(i)},\alpha_{kj}^{(i)},\beta_{kj}^{(i)}$ $(i=1,\ldots,r)$ $(k=1,\ldots,r)$ are positive numbers, $a_j^{(i)}$, $b_j^{(i)}$ $(i=1,\ldots,r)$, a_{kj}, b_{kj} $(k=2,\ldots,r)$ are complex numbers and here $m^{(i)}, n^{(i)}, p^{(i)}, q^{(i)}$ $(i=1,\ldots,r)$, n_k, p_k, q_k $(k=2,\ldots,r)$ are non-negative integers where $0\le m^{(i)}\le q^{(i)}$, $0\le n^{(i)}\le p^{(i)}$, $q^k\ge 0$, $0\le n_k\le p_k$. Here (i) denotes the numbers of dashes. The contours L_i in the complex s_i–plane is of the Mellin-Barnes type which runs from $-w\infty$ to $+w\infty$ with identations, if necessary, to ensure that all the poles of $\Gamma\left(b_j^{(i)}-\beta_j^{(i)}s_i\right)\left(j=1,\ldots,m^{(i)}\right)$ are separated from those of $\Gamma\left(1-a_j^{(i)}+\alpha_j^{(i)}s_i\right)\left(j=1,\ldots,n^{(i)}\right)$, $\Gamma\left(1-a_{2j}+\sum_{i=1}^{2}\alpha_{2j}^{(i)}s_i\right)\left(j=1,\ldots,n_2\right),\ldots,$ $\Gamma\left(1-a_{rj}+\sum_{i=1}^{r}\alpha_{rj}^{(i)}s_i\right)\left(j=1,\ldots,n_r\right)$.

For further details and asymptotic expansion of the I-function one can refer to the original paper by Prasad[1]. I function includes, as special cases, the functions studied by Fox[14], Agarwal[15] and Braaksma[16].

In what follows, the multivariable I-function defined by (1) will be represented in the contracted notation.

$$I^{0,n_2:\ldots:0,n_r:(m',n'):\ldots:\left(m^{(r)},n^{(r)}\right)}_{p_2,q_2:\ldots:p_r,q_r:(p',q'):\ldots:\left(p^{(r)},q^{(r)}\right)}\left[z_1,\ldots,z_r\right]$$

or simply by $I(z_1,\ldots,z_r)$.

Integral Operators

We introduce the fractional integration operators by means of the following integral equations

$$(K_r)^{\eta,\alpha}A_x^{\xi}f(x)=\xi x^{-\eta-\xi\alpha-1}\int_0^x t^{\eta}\left(x^{\xi}-t^{\xi}\right)^{\alpha}f(t).I(K_1U,\ldots,K_rU)dt \tag{4}$$

$$(K_r)^{\delta,\alpha}B_x^{\xi}f(x)=\xi x^{\delta}\int_x^{\infty} t^{-\delta-\xi\alpha-1}\left(t^{\xi}-x^{\xi}\right)^{\alpha}f(t).I(K_1V,\ldots,K_rV)dt \tag{5}$$

where

$$U=\left(\frac{t^{\xi}}{x^{\xi}}\right)^{m_i}\left(1-\frac{t^{\xi}}{x^{\xi}}\right)^{n_i},\quad V=\left(\frac{x^{\xi}}{t^{\xi}}\right)^{m_i}\left(1-\frac{x^{\xi}}{t^{\xi}}\right)^{n_i}$$ and ξ, mi, ni are positive numbers.

The condition of the validity of these operators are as follows :

(i) $1\le p,\ q<\infty,\ p^{-1}+q^{-1}=1$

(ii) $$\mathrm{Re}\left(\eta+\xi\sum_{i=1}^{r}m_i\frac{b_j^{(i)}}{\beta_j^{(i)}}\right)>-\frac{1}{q},$$

$$\mathrm{Re}\left(\alpha+\sum_{i=1}^{r}n_i\frac{b_j^{(i)}}{\beta_j^{(i)}}\right)>-\frac{1}{q\xi},$$

$$\mathrm{Re}\left(\delta+1+\xi\sum_{i=1}^{r}m_i\frac{b_j^{(i)}}{\beta_j^{(i)}}\right)>\frac{1}{p},\quad j=1,\ldots,M_i;\quad i=1,\ldots,r$$

(iii) $f(x)\in L_p(0,\infty)$

The last condition ensures that both the operators exist and also that both belong to $L_p(0,\infty)$.

A Particular Case :

If we set $n_2=n_3=\ldots=n_{r-1}=0=p_2=p_3=\ldots=p_{r-1}$ and $q_2=q_3=\ldots=q_{r-1}=0$, we obtain the operators defined by Banerji and Sethi[13] which themselves are the generalizations of the operators due to other workers[2-5,6,8,11,12,17].

The Mellin transform of $f(x)$ will be denoted by $M[f(x)]$ or by $F(s)$. We write $s = p^{-1} + it$, where p and t are real. If $p \geq 1, f(x) \propto L_p(0,\infty)$, then

$$p = 1,\ M[f(x)] = F(s) = \int_0^\infty f(x)x^{s-1}dx \tag{6}$$

$$p > 1,\ M[f(x)] = F(s) = \text{l.i.m.} \int_{1/x}^{x} f(x)x^{s-1}dx \tag{7}$$

where l.i.m. denotes the usual limit in the mean of L_p–spaces.

Theorems

We now enunciate the three main theorems of this paper.

Theorem 1: If $f(x) \in L_p(0,\infty), 1 \leq p \leq 2$ [or $f(x) \in M_p(0,\infty)$ and $p > 2$],

$$|\arg K_i| < \frac{1}{2}\lambda_i\pi, \left[(\lambda_i),(K_i)\right] > 0, \operatorname{Re}\left(\alpha + \sum_{i=1}^{r} n_i \frac{b_j^{(i)}}{\beta_j^{(i)}}\right) > -\frac{1}{q}, \operatorname{Re}\left(\frac{\eta - s - \xi + 1}{\xi} + \sum_{i=1}^{r} m_i \frac{b_j^{(i)}}{\beta_j^{(i)}}\right)$$

$> -\frac{1}{q}, j = 1,\ldots,M_i; i = 1,\ldots,r, p^{-1} + q^{-1} = 1$, then

$$M\left\{(K_r)^{\eta,\alpha} A_x^{\xi} f(x)\right\} = I^{0,n_2:\ldots:0,n_r+2:(m',n'):\ldots:(m^{(r)},n^{(r)})}_{p_2,q_2:\ldots:p_r+2,q_r+1:(p',q'):\ldots:(p^{(r)},q^{(r)})}$$

$$\left[K_1,\ldots,K_r \middle| \begin{matrix} \left(a_{2j};\alpha'_{2j},\alpha''_{2j}\right)_{1,p_2}:\ldots \\ \left(b_{2j};\beta'_{2j},\beta''_{2j}\right)_{1,q_2}:\ldots \end{matrix} \right.$$

$$:\left(a_{rj};\alpha'_{rj},\ldots,\alpha^{(r)}_{rj}\right)_{1,p_r}:\left(\frac{\xi + s + 1 - \eta}{\xi};m_1,\ldots,m_r\right)$$

$$:\left(b_{rj};\beta'_{rj},\ldots,\beta^{(r)}_{rj}\right)_{1,q_r}$$

$$:(-\alpha;n_1,\ldots,n_r)$$

$$:\left(\frac{s - \eta - \xi\alpha - 1}{\xi};m_1 + n_1,\ldots,m_r + n_r\right)$$

$$\left. \begin{matrix} :\left(a'_j,\alpha'_j\right)_{1,p}:\ldots:\left(a_j^{(r)},\alpha_j^{(r)}\right)_{1,p}{}^{(r)} \\ :\left(b'_j,\beta'_j\right)_{1,q}:\ldots:\left(b_j^{(r)},\beta_j^{(r)}\right)_{1,q^{(r)}} \end{matrix} \right] M[f(x)], \tag{8}$$

where $M(0,\infty)$ denotes the class of all functions $f(x)$ of $L_p(0,\infty)$ with $p>2$, which are inverse Mellin transforms of functions of $L_q(-\infty,\infty)$.

Theorem 2: If $f(x)\in L_p(0,\infty), 1\le p\le\left[\text{or } f(x)\in M_p(0,\infty),\ p>2\right]$, $|\arg K_i|<\frac{1}{2}\lambda_i\pi$,

$$\left[(K_i),(\lambda_i)\right]>0, \operatorname{Re}\left(\alpha+\sum_{i=1}^{r} n_i\frac{b_j^{(i)}}{\beta_j^{(i)}}\right)>-\frac{1}{q}, \operatorname{Re}\left(\frac{\delta+s-\xi}{\xi}+\sum_{i=1}^{r} m_i\frac{b_j^{(i)}}{\beta_j^{(i)}}\right)>-\frac{1}{q},$$

$p^{-1}+q^{-1}=1, j=1,\ldots,M_i;\ i=1,\ldots,r;$ then

$$M\left\{(K_r)^{\delta,\alpha}B_x^{\xi}f(x)\right\}=I^{0,n_2:\ldots:0,n_r+2:\left(m',n'\right):\ldots:\left(m^{(r)},n^{(r)}\right)}_{p_2,q_2:\ldots:p_r+2,q_r+1:\left(p',q''\right):\ldots:\left(p^{(r)},q^{(r)}\right)}$$

$$\left[K_1,\ldots,K_r\left|\begin{matrix}\left(a_{2j};\alpha'_{2j},\alpha''_{2j}\right)_{1,p_2}:\ldots:\left(a_{rj};\alpha'_{rj},\ldots,\alpha^{(r)}_{rj}\right)_{1,p_r}\\ \left(b_{2j};\beta'_{2j},\beta''_{j}\right)_{1,q_2}:\ldots:\left(b_{rj};\beta'_{rj},\ldots,\beta^{(r)}_{rj},\ldots,\beta^{(r)}_{rj}\right)_{1,q_r}\end{matrix}\right.\right.$$

$$:\left(\frac{\xi-\delta-s}{\xi};m_1,\ldots,m_r\right):(-\alpha;n_1,\ldots,n_r)$$

$$:\left(-\frac{\delta+s+\xi\alpha}{\xi};m_1+n_1,\ldots,m_r+n_r\right)$$

$$\left.\begin{matrix}:\left(a'_j,\alpha'_j\right)_{1,p'}:\ldots:\left(a_j^{(r)},\alpha_j^{(r)}\right)_{1,p^{(r)}}\\ :\left(b'_j,\beta''\right)_{1,q'}:\ldots:\left(b_j^{(r)},\beta_j^{(r)}\right)_{1,q^{(r)}}\end{matrix}\right]M\left[f(x)\right] \tag{9}$$

Thorem 3: If $f(x)\in L_p(0,\infty), p^{-1}+q^{-1}=1, g(x)\in L_q(0,\infty), \operatorname{Re}\left(\alpha+\sum_{i=1}^{r} n_i\frac{b_j^{(i)}}{\beta_j^{(i)}}\right)>-\frac{1}{q\xi}$,

$$\operatorname{Re}\left(\eta+\xi\sum_{i=1}^{r} m_i\frac{b_j^{(i)}}{\beta_j^{(i)}}\right)>-\frac{1}{q}, \operatorname{Re}\left(\delta+1+\xi\sum_{i=1}^{r} m_i\frac{b_j^{(i)}}{\beta_j^{(i)}}\right)>\frac{1}{p}, |\arg K_i|<\frac{1}{2}\lambda_i\pi, \left[(\lambda_i),(K_i)\right]>0,$$

then

$$\int_0^x g(x)(K_r)^{\eta,\alpha}A_x^{\xi}\{f(x)\}dx=\int_0^x f(x)(K_r)^{\delta,\alpha}B_x^{\xi}\{g(x)\}dx \tag{10}$$

Proof of Theorem 1 : From (4), it follows that

$$M\left\{(K_r)^{\eta,\alpha}A_x^{\xi}f(x)\right\}\int_0^{\infty}x^{s-1}\xi x^{-\eta-\xi\alpha-1}\int_0^{x}t^{\eta}\left(x^{\xi}-t^{\xi}\right)^{\alpha}J(K_1U,\ldots,K_rU)f(t)\,dt.dx$$

On changing the order of integration which is permissible[18] under the conditions stated with the theorem, we obtain

$$\xi\int_0^{\infty}t^{\eta}f(t)dt\int_t^{\infty}x^{s-\eta-\xi\alpha-2}\left(x^{\xi}-t^{\xi}\right)^{\alpha}I(K_1U,\ldots,K_rU)dx$$

The theorem now follows on evaluating the x-integral by means of the formula

$$\int_0^1 x^{\alpha-1}(1-x)^{\beta-1}I\left[a_1x^{m_1}(1-x)^{n_1},\ldots,a_rx^{m_r}(1-x)^{n_r}\right]dx$$

$$=I^{0,n_2;\ldots;0,n_r+2:(m',n'):\ldots:\left(m^{(r)},n^{(r)}\right)}_{p_2,q_2;\ldots;p_r+2.q_r+1:(p',q'):\ldots:\left(p^{(r)},q^{(r)}\right)}\left[a_1,\ldots,a_r\middle|\begin{matrix}\left(a_{2j};\alpha'_{2j},\alpha''_{2j}\right)_{1,p_2}:\ldots:\left(a_{rj};\alpha'_{rj},\ldots,\alpha^{(r)}_{rj}\right)_{1,p_r}\\ \left(b_{2j};\beta'_{2j},\beta''_{2j}\right)_{1,q_2}:\ldots:\left(b_{rj};\beta'_{rj},\ldots,\beta^{(r)}_{rj}\right)_{1,q_r}\end{matrix}\right.$$

$$\left.\begin{matrix}:(1-\alpha;m_1,\ldots,m_r):(1-\beta;n_1,\ldots,n_r):\left(a'_j,\alpha'_j\right)_{1,p}:\ldots:\left(a^{(r)}_j,\alpha^{(r)}_j\right)_{1,p^{(r)}}\\ :(1-\alpha-\beta;m_1+n_1,\ldots,m_r+n_r):\left(b'_j,\beta'_j\right)_{1,q}:\ldots:\left(b^{(r)}_j,\beta^{(r)}_j\right)_{1,q^{(r)}}\end{matrix}\right] \tag{11}$$

where $\mathrm{Re}\left(\alpha+\sum_{i=1}^{r}m_i\frac{b_j^{(i)}}{\beta_j^{(i)}}\right)>0$, $\mathrm{Re}\left(\beta+\sum_{i=1}^{r}n_i\frac{b_j^{(i)}}{\beta_j^{(i)}}\right)>0$, $(j=1,2,\ldots,Mi;\ i=1,\ldots,r)$

$$|\arg a_i|<\frac{1}{2}U_i\pi;\ \left[(a_i),(U_i)\right]>0$$

where $U_i=\sum_{j=1}^{n^{(i)}}\alpha_j^{(i)}-\sum_{j=n^{(i)}+1}^{p^{(i)}}\alpha_j^{(i)}+\sum_{j=1}^{m^{(i)}}\beta_j^{(i)}-\sum_{j=m^{(i)}+1}^{q^{(i)}}\beta_j^{(i)}+\left(\sum_{j=1}^{n_2}\alpha_{2j}^{(i)}-\sum_{j=n_2+1}^{p_2}\alpha_{2j}^{(i)}\right)$

$$+\left(\sum_{j=1}^{n_3}\alpha_{3j}^{(i)}-\sum_{j=n_3+1}^{p_3}\alpha_{3j}^{(i)}\right)+\ldots+\left(\sum_{j=1}^{n_r}\alpha_{rj}^{(i)}-\sum_{j=n_r+1}^{p_r}\alpha_{rj}^{(i)}\right)-\left(\sum_{j=1}^{q_2}\beta_{2j}^{(i)}+\sum_{j=1}^{q_3}\beta_{3j}^{(i)}+\ldots+\sum_{j=1}^{q_r}\beta_{rj}^{(i)}\right),$$

which follows from the Beta function formula and includes Goyal's formula[19].

Theorem 2 can be established in the same way. Theorem 3 follows immediately on interpreting it with the help of (4) and (5).

Formal Properties of the Operators

We give some formal properties of the operators which follow as a consequence of the definitions (4) and (5).

(i) $x^{-1}(K_r)^{\eta,\alpha}A^{\xi}_{1/x}[f(1/x)] = (K_r)^{\eta,\alpha}B^{\xi}_{x}\left[x^{-1}f(x)\right]$

(ii) $x^{-1}(K_r)^{\delta,\alpha}B^{\xi}_{1/x}[f(1/x)] = (K_r)^{\delta,\alpha}A^{\xi}_{x}\left[x^{-1}f(x)\right]$

(iii) $x^{\beta}(K_r)^{\eta,\alpha}A^{\xi}_{x}[f(x)] = (K_r)^{\eta-\beta,\alpha}A^{\xi}_{x}\left[x^{s}f(x)\right]$

(iv) $x^{\beta}(K_r)^{\delta,\alpha}B^{\xi}_{x}[f(x)] = (K_r)^{\delta-\beta,\alpha}B^{\xi}_{x}\left[x^{\beta}f(x)\right]$

(v) If $(K_r)^{\eta,\alpha}A^{\xi}_{x}[f(x)] = g(x)$

then $(K_r)^{\eta,\alpha}A^{\xi}_{x}[f\{cx\}] = g\{cx\}$

(vi) and If $(K_r)^{\delta,\alpha}B^{\xi}_{x}[f(x)] = \phi(x)$

then $(K_r)^{\delta,\alpha}B^{\xi}_{x}[f\{cx\}] = \phi\{cx\}$

References

1. Prasad, Y.N. (1986) *Vijnana Parishad Anusandhan Patrika* **29**: 232.
2. Kober, H. (1940) *Q. Jl. Math. (Oxford)* II:193.
3. Erdelyi, A. (1950-51) *Re. Sem. Math. Univ. Torino* **10** : 217.
4. Saxena, R.K. & Kumbhat, R.K. (1973) *Proc. Indian Acad. Sci.* A **78** : 177.
5. Saxena, R.K. & Kumbhat, R.K. (1974) *J. Pure and Appl. Math. India* **5** : 1.
6. Kalla, S.L. & Saxena, R.K. (1969) *Math. Z.* **108** : 231.
7. Mathur, B.L. (1977) *J.M.A.C.T.* **10** : 123.
8. Parasher, B.P. (1968) *Math. Japan* **12** : 141.
9. Lowndes, J.S. (1970) *Proc. Edinburgh Math. Soc.* **17** : 139.
10. Mourya, D.P. (1970) *Proc. Indian Acad. Sci.* A **62** : 175.
11. Kiryakova, V.S. (1986) *Compt. Rend. Acad. Bulg. Sci.* **39** : 25.
12. Kiryakova, V.S. (1988) *Compt. Rend. Acad. Bulg. Sci.* **41** : 11.
13. Banerji, P.K. & Sethi, P.L. (1978) *Math. Student* **2** : 152.
14. Fox, C. (1961) *Trans. Amer. Math. Soc.* **98** : 395.
15. Agarwal, R.P. (1965) *Proc. Nat. Inst. Sci. India* A**3** : 536.
16. Braaksma, B.L.J. (1963) *Compt. Math.* **15** : 239.
17. Saxena, R.K. (1967) *Math. Z.* **96** : 288.
18. Bromwich, T.J.I. (1954) *An introduction to the theory of infinite series*, Mcmillan, London.
19. Goyal, G.K. (1969) *Proc. Nat. Acad. Sci. India* **39**A : 201.

PROC. NAT. ACAD. SCI. INDIA, 61(A), II, 1991

On modes of propagation of weak discontinuity in two-phase homogeneous conducting system

(Key words : two-phase system/weak discontinuity/shock relations/Alfven velocity)

P. N. MISHRA*+ and K. S. UPADHAYAYA**

* *Management Development Institute, Mehrauli Road, Gurgaon, India.*

** *Department of Mathematics and Statistics, University of Allahabad, Allahabad-211 002, India.*

+ *Present Address : Institute of Management Studies, Devi Ahilya University, Indore-452 001, India.*

Received August 14, 1989; Revised April 30, 1990; Accepted July 14, 1990.

Abstract

The two-phase homogeneous conducting system has been reduced to a corresponding single phase system with the help of two suitably defined quantities for the mixture-uniform density ρ_m and permeability coefficient μ_m. The equations governing the flow have been integrated across the shock surface to give shock relations. The presence of magnetic field affects the propagation of weak discontinuity in such a way that, in place of one, three modes of propagation of surface of weak discontinuity have been obtained. It has been observed that Alfven velocity is independent of velocity of propagation of sound in the mixture while the slow and fast wave velocities depend upon sonic velocity.

Introduction

Two phase hydrodynamical systems have not been investigated as deeply as single phase hydrodynamical system for the want of appropriate mathematical formulation. As a matter of fact, single phase system is only an ideal mathematical formulation far away from the natural reality. Most of the natural phenomena are represented by two phase/multi-phase system only. The study of two phase system is equally important for subsonic and supersonic flows. Some of the initial work in this field has been done by Carrier[1] and Campbell and Pitcher[2]. But they have started with jump conditions across the shock without going into the details of formulation governing the flow. The work was extended by Miura[3], Moore[4], Rudinger[5] and Wizngaarden[6] etc. Upadhyaya and Singh[7] have recently formulated the problem in somewhat more general sense and have observed that the results obtained by Campbell and Pitcher[2] for homogeneous gas liquid mixture are also true for conducting, non conducting and viscous conducting fluids.

Our two-phase conducting system is a liquid-gas mixture in the presence of magnetic field. The former (liquid) is incompressible where as latter (gas) is compressible. In the mixture the gas is supposed to be in the form of bubbles. An incompressible fluid mixed with gas bubbles behaves like compressible one and thus its fundamental characteristic is changed. Formulation of a two phase system is a difficult task. Presence of magnetic field makes it more complicated. In Campbell and Pitcher's formulation[2] relative velocity between the phases was not accounted for. Wallis[8] made some improvement in the approach of Campbell and Pitcher. Some workers[9-11] have made significant contribution by improving the formulation available earlier. Miura's[3] formulation can be treated as an improvement on the

earlier formulations but the formulation proposed by Upadhyaya and Singh[7] is more appropriate and has been used here.

Formulation

The bubbles affect and are affected by the motion of liquid. The effect of gas bubbles is proportional to the space that they occupy. Let us assume that X be the space occupied by the gas in liquid-gas mixture of unit volume; the space occupied by the liquid will be (1-X). The liquid and gas are supposed to be moving with the same velocity. Thus, there is no interaction between the phases[2]. Since the maghetic field has no impact on mass, concentrating on liquid and gas portions separately and applying the law of conservation of mass, equations of continuity for the individual phases can be given as

$$\rho^* \frac{\partial(1-X)}{\partial t} + \rho^* \{(1-X)v_i\}_{,i} = 0 \tag{1a}$$

$$\frac{\partial(X\rho)}{\partial t} + (X\rho v_i)_{,i} = 0 \tag{1b}$$

where v_i is the common velocity of liquid and gas and comma followed by Latin index 'i' denotes partial differentiation with respect to x_i, ρ and ρ^* stand for gas and liquid densities respectively. Every term of field equation contains magnetic field intensity (H). The field equations can be directly written as

$$H_{i,i} = 0 \tag{2a}$$

$$\frac{\partial H_i}{\partial t} + v_j H_{i,j} - H_j v_{i,j} + H_i v_{j,j} = 0 \tag{2b}$$

Unlike mass, the magnetic field has impact on moving fluid which is directly related to its velocity. Applying laws of conservation of momentum and energy, we get the equations of motion and energy for liquid and gas separately as

$$(1-X)\rho^* \frac{\partial v_i}{\partial t} + (1-X)\rho^* v_j v_{i,j} + \left\{(1-X)_p\right\}_{,i} + \frac{1}{4\pi}\left\{\mu_e(1-X)\left(\frac{H^2}{2}\delta_{ij} - H_i H_j\right)\right\}_{,j} = 0 \tag{3a}$$

$$X\rho \frac{\partial v_i}{\partial t} + X\rho + v_j v_{i,j} + (Xp)_{,i} + \frac{1}{4\pi}\left\{\mu_g X\left(\frac{H^2}{2}\delta_{ij} - H_i H_j\right)\right\}_{,j} = 0 \tag{3b}$$

and

$$\frac{\partial\left\{(1-X)\rho^*\left(\frac{1}{2}v^2 + c^*T\right) + \frac{\mu_e}{8\pi}(1-X)H^2\right\}}{\partial t} + \left\{(1-X)\rho^* v_j\left(\frac{1}{2}v^2 + c^*T + \frac{p}{\rho^*}\right)\right\}_{,j}$$

$$-\frac{\mu_e}{8\pi}(1-X)H^2 v_{j,j} - (1-X)p v_{i,i} + \frac{1}{4\pi}\left\{\mu_e(1-X)v_i\left(H^2\delta_{ij} - H_i H_j\right)\right\}_{,j} = 0 \tag{4a}$$

$$\frac{\partial\left\{X\rho\left(\frac{1}{2}v^2+c_vT\right)+\frac{\mu_g}{8\pi}XH^2\right\}}{\partial t}+\left\{X\rho v_j\left(\frac{1}{2}v^2+c_vT+\frac{p}{\rho}\right)\right.$$

$$\left.+\frac{\mu_g}{4\pi}Xv_i\left(H^2\delta_{ij}-H_iH_j\right)\right\}_{,j}+\left(p+\frac{\mu_gH^2}{8\pi}\right)(1-X)v_{j,j}=0 \tag{4b}$$

where μ_e and μ_g stand for magnetic permeability of liquid and gas respectively. c_v, c^* and T are respectively the specific heat of gas at constant volume, specific heat of liquid and temperature of the media.

The two media have got different permeabilities and densities. Therefore, we have obtained separate equations of continuity, motion and energy for respective phases. To combine the equations of continuity, motion and energy, we define two quantities ρ_m and μ_m respectively for density and magnetic permeability of the mixture as

$$\rho_m=X\rho+(1-X)\rho^* \tag{5}$$

$$\mu_m=(1-X)\mu_e+X\mu_g \tag{6}$$

We combine the set of eqn. (1), (3) and (4) by using (5) and (6) to give

$$\frac{\partial\rho_m}{\partial t}+v_i\rho_{m,i}+\rho_mv_{i,i}=0 \tag{7}$$

$$\rho_m\frac{\partial v_i}{\partial t}+\rho_mv_jv_{i,j}+p_{,i}+\frac{1}{4\pi}\left\{\mu_m\left(\frac{H^2}{2}\delta_{ij}-H_iH_j\right)\right\}_{,j}=0 \tag{8}$$

$$\frac{\partial\left\{\rho_m\left(\frac{1}{2}v^2+c_{mv}T\right)+\frac{\mu_m}{8\pi}H^2\right\}}{\partial t}+\left\{\rho_mv_j\left(\frac{1}{2}v^2+c_{mv}T+\frac{p}{\rho_m}\right)\right.$$

$$\left.+\frac{\mu_m}{4\pi}v_i\left(H^2\delta_{ij}-H_iH_j\right)\right\}_{,j}=0 \tag{9}$$

where $c_{mv}=\dfrac{mc^*+c_v}{1+m}$ (10)

c_{mv} represents specific heat of the mixture and m is mass ratio of the liquid to gas such that

$$m=\frac{(1-X)\rho^*}{X\rho} \tag{11}$$

and can be treated as constant without affecting the general results[2].

Shock Relations

In order to obtain the shock relations, we intergate the eqn. (2), (7), (8) and (9). For this purpose, let us consider a cylindrical fluid volume $\bar{V}$, with base Σ_1 and Σ_2 and curved surface $\bar{S}$ containing the portion Σ of the shock surface in it. Obviously, $\bar{S}$ is formed of the stream lines of the particles crossing the outer boundary of Σ_1 at a particular time and reaching the corresponding boundary of Σ_2. The cylindrical volume of length l is assumed to be stationary with the shock surface. The integration of the representative equation of the set of equations governing the flow, i.e.,

$$\frac{\partial I}{\partial t} + F_{i,i} = 0 \tag{12}$$

over the volume $\bar{V}$, under the conditions l, $\bar{V}$, and $\bar{S}$ tending to zero and Σ_1 and Σ_2 tending to Σ yields[12]

$$\iint_{\Sigma} [F_i n_i] d\Sigma = 0 \tag{13}$$

where [ ] denotes the difference of the quantity on the two surfaces Σ_1 and Σ_2 of the volume. The eqn. (13) holds good for arbitrary point in the surface area Σ, therefore, we have

$$[F_i n_i] = 0 \tag{14}$$

Using the result (14) and integrating (2), (7), (8) and (9), we get

$$[H_{n/}] = 0 \tag{15}$$

$$[V_{n/} H_i] - H_{1n/}[V_i] = 0 \tag{16}$$

$$[\rho_m V_{n/}] = 0 \tag{17}$$

$$\rho_{1m} V_{1n/}[V_i] + [p^*] n_i - \frac{\mu_m}{4\pi} H_{1n/}[H_i] = 0 \tag{18}$$

where $p^* = p + \frac{\mu_m}{4\pi} \cdot \frac{H^2}{2}$ and $V_i = v_i - G n_i$,

G denotes the speed of Shock Surface, and

$$\rho_{1m} V_{1n/} \left[\frac{1}{2} V^2 + c_{mv} T + \frac{p}{\rho_m} \right] + \frac{\mu_m}{4\pi} \left[V_i \left(H^2 n_i - H_{n/} H_i \right) \right] = 0 \tag{19}$$

The suffix $n/$ is used to denote the dot product of the quantity concerned with the unit normal vector n_i to the shock surface

The eqn. (15) to (19) are the shock relations for liquid-gas mixture in the presence of magnetic field. Putting magnetic field intensity $H = 0$, we get the results for two phase non-conducting system which are in full agreement with previous results[7].

Propagation of Weak Discontinuity

Let $\Sigma_{(t)}$ denote the surface of weak discontinuity moving in the homogeneous liquid-gas mixture with velocity G. Obviously the flow parameters are continuous across $\Sigma_{(t)}$ i.e.,

$$[Z] = 0 \tag{20}$$

while the first and higher order derivatives are discontinuous across it. Moreover, under the proper assumption of the regularity of the surface $\Sigma_{(t)}$ and the existence of limiting values of the functions and their derivatives as they approach this surface from each side, it is well known that

$$[Z, i] = \beta n_i \tag{21}$$

and

$$\left[\frac{\partial Z}{\partial t}\right] = -\beta G \tag{22}$$

where B is the normal derivative of flow parameter.

For obtaining the jumps of normal derivatives of the flow parameters, we would like to use the equation of the state for the mixture in place of equation of energy, as former is sufficient for our purpose and latter is cumbersome to handle. Equation of state for the mixture under constant entropy can be written as

$$p = p(\rho_m) \tag{23}$$

which implies

$$\frac{\partial p}{\partial t} + v_i p_{,i} - c_m^2\left(\frac{\partial \rho_m}{\partial t} + v_i \rho_{m,i}\right) = 0 \tag{24}$$

with the help of (7), (24) gives

$$\frac{\partial p}{\partial t} + v_i p_{,i} + c_m^2 \rho_m v_{i,i} = 0 \tag{25}$$

Now taking the jumps of (2), (7), (8) and (25) and making use of first order compatibiliy conditions[13], we get

$$\epsilon_N = 0 \tag{26}$$

where

$$\left[H_{i,j}\right]n_j = \epsilon_i$$

$$V_{n/}\epsilon_i - H_n\lambda_i + H_i\lambda_{n/} = 0 \tag{27}$$

$$V_{n/}\varsigma + \rho_m\lambda_{n/} = 0 \tag{28}$$

$$\rho_m V_{n/}\lambda_i + \mu n_i + \frac{\mu_m}{4\pi}\left\{H_j \epsilon_j n_i - H_{n/}\epsilon_i\right\} = 0 \tag{29}$$

$$V_{n/}\mu + \rho_m c_m^2 \lambda_{n/} = 0 \tag{30}$$

Before solving (26) to (30), we observe that the situation is not exactly similar to its counter part for non-conducting flow[7]. Therefore, we follow a different approach. Eliminating unknown quantities other than i from (26) to (30) and substituting

$l_i = H_i / H$, we get

$$V_{n/}^2\lambda_i = a_{ij}\lambda_j \tag{31}$$

where

$$a_{ij} = \left\{\frac{\mu H^2 l_{n/}^2}{4\pi\rho_m}\delta_{ij} + \left(c_m^2 + \frac{\mu H^2}{4\pi\rho_m}\right)n_i n_j - \frac{\mu H^2 l_{n/}}{4\pi\rho_m}\left(l_j n_i + n_j l_i\right)\right\}$$

(31) implies

$$\lambda_j\left\{V_{n/}^2\delta_{ij} - a_{ij}\right\} = 0 \tag{32}$$

which gives

$$\left|V_{n/}^2\delta_{ij} - a_{ij}\right| = 0 \tag{33}$$

as $\lambda_j \neq 0$.

Taking (x_i) parallel to x_1 - axis and (l_i) in the plane of (x_1, x_2) at an angle θ with x_1 and substituting

$$\frac{\mu_m H^2}{4\pi\rho_m} = b^2$$

(33) yields

$$\begin{vmatrix} \left(V_{n/}^2 + b^2 l_{n/}^2 - c_m^2 - b^2\right) & \left(b^2 l_{n/} \sin\theta\right) & 0 \\ \left(b^2 l_{n/} \sin\theta\right) & \left(V_{n/}^2 - b^2 l_{n/}^2\right) & 0 \\ 0 & 0 & \left(V_{n/}^2 - b^2 l_{n/}^2\right) \end{vmatrix} = 0 \tag{34}$$

which on simplification reduces to

$$\left(V_{n/}^2 - b^2 l_{n/}^2\right)\left\{V_{n/}^4 + b^2 l_{n/}^2 c_m^2 - V_{n/}^2\left(c_m^2 + b^2\right)\right\} = 0 \tag{35}$$

Eqn. (35) is a third degree equation in $V^2_{n/}$, therefore, it will give three values of $V^2_{n/}$ and consequently three values of velocity of propagation of weak discontinuity. From (35), we infer

$$V_{n/}^2 = b^2 l_{n/}^2 \tag{36a}$$

$$V_{n/}^2 = \frac{1}{2}\left\{c_m^2 + b^2 + \sqrt{c_m^4 + b^4 + b^2 c_m^2\left(1 - 2l_{n/}^2\right)}\right\} \tag{36b}$$

$$V_{n/}^2 = \frac{1}{2}\left\{c_m^2 + b^2 - \sqrt{c_m^4 + b^4 + b^2 c_m^2\left(1 - 2l_{n/}^2\right)}\right\} \tag{36c}$$

The set of eqn. (36) gives magnitudes of three velocities of propagation of surface of weak discontinuity relative to the medium. If medium ahead is at rest ; they yield

$$G_a^2 = b^2 l_{n/}^2 \tag{36a'}$$

$$G_f^2 = \frac{1}{2}\left\{c_m^2 + b^2 + \sqrt{c_m^4 + b^4 + 2b^2 c_m^2\left(1 - 2l_{n/}^2\right)}\right\} \tag{36b'}$$

$$G_s^2 = \frac{1}{2}\left\{c_m^2 + b^2 - \sqrt{c_m^4 + b^4 + 2b^2 c_m^2\left(1 - 2l_{n/}^2\right)}\right\} \tag{36c'}$$

where G_a, G_f and G_s are respectively magnitudes of Alfven, fast and slow wave velocities.

A velocity is determined completely only when its direction and magnitude both are determined. It is obvious that respective directions of Alfven, fast and slow velocities are given by eigen vectors of symmetric matrix (a_{ij}).

Determination of Eigen Vectors of Symmetric Matrix (a_{ij}) :

Let L_i be the eigen vector of the symmetric matrix (a_{ij}) with principal value L. We obtain from (31)

$$V_{n/}^2 L_i \lambda_i = a_{ij} L_i \lambda_j = L L_j \lambda_j \tag{37}$$

which implies

$$\left(V_{n/}^2 - L\right) L_i \lambda_i = 0 \tag{38}$$

Consequently $L = V_{n/}^2$. That is, λ_i is an eigen vector of (a_{ij}) with principal value $V_{n/}^2$.

Since (a_{ij}) is a symmetric matrix of rank 3, therefore, it possesses three mutually perpendicular eigen vectors. These three vectors are corresponding to three values of velocity of propagation of weak discontinuity given by (36). Let us denote them by L_i^a, L_i^f and L_i^s.

Surface of discontinuity is the surface formed by θ and ϕ parametric curves. Its normal $\hat{n}$ is inclined with x_3-axis at an angle θ.

We obviously have

$$\hat{n} = (\sin\theta\cos\phi,\ \sin\theta\sin\phi,\ \cos\theta) \tag{39}$$

$$\hat{m} = (\cos\theta\cos\phi,\ \cos\theta\sin\phi,\ -\sin\theta) \tag{40}$$

$$\hat{k} = (-\sin\phi,\ \cos\phi,\ 0) \tag{41}$$

where $\hat{m}$ and $\hat{k}$ are unit vectors tangential to θ and ϕ parametric curves respectively.

Now it is easy to show that $\hat{k}$ is an eigen vector of the matrix (a_{ij}) with the principal value as Alfvan velocity. Thus we have

$$L_i^a = k_i \quad \text{for} \quad i = 1,2,3. \tag{42}$$

Since λ_i is an eigen vector of the matrix (a_{ij}) and eigen vectors are perpendicular to each other, we can write

$$\lambda_i = \left(\cos\phi,\ \sin\phi,\ \bar{M}\right) \tag{43}$$

In view of (43), eqn. (31) yields

$$\bar{M} = \frac{V_{n/}^2 - b^2 - c_m^2 \sin^2\theta}{c_m^2 \sin\theta\cos\theta} \tag{44}$$

hence the corresponding eigen vectors are

$$L_i^f = \left(\cos\phi,\ \sin\phi,\ \frac{V_{n/f}^2 - b^2 - c_m^2 \sin^2\theta}{c_m^2 \sin\theta\cos\theta} \right) \tag{45}$$

$$L_i^s = \left(\cos\phi,\ \sin\phi,\ \frac{V_{n/s}^2 - b^2 - c_m^2 \sin^2\theta}{c_m^2 \sin\theta\cos\theta} \right) \tag{46}$$

As it has been already stated, unique solution, for the velocity of propagation of surface of weak discontinuity in presence of magnetic field is not possible. That is why we have obtained three magnitudes of velocities given by set of eqn. (36) and three different directions given by (42), (45) and (46). Mere observation of eqn. (36), (42), (45) and (46) reveals that

(i) The velocity of propagation depends upon the magnetic strength.

(ii) The Alfven velocity is independent of velocity of propagation of sound in the mixture while the slow and fast wave velocities depend upon sonic velocity.

(iii) In the absence of magnetic field, the velocity of fast wave reduces to te velocity of propagation of weak discontinuity while the remaining two velocities vanish.

(iv) In the absence of magnetic field the direction of the fast wave coincides with the direction of propagation of wave.

References

1. Carrier, G.F. (1958) *J. Fluid Mech.* **4** : 376.
2. Campbell, I.J. & Pitcher, A.S. (1958) *Proc. Roy Soc.* A **243** : 534.
3. Miura, H. (1972) *J. Phys. Soc. Japan* **33** : 1688
4. Moore, D.W. (1959) *J. Fluid Mech.* **6** : 113.
5. Rudinger, G. (1964) *Phys. Fluids* **7** : 658.
6. Wizngaarden, L.V. (1968) *J. Fluid Mech.* **33** : 465.
7. Upadhyaya, K.S. & Singh, P. (1985) *Nat. Acad. Sci. Letters* **8** : 43.
8. Wallis, G.B. (1961) *A.S.M.E.* **2** : 330.
9. Crespo, A. (1969) *Phys. Fluids* **12** : 2274.
10. Witte, J.H. (1969) *J. Fluid Mech.* **36** : 639.
11. Webb, D.R. (1970) *Ph.D. Thesis*, Cambridge University, Cambridge.
12. Pant, J.C. & Mishra, R.S. (1963) *Rend. Circt. Mat. Polermo.* **12** : 59.
13. Thomas, T.Y. (1957) *J. Math. Mech.* **6** : 311.

PROC. NAT. ACAD. SCI. INDIA, 61 (A), II, 1991

Temperature distribution in laminar flow through a uniform circular pipe

(Key words : fluid mechanics/laminar flow/energy equation)

J. P. MANI and S. PRASAD

Mechanical Engineering Department, M.M.M. Engineering College, Gorakhpur-273 010, India.

**Kamla Nehru Institute of Technology, Sultanpur-228 118, India.*

Received August 28, 1989; Accepted July 14, 1990.

Abstract

The effect of suction on the temperature distribution and heat transfer in a uniform circular pipe taking small outward normal suction has been studied using perturbation method. The solution of energy equation in cylindrical polar coordinates has been obtained under suitable condition. It is shown that in the region of no-back flow, the maximum of temperature exists on the axis of the pipe, while in the region of back flow the surface of maximum temperature is near the wall due to suction.

Introduction

The solution for the temperature distribution of a fluid flowing in a circular pipe has been given by Goldstein[1]. The heat transfer of a fluid flowing between two parallel plates of which one is at rest, the other moving with constant velocity in its own plane is well known[2].

Yuan and Finkelstein[3] have discussed the problem of laminar flow through a pipe of porous wall with injection and suction under the assumption that the maximum velocity of the Hagen-Poiseuille flow exists at the centre of the mouth of the pipe. But it is found that the pressure gradient along the axis, at mouth of pipe, is not the same as the pressure gradient of the Hagen-Poiseuille flow. Verma and Bansal[4] have found the exact solution of the Navier-Stokes equations for the flow of a liquid between two parallel plates, one in uniform motion and the other at rest with uniform suction at the stationary plate.

Bansal[5] has considered the steady flow of a viscous incompressible fluid through a circular pipe with small outward normal suction under the assumption that the flow is due to pressure gradient of the Hagen-Poiseuille flow at the mouth and that the suction at the wall is uniform and small. Moreover, he has used a perturbation method to determine the motion instead of assuming the form of stream function as done by Yuan and Finkelstein. He has also assumed that the radial velocity which vanishes in the Poiseuille flow has a finite magnitude except at the axis of the pipe where it vanishes.

Verma and Bansal[6] have further discussed the effect of suction on the temperature distribution of the problem of Bansal[5] in a porous circular pipe with small suction at the porous wall. They have determined the solution of energy equation in cylindrical polar coordinates with the following assumptions : (i) The wall temperature is constant, (ii) The suction parameter is small, (iii) No diffusion takes place and (iv) Fluid is incompressible and heat conduction is negligible.

In the present paper the effect of suction on the temperature distribution and heat transfer in a uniform circular pipe with small outward normal suction has been considered with the same assumptions as made by Verma and Bansal by perturbation method. It has been found that in the region of no-back flow, the maximum of temperature exists on the axis of the pipe, while in the region of back flow the surface of maximum temperature is near the wall due to suction.

Formulation of the Problem

Let us consider the steady laminar flow of a viscous incompressible fluid through a porous pipe of uniform circular cross-section with small suction at the porous wall. The temperature of the wall of the pipe is maintained constant.

In cylindrical polar coordinates (x,r,θ), the equations of conservation of mass, momentum and energies are

$$\frac{\partial u}{\partial x}+\frac{1}{r}\frac{\partial}{\partial r}(v,r)=0 \tag{1}$$

$$u\frac{\partial u}{\partial x}+v\frac{\partial u}{\partial r}=-\frac{1}{\rho}\frac{\partial p}{\partial x}+\upsilon\left(\frac{\partial^2 u}{\partial r^2}+\frac{1}{r}\frac{\partial u}{\partial r}+\frac{\partial^2 u}{\partial x^2}\right) \tag{2}$$

$$u\frac{\partial v}{\partial x}+v\frac{\partial v}{\partial r}=-\frac{1}{\rho}\frac{\partial p}{\partial x}+\upsilon\left(\frac{\partial^2 v}{\partial r^2}+\frac{1}{r}\frac{\partial v}{\partial r}+\frac{\partial^2 v}{\partial x^2}-\frac{v}{r^2}\right) \tag{3}$$

and

$$\rho C_p\left(u\frac{\partial T}{\partial x}+v\frac{\partial T}{\partial r}\right)=K\left(\frac{\partial^2 T}{\partial r^2}+\frac{1}{r}\frac{\partial T}{\partial r}+\frac{\partial^2 T}{\partial x^2}\right)+\mu\varphi \tag{4}$$

where

$$\varphi=2\left[\left(\frac{\partial u}{\partial x}\right)^2+\left(\frac{\partial v}{\partial r}\right)^2+\left(\frac{v}{r}\right)^2\right]+\left(\frac{\partial v}{\partial x}+\frac{\partial u}{\partial r}\right)^2 \tag{5}$$

x is taken as the axis of the pipe, r is the radial direction, θ is the azimuthal angle and all the quantities are independent of θ.

The boundary conditions are :

$$r=R: v=v_0,\ u=0,\ T=T_0,\ \frac{\partial v}{\partial x}=0 \tag{6}$$

$$r=0: v=\text{finite},\ u=\text{finite},\ \frac{\partial T}{\partial r}=0$$

Since there is uniform suction, $\partial v/\partial x = 0$ i.e. v is independent of x and, therefore, it is a function of r only. Now, it is evident from eqn. (1) that $\partial^2 u/\partial x^2 = 0$.

Thus eqn. (1) to (5) become

$$\frac{\partial u}{\partial x} + \frac{\partial v}{\partial r} + \frac{v}{r} = 0 \tag{7}$$

$$u\frac{\partial u}{\partial x} + v\frac{\partial u}{\partial r} = -\frac{1}{\rho}\frac{\partial p}{\partial x} + \upsilon\left(\frac{\partial^2 u}{\partial r^2} + \frac{1}{r}\frac{\partial u}{\partial r}\right) \tag{8}$$

$$v\frac{\partial v}{\partial r} = -\frac{1}{\rho}\frac{\partial p}{\partial r} + \upsilon\left(\frac{\partial^2 v}{\partial r^2} + \frac{1}{r}\frac{\partial v}{\partial r} - \frac{v}{r^2}\right) \tag{9}$$

and

$$\rho C_p\left(u\frac{\partial T}{\partial x} + v\frac{\partial T}{\partial r}\right) = K\left(\frac{\partial^2 T}{\partial r^2} + \frac{1}{r}\frac{\partial T}{\partial r} + \frac{\partial^2 T}{\partial x^2}\right) + \mu\left[2\left\{\left(\frac{\partial u}{\partial x}\right)^2 + \left(\frac{\partial v}{\partial r}\right)^2 + \left(\frac{v}{r}\right)^2\right\} + \left(\frac{\partial u}{\partial r}\right)^2\right] \tag{10}$$

Let us introduce the non-dimensional quantities as follows

$$\bar{u} = \frac{u}{U_m},\quad \bar{V} = \frac{v}{v_0},\quad \eta = \frac{r}{R},\quad \bar{x} = \frac{x}{R},\quad \bar{p} = \frac{p}{\rho U_m^2}$$

$$\bar{\theta} = \frac{T - T_0}{T_1 - T_0},\ R_e = \frac{U_m R}{\upsilon}\ \text{(Reynold number)},\ P_r = \frac{\mu C_p}{K}\ \text{(Prandtl number)}, \tag{11}$$

$$\sigma = \frac{v_0 R}{\upsilon}\ \text{(suction parameter)}$$

where U_m is the maximum velocity of the Hagen-Poiseuille flow and T_1 is the finite temperature at the axis when there is no suction such that

$$T_1 = T_0 + \frac{\mu U_m^2}{4K} \tag{12}$$

Hence eqn. (7) to (10) in non-dimensional form are

$$\frac{\partial \bar{u}}{\partial \bar{x}} + \frac{\sigma}{R_e}\left(\frac{\partial \bar{v}}{\partial \eta} + \frac{\bar{v}}{\eta}\right) = 0 \tag{13}$$

$$\bar{u}\frac{\partial \bar{u}}{\partial \bar{x}} + \frac{\sigma}{R_e}\bar{v}\frac{\partial \bar{u}}{\partial \eta} = -\frac{\partial \bar{p}}{\partial \bar{x}} + \frac{1}{R_e}\left(\frac{\partial^2 \bar{u}}{\partial \eta^2} + \frac{1}{\eta}\frac{\partial \bar{u}}{\partial \eta}\right) \tag{14}$$

$$\bar{v}\frac{\partial \bar{v}}{\partial \eta} = -\frac{R_e^2}{\sigma^2}\frac{\partial \bar{p}}{\partial \eta} + \frac{1}{\sigma}\left(\frac{\partial^2 \bar{v}}{\partial \eta^2} + \frac{1}{\eta}\frac{\partial \bar{v}}{\partial \eta} - \frac{\bar{v}}{\eta}\right) \tag{15}$$

$$R_e P_r\left(\bar{u}\frac{\partial \bar{\theta}}{\partial x} + \frac{\sigma}{R_e}\bar{v}\frac{\partial \bar{\theta}}{\partial \eta}\right) = \frac{\partial^2 \bar{\theta}}{\partial \eta^2} + \frac{1}{\eta}\frac{\partial \bar{\theta}}{\partial \eta} + \frac{\partial^2 \bar{\theta}}{\partial \bar{x}^2}$$
$$+4\left[2\left\{\left(\frac{\partial \bar{u}}{\partial \bar{x}}\right)^2 + \frac{\sigma^2}{R_e^2}\left(\frac{\partial \bar{v}}{\partial \eta}\right)^2 + \frac{\sigma^2}{R_e^2}\left(\frac{\bar{v}}{\eta}\right)^2\right\} + \left(\frac{\partial \bar{u}}{\partial \eta}\right)^2\right] \tag{16}$$

The boundary conditions (6) with the help of eqn. (11) are

$$\eta = 1 : \bar{v} = 1, \quad \bar{u} = 0, \quad \bar{\theta} = 0, \quad \frac{\partial \bar{v}}{\partial \eta} = 0$$
$$\eta = 0 : \bar{v} = \text{finite}, \quad \bar{u} = \text{finite}, \quad \frac{\partial \bar{\theta}}{\partial \eta} = 0 \tag{17}$$

Let

$$\begin{aligned} \bar{p}(\bar{x}, \eta) &= p_0 + p'(\bar{x}, \eta) \\ \bar{u}(\bar{x}, \eta) &= u_0 + u'(\bar{x}, \eta) \\ \bar{v}(\eta) &= v'(\eta) \end{aligned} \tag{18}$$

and $\bar{\theta}(\bar{x}, \eta) = \theta_0 + \theta'(\bar{x}, \eta)$

where the primed quantities are the perturbations caused by the suction and p_0, u_0, θ_0 are the known quantities for flow when there is no suction (i.e. Hagen - Poiseuille flow in a circular pipe), satisfying the equations

$$\frac{\partial p_0}{\partial \eta} = 0, \quad \frac{\partial u_0}{\partial \bar{x}} = 0, \quad \frac{\partial p_0}{\partial \bar{x}} = a_0 = \frac{1}{R_e}\left(\frac{\partial^2 u_0}{\partial \eta^2} + \frac{1}{\eta}\frac{\partial u_0}{\partial \eta}\right)$$

and $$\frac{\partial^2 \theta_0}{\partial \eta^2} + \frac{1}{\eta}\frac{\partial \theta_0}{\partial \eta} + 4\left(\frac{\partial u_0}{\partial \eta}\right)^2 = 0 \tag{19}$$

Here we have p_0 independent of η

$$u_0 = A\left(\eta^2 - 1\right) \quad \text{where } A = \frac{R_e}{4}\frac{\partial p_0}{\partial \bar{x}} = \frac{R_e}{4} a_0 \text{ and } \theta_0 = B\left(1 - \eta^4\right) \tag{20}$$

Substituting eqn. (18) in eqn. (13) to (16) and after simplification with the help of eqn. (20), we get

$$\frac{\partial u'}{\partial \bar{x}} + \frac{\sigma}{R_e}\left(\frac{\partial v'}{\partial \eta} + \frac{v'}{\eta}\right) = 0 \tag{21}$$

$$\left(u_0 + u'\right)\left(\frac{\partial u'}{\partial \bar{x}}\right) + \frac{\sigma}{R_e} v'\left(\frac{\partial u_0}{\partial \eta} + \frac{\partial u'}{\partial \eta}\right) = -\frac{\partial p'}{\partial \bar{x}} + \frac{1}{R_e}\left(\frac{\partial^2 u'}{\partial \eta^2} + \frac{1}{\eta}\frac{\partial u'}{\partial \eta}\right) \tag{22}$$

$$v'\frac{\partial v'}{\partial \eta} = -\frac{R_e^2}{\sigma^2}\frac{\partial p'}{\partial \eta} + \frac{1}{\sigma}\left(\frac{\partial^2 v'}{\partial \eta^2} + \frac{1}{\eta}\frac{\partial v'}{\partial \eta} - \frac{v'}{\eta^2}\right) \tag{23}$$

and

$$\begin{aligned} R_e P_r\left[\left(u_0 + u'\right)\frac{\partial \theta'}{\partial \bar{x}} + \frac{\sigma}{R_e} v'\left(\frac{\partial \theta_0}{\partial \eta} + \frac{\partial \theta'}{\partial \eta}\right)\right] &= \frac{\partial^2 \theta'}{\partial \eta^2} + \frac{1}{\eta}\frac{\partial \theta'}{\partial \eta} + \frac{\partial^2 \theta'}{\partial \bar{x}^2} \\ &+ 4\left[2\left\{\left(\frac{\partial u'}{\partial \bar{x}}\right)^2 + \frac{\sigma^2}{R_e^2}\left(\frac{\partial v'}{\partial \eta}\right)^2 + \frac{\sigma^2}{R_e^2}\left(\frac{v'}{\eta}\right)^2\right\} + \left(\frac{\partial u'}{\partial \eta}\right)^2 + 2\frac{\partial u_0}{\partial \eta}\frac{\partial u'}{\partial \eta}\right] \\ &+ \left[B\left(-12\eta^2\right) + \frac{1}{\eta}B\left(-4\eta^3\right) + 4\left(-A.2\eta\right)^2\right] \end{aligned} \tag{24}$$

From the last eqn. of (19) and (20) $B = A^2$.

The boundary conditions (17) with the help of eqn. (18) are

$$\begin{aligned} &\eta = 1, \quad v' = 1, \quad u' = 0, \frac{\partial v'}{\partial \eta} = 0, \quad \theta' = 0 \\ &\eta = 0, \quad v' = \text{finite}, \quad u' = \text{finite}, \quad \frac{\partial \theta'}{\partial \eta} = 0 \end{aligned} \tag{25}$$

The solution of eqn. (21-23) with the help of the boundary conditions (25) is

$$u' = -\frac{\sigma}{R_e}\bar{x}\left[f'(\eta) + \frac{1}{\eta} f(\eta)\right] + F(\eta), \; v' = f(\eta) \tag{26}$$

where

$$f(\eta)=\left[\frac{3}{2}\eta-\frac{1}{2}\eta^3\right]+\sigma\left[\frac{7}{144}\eta-\frac{5}{48}\eta^3+\frac{1}{16}\eta^5-\frac{1}{144}\eta^7\right]$$
$$+\sigma^2\left[\frac{103}{9600}\eta-\frac{101}{4320}\eta^3+\frac{13}{864}\eta^5-\frac{5}{1728}\eta^7+\frac{1}{1920}\eta^9-\frac{1}{43200}\eta^{11}\right] \tag{27}$$

and

$$F(\eta)=\sigma\frac{\bar{x}}{R_e}+\sigma A\left[\frac{1}{36}\eta^6-\frac{1}{8}\eta^4+\frac{3}{4}\eta^2-\frac{47}{72}\right]+\sigma^2\frac{\bar{x}}{R_e}\left(\frac{5}{8}-\frac{3}{4}\eta^2+\frac{1}{8}\eta^4\right)$$
$$+\sigma^2\left(\frac{1}{256}\eta^8-\frac{1}{24}\eta^6+\frac{9}{64}\eta^4-\frac{79}{786}\right)+\sigma^2A\left(-\frac{28337}{86400}+\frac{37}{72}\eta^2-\frac{143}{576}\eta^4\right.$$
$$\left.+\frac{59}{864}\eta^6-\frac{7}{1152}\eta^8+\frac{1}{7200}\eta^{10}\right) \tag{28}$$

$$f_0=\frac{3}{2}\eta-\frac{1}{2}\eta^3,\ f_i=\left(\frac{7}{144}\eta-\frac{5}{48}\eta^3+\frac{1}{16}\eta^5-\frac{1}{144}\eta^7\right)$$

and so on

$$F_0=0,\ F_1=\frac{\bar{x}}{R_e}+A\left(\frac{1}{36}\eta^6-\frac{1}{8}\eta^4+\frac{3}{4}\eta^2-\frac{47}{72}\right)$$

and so on.

Now, after substituting the values of u_0, v_0, u' and v' from eqn. (20), (26), (27) and (28), the eqn. (24) becomes

$$R_eP_r\left[\frac{1}{4}R_ea_0(\eta^2-1)-\frac{\sigma}{R_e}\bar{x}f'-\frac{\sigma}{R_e}\bar{x}\frac{1}{\eta}f+F\right]\frac{\partial\theta'}{\partial\bar{x}}+\sigma P_r\left[\left(-B.4\eta^3\right)+\left(\frac{\partial\theta'}{\partial\eta}\right)\right]f$$
$$=\frac{\partial^2\theta'}{\partial\eta^2}+\frac{1}{\eta}\frac{\partial\theta'}{\partial\eta}+\frac{\partial^2\theta}{\partial\bar{x}^2}+4\left[\frac{4\sigma^2}{R_e^2}\left(f'^2+\frac{1}{\eta^2}f^2+\frac{1}{\eta}ff'\right)\right.$$
$$\left.+\left\{\frac{\sigma\bar{x}}{R_e}\left(\frac{f}{\eta^2}-\frac{f'}{\eta}-\frac{f''}{1}\right)+F'\right\}^2+R_ea_0\eta\left\{\frac{\sigma\bar{x}}{R_e}\left(\frac{f}{\eta^2}-\frac{f'}{\eta}-\frac{f''}{1}\right)+F'\right\}\right] \tag{29}$$

Solution of Equation 29

$$\text{Let } \theta'=\varphi(\eta)+\bar{x}\,\psi(\eta)+\bar{x}^2\xi(\eta) \tag{30}$$

where $\varphi(\eta)$, $\psi(\eta)$ and $\xi(\eta)$ are unknown functions of η to be determined.

By substituting eqn. (30) into eqn. (29) and equating the coefficient of like powers of x,

we get the following set of equations

$$\xi''+\frac{1}{\eta}\xi'+\frac{4\sigma^2}{R_e^2}\left(\frac{f}{\eta^2}-\frac{f'}{\eta}-\frac{f''}{1}\right)^2+2\sigma P_r f'\xi+\frac{2\sigma}{\eta}P_r f\,\xi-\sigma P_r\xi' f=0 \tag{31}$$

$$\psi''+\frac{\psi'}{\eta}+4\left[\frac{2\sigma}{R_e}\left(\frac{f}{\eta^2}-\frac{f'}{\eta}-\frac{f''}{1}\right)F'+a_0\eta\sigma\left(\frac{f}{\eta^2}-\frac{f'}{\eta}-\frac{f''}{1}\right)\right]$$

$$-\sigma P_r f\psi'+\sigma P_r f'\psi+\frac{\sigma P_r}{\eta}f\,\psi-2R_e P_r\left[\frac{1}{4}R_e a_0\left(\eta^2-1\right)+F\right]\xi=0 \tag{32}$$

$$\varphi''+\frac{1}{\eta}\varphi+\frac{16\sigma^2}{R_e^2}\left(\frac{f'^2}{1}+\frac{f^2}{\eta^2}-\frac{f\,f'}{\eta}\right)+4F'^2+4R_e a_0\eta F'$$

$$B_4\sigma P_r\eta^3 f-\sigma P_r f\varphi'-R_e P_r\left[\left\{\frac{1}{4}R_e a_0\left(\eta^2-1\right)+F\right\}\psi\right]+2\xi=0 \tag{33}$$

The boundary conditions (25) with the help of eqn. (30) become

$$\eta=1:\xi(\eta)=0;\quad \psi(\eta)=0;\quad \varphi(\eta)=0$$

$$\eta=0:\frac{\partial\xi}{\partial\eta}=0;\ \frac{\partial\psi}{\partial\eta}=0;\ \frac{\partial\varphi}{\partial\eta}=0 \tag{34}$$

Now, the solution of eqn. (31) can be expressed for small values σ of by a power series developed near $\sigma=0$ as follows

$$\xi=\xi_0+\sigma\,\xi_1+\sigma^2\xi_2+\ldots\sigma^n\xi_n \tag{35}$$

where ξ_n's are taken to be independent of σ.

By substituting eqn. (35) in eqn. (31) and equating like powers of σ, we get the following set of equations

$$\xi_0''+\frac{1}{\eta}\xi_0'=0 \tag{36}$$

$$\xi_1''+\frac{1}{\eta}\xi_1'-\frac{P_r}{1}f_0\,\xi_0'+2P_r\left(f_0'+\frac{f_0}{\eta}\right)\xi_0=0 \tag{37}$$

$$\xi_2''+\frac{1}{\eta}\xi_2'+2P_r f_0'\xi_1+2P_r f_1'\xi_0+\frac{2P_r}{\eta}f_0\,\xi_1+\frac{2P_r}{\eta}f_1\,\xi_0-P_r f_0\,\xi_1'-P_r f_1\,\xi_0'$$

$$+\frac{4}{R_e^2}\left(\frac{f}{\eta^2}-\frac{f'}{\eta}-\frac{f''}{1}\right)^2=0 \tag{38}$$

The boundary conditions to be satisfied by the ξ_n's are

$$\xi_n(0) = 0,\ \xi_n(1) = 0 \text{ for all } n \tag{39}$$

Now from eqn. (36) to (38), we get

$$\xi_0 = 0,\ \xi_1 = 0 \text{ and } \xi_2 = \frac{4}{R_e^2}\left(1-\eta^4\right)$$

Hence the second order perturbation solution in σ of (31) is

$$\xi(\eta) = \frac{4\sigma^2}{R_e^2}\left(1-\eta^4\right) \tag{40}$$

Now the solution of eqn. (32) can be expressed for small values of σ by a power series developed near $\sigma = 0$ as follows

$$\psi = \psi_0 + \sigma\psi_1 + \sigma^2\psi_2 + \ldots \sigma^n\psi_n$$

where ψ_n's are taken to be independent of σ.

Substituting this power series in eqn. (32) and equating the coefficients of like powers of σ, we get the following set of equations

$$\psi_0'' + \frac{1}{\eta}\psi_0' = 0 \tag{41}$$

$$\psi_1'' + \frac{1}{\eta}\psi_1' + 4\left[\left(\frac{f_0}{\eta^2} - \frac{f_0'}{\eta} - \frac{f_0''}{1}\right)a_0\eta\right] = 0 \tag{42}$$

and

$$\psi_2'' + \frac{1}{\eta}\psi_2'' - P_r f_0\psi_1' + P_r f_0'\psi_1 + \frac{P_r}{\eta}f_0\psi_1 - 2R_eP_r\left[\frac{1}{4}R_e a_0\left(\eta^2-1\right)\right]\left[\frac{4}{R_e^2}\left(1-\eta^2\right)\right]$$
$$+4a_0\eta\left(\frac{f_1}{\eta^2} - \frac{f_1'}{\eta} - \frac{f_1''}{1}\right) + \frac{8}{R_e}\left(\frac{f_0}{\eta^2} - \frac{f_0'}{\eta} - \frac{f_0''}{1}\right)F_1' = 0 \tag{43}$$

Proceeding exactly as before, the second order perturbation solution in σ of (32) is

$$\psi(\eta) = a_0\sigma\left(1-\eta^4\right) + \frac{\sigma^2}{576}\left[\frac{16A}{R_e}\left(95 - 108\eta^4 + 16\eta^6 - 3\eta^8\right)\right.$$
$$\left.+12a_0\left(3 - 10\eta^4 + 8\eta^6 - \eta^8\right) + a_0P_r\left\{307 - 288\eta^2 + 36\eta^4 - 64\eta^6 + 9\eta^8\right\}\right] \tag{44}$$

Similarly we proceed to find out the solution of eqn. (33) by substituting the power series in φ, as usual, we obtain the second order perturbation solution in σ as

$$\varphi(\eta) = \varphi_0 + \sigma\varphi_1 + \sigma^2\varphi_2 \tag{45}$$

where

$$\varphi_0 = 0, \varphi_1 = \frac{R_e a_0 A}{288}\left(95 - 108\eta^4 + 16\eta^6 - 3\eta^8\right) + \frac{B.P_r}{96}\left(13 - 16\eta^6 + 3\eta^8\right)$$
$$+ \frac{R_e^2 a_0^2 P_r}{2304}\left(101 - 144\eta^2 + 36\eta^4 + 16\eta^6 - 9\eta^8\right)$$

and

$$\varphi_2 = \frac{1}{9R_e^2}\left(77 - 99\eta^2 + 27\eta^4 - 5\eta^6\right)$$
$$+ \frac{R_e^2 a_0^2}{720}\left(\frac{1}{1440}\right)\left(72449 - 103050\eta^4 + 39400\eta^6 - 9675\eta^8 + 936\eta^{10} - 60\eta^{12}\right)$$
$$- \frac{a_0\bar{x}}{72}\left(23 - 27\eta^4 + 4\eta^6\right) + \frac{R_e a_0}{1600}\left(77 - 100\eta^6 + 25\eta^8 - 2\eta^{10}\right)$$
$$+ \frac{BP_r}{36}\left(\frac{1}{129600}\right)\left(5589 - 25200\eta^6 + 30375\eta^8 - 11664\eta^{10} + 900\eta^{12}\right)$$
$$+ \frac{P_r R_e^2 a_0^2}{576}\left(\frac{1}{7200}\right)\left(293091 - 356400\eta^2 + 95400\eta^4 - 2200\eta^6\right.$$
$$\left. - 11475\eta^8 + 1584\eta^{10} - 200\eta^{12}\right)$$
$$- \frac{P_r a_0}{36}\left(8 - 9\eta^2 + \eta^6\right) + \frac{B.P_r^2}{28800}\left(148 - 375\eta^8 + 252\eta^{10} - 25\eta^{12}\right)$$
$$+ \frac{P_r^2 R_e^2 a_0^2}{2304}\left(\frac{1}{1600}\right)\left[103764 - 122800\eta^2 + 16300\eta^4 + 1600\eta^6\right.$$
$$\left. + 4300\eta^8 - 3664\eta^{10} + 500\eta^{12}\right]$$

The temperature distribution obtained with the help of eqn. (18), (20) and (30) is

$$\bar{\theta} = \left(1 - \eta^4\right) + \varphi(\eta) + \bar{x}\psi(\eta) + \bar{x}^2\xi(\eta) \tag{46}$$

where $\xi(\eta)$, $\psi(\eta)$ and $\varphi(\eta)$ are given by the eqn. (40), (44) and (45) respectively.

Now by keeping $A = -1$, we have $B = 1$ and $R_e a_0 = -4$. Further by putting $R_e = 1000$,

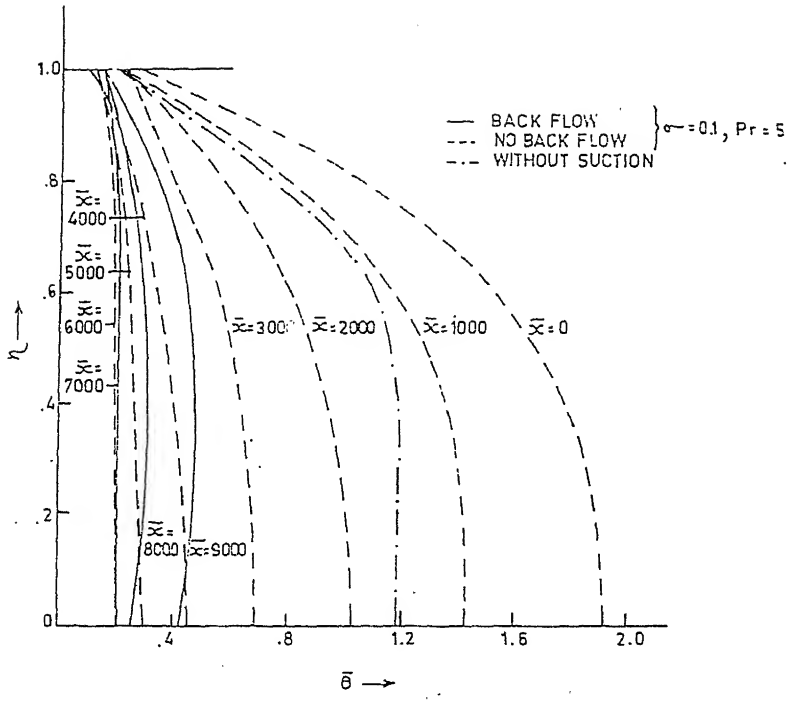

Fig. 1- Temperature distribution in pipe flow without suction.

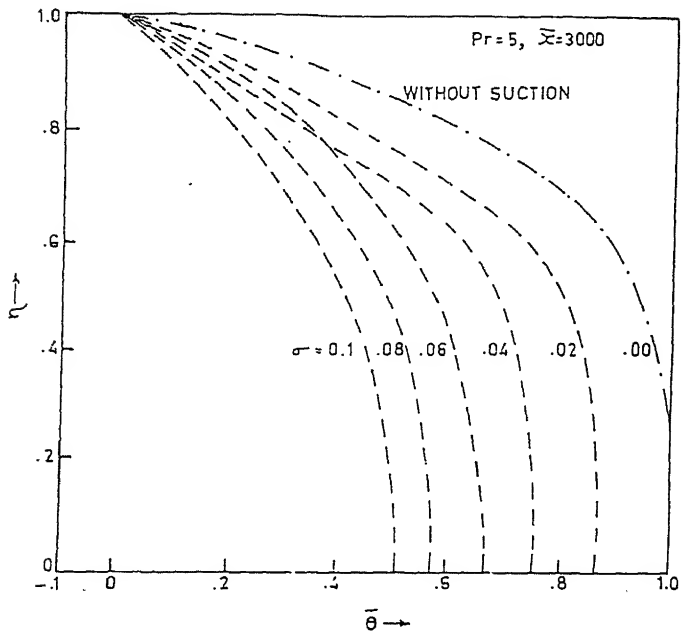

Fig. 2 - Temperature profiles $\bar{\theta} - \eta$.

$P_r = 5$ and $\sigma = 0.1$ in eqn. (46), we get after simplification

$$\bar{\theta} = 1.727 - 0.702\eta^2 - 1.0049\eta^4 + \frac{\bar{x}}{1000}\left(-0.523 + 0.10\eta^2 + 0.4108\eta^4\right) + \frac{\bar{x}^2}{(1000)^2}\left(0.04 - 0.04\eta^4\right) \tag{47}$$

The temperature profiles $\left(\bar{\theta}\ vs.\ \eta\right)$ are shown in Fig. 1 for various values of $\bar{x}$.

Similarly by putting $B = 1, P_r = 5, R_e = 1000$ and $\bar{x} = 3000$ in eqn. (46), we get

$$\bar{\theta} = 1 - \eta^4 + \sigma\left(-6.52 - 5\eta^2 + 11.75\eta^4\right) + \sigma^2\left(17.115 + 9.81\eta^2 - 30.74\eta^4\right) \tag{48}$$

The temperature profiles $\left(\bar{\theta}\ vs.\ \eta\right)$ are shown in Fig. 2 for various values of σ.

Discussion

The temperature profiles in Fig. 1 are divided into two parts : (a) The region of back flow and, (b) The region of no-back flow.

It is observed that the maximum of the temperature distribution exists on the axis of the pipe in the region of no-back flow, whereas the surface of the maximum temperature distribution is near the wall in the region of back flow.

The temperature on the axis of the pipe decreases and remains always positive in the region of no-back flow, whereas there is a continuous rise in temperature after $\bar{x} = 7000$ in the region of back flow.

The effect of the variation of suction parameter σ is shown in Fig. 2. It is seen that the temperature decreases with suction parameter σ in the region of no-back flow. The temperature profile without suction is also drawn for comparison.

Proceeding to the limit $\sigma = 0$, we have $\bar{\theta} = 1 - \eta^4$ as in the case of Hagen-Poiseuille flow.

References

1. Goldstein, S. (1965) *Modern Developments in Fluid Dynamics*, Dover Publication Inc., New York.
2. Schlichting, H. (1968) *Boundary Layer Theory*, Mc-Graw Hill Book Co., New York.
3. Yuan, S.W. & Finkelstein, A.B. (1956) *Trans. A.S.M.E.* 78 : 719.
4. Verma, P.D. & Bansal, J.L. (1966) *Proc. Ind. Acad. Sci.* 64 : 385.
5. Bansal, J.L. (1967) *Proc. Nat. Inst. Sci.* 32 : 368.
6. Verma, P.D. & Bansal, J.L. (1968) *Ind. J. Pure & Applied Physics* 9 : 506.

PROC. NAT. ACAD. SCI. INDIA, 61(A), II, 1991

Incompressible laminar viscous flow over a semi-infinite wavy wall

(Key words : viscous flow/wavy wall/vorticity equation/Reynolds number)

J. DEY and G. NATH*+

Department of Mechanical Engineering, Indian Institute of Science, Bangalore-560 0012, India.
**Department of Applied Mathematics, Indian Institute of Science, Bangalore-560 012, India.*
+ Author for correspondence.

Received March 4, 1990; Accepted July 14, 1990.

Abstract

Local similarity solution of the vorticity equation for flow over a sinusoidal wall for both low and large Reynolds numbers has been presented without using the perturbation method and the linearized boundary conditions.

Introduction

The flow problem over a wavy wall is important in connection with the study of the effect of inhomogeneities on boundary layer separation, aerodynamic heating and the surface distribution of the stresses created by the fluid flow. It is also useful in investigating the hydrodynamic instability of a protective layer of fluid injected as a coolent[1]. Inspite of its importance, it has attracted the attention of only a few research workers. Bejamin[2] was probably the first to consider this problem. His analysis is based on the assumption that the basic flow (defined in the absence of waviness) is parallel. Singh and Lumley[3] studied the effect of an isolated component of wall roughness on the average velocity distribution. Lessen and Gangwani[4] studied the flow stability under boundary-layer approximation. Other studies include the Rayleigh problem[5] and the free convection problem[6]. These studies[3,4,6] were aimed at seeking a perturbation solution about a basic flow which is either a function of y (co-ordinate transverse to the flow direction) only[2,3] or an average of the flow quantities over a wave length with similarity transformations incorporated[4] or fully developed flow[6] satisfying the linearized wall condition[3,4,6]. The boundary-layer approximation holds true for large Reynolds number (based on the axial distance and the free stream velocity). For low or moderately large Reynolds number describing the early flow region, the perturbation solution about a y-dependent basic flow will be inappropriate since it has been well established[7,8] that such basic flow also depends on the axial co-ordinate (x). As such, a perturbation solution will involve a basic flow which is function of x and y.

To the authors knowledge, no attempt has been made earlier to study a steady incompressible flow over a wavy wall for both low and moderately large Reynolds numbers. To study this problem, one is tempted to seek a perturbation solution about a known flat plate solution, which is a function of x^* and y^*, satisfying the linearized wall condition. These complicate the perturbation method, which is an approximate one. Also, the use of linearized wall condition provides information regarding flow at the mean position and as such Singh and Lumley[3] have suggested that the solution with linearized boundary condition is not valid

near the wall. In order to circumvent these difficulties, it would be appropriate to solve the Navier-Stokes equations satisfying the actual boundary conditions prevailing on the wavy surface. It appears that this is possible *via* some simple transformations, which permit one to obtain exact solution of the Navier-Stokes equations for both low and high Reynolds numbers. Such results have been presented in this paper.

Governing Equations

We consider a two-dimensional steady laminar incompressible flow over a wavy wall. Let u^* and v^* denote the two velocity components in the x^* and y^* directions, respectively (Fig. 1a). The wavy wall is defined by

$$y_w^* = \varepsilon^* \sin(2\pi x^*/\lambda) \tag{1}$$

where ε^* is the waviness amplitude and λ is the wave length. Following dimensionless quantities are introduced to obtain the non-dimensional vorticity equation

$$\begin{aligned} x &= x^*U/\upsilon \quad ; \quad y = y^*U/\upsilon \\ u &= u/U \quad ; \quad v = v/U \\ P &= p^*/U^2 \quad ; \quad \varepsilon = \varepsilon U/\upsilon \\ R_\lambda &= \lambda U/\upsilon \end{aligned} \tag{2}$$

where U denotes the uniform free stream velocity, ρ is the fluid density, υ is the kinematic viscosity and p^* is the dimensional static pressure. The non-dimensional form of the wall is $y_w = \varepsilon \sin(2\pi X/R_\lambda)$, where R_λ is the Reynolds number based on the wave length λ.

The governing non-dimensional vorticity equation is

$$u\beta_x + v\beta_y = \nabla_1^2 \beta \tag{3}$$

where suffixes x and y denote partial derivatives with respect to x and y, respectively. $\beta(=v_x - u_y)$ is the vorticity and $\nabla_1^2\left(= \partial^2/\partial x^2 + \partial^2/\partial y^2\right)$ is the two-dimensional Laplacian operator.

The boundary conditions are

$$\begin{aligned} u = v &= 0 \quad \text{at} \quad y = y_w \\ u &\to 1 \quad \text{as} \quad y \to \infty \end{aligned} \tag{4}$$

It has been assumed that the disturbance dies out as $y \to \infty$, which is of course obvious.

We define the non-orthogonal co-ordinates (X, Y), similar to those of Shankar and Sinha[5], such that

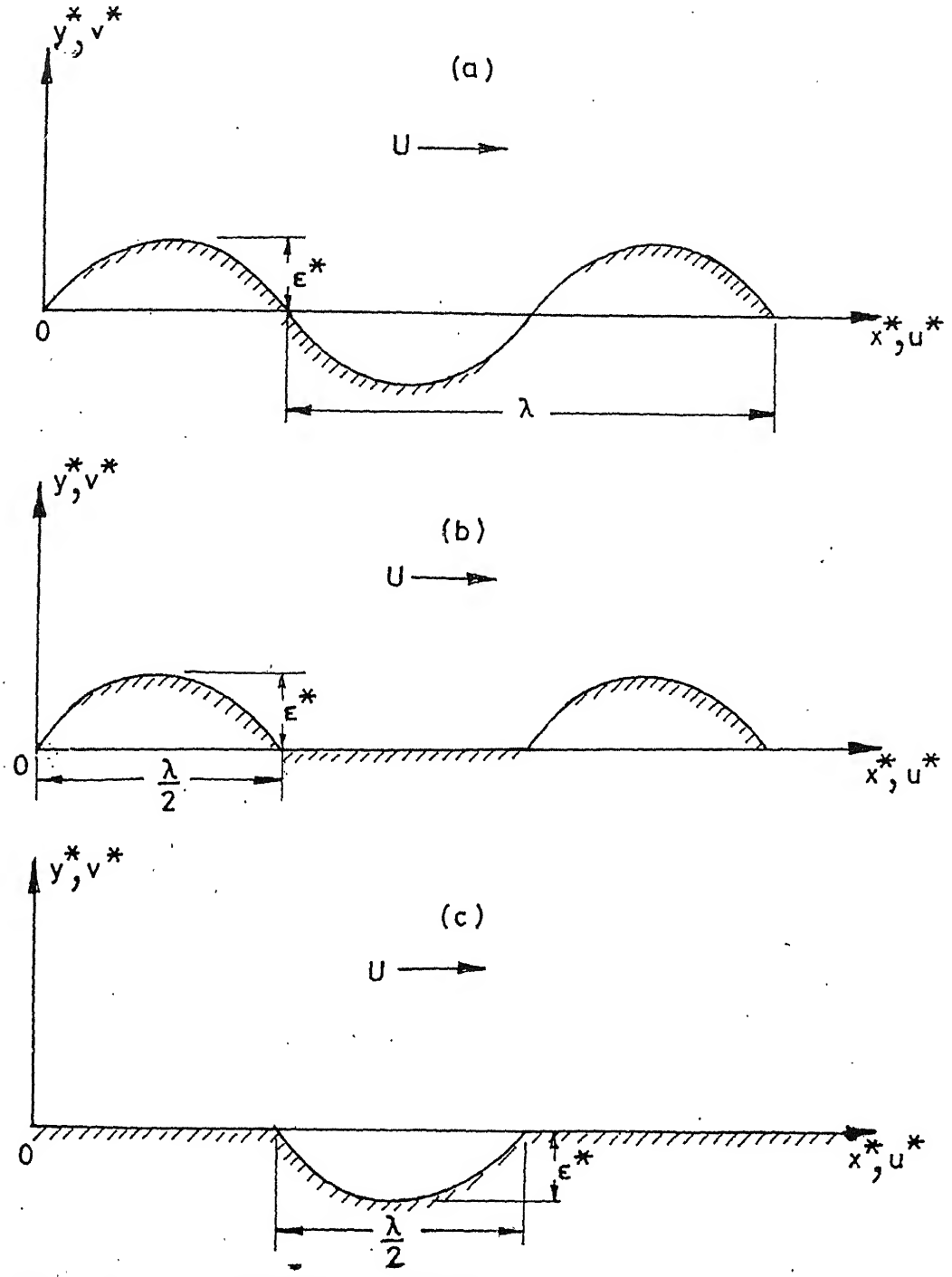

Fig. 1 – Flow configurations (a) Flow configuration considered, (b) and (c) other possible flow configurations.

$$X = x\ ;\ Y = y - \varepsilon \sin\left(2\pi x / R_\lambda\right) \tag{5}$$

which set the range of Y as $0 \le Y < \infty$, i.e., the flow geometry has been transferred to the positive Y plane. The vorticity eqn. (3) then becomes

$$\varphi_Y\left(\nabla^2\varphi\right)_X - \varphi_X\left(\nabla^2\varphi\right)_Y = \nabla^2\nabla^2\varphi \tag{6}$$

where φ is the non-dimensional stream function and ∇^2 is given by

$$\nabla^2 = \frac{\partial^2}{\partial X^2} + \left\{1 + \left(\varepsilon\ 2\pi / R_\lambda\right)^2 \cos^2\left(2\pi X / R_\lambda\right)\right\}\frac{\partial^2}{\partial Y^2}$$
$$-2\varepsilon\left(2\pi / R_\lambda\right)\cos\left(2\pi X / R_\lambda\right)\frac{\partial^2}{\partial Y\ \partial X}$$
$$+\varepsilon\left(2\pi / R_\lambda\right)^2 \sin\left(2\pi X / R_\lambda\right)\frac{\partial}{\partial Y} \tag{7}$$

The solution of (6) being intractable in the present form, we define the parabolic co-ordinates (σ, η) such that

$$X + i\left[Y + \varepsilon \sin\left(2\pi X / R_\lambda\right)\right] = (\sigma + i\eta)^2 / 2$$
$$\sigma = \pm\left\{X + \left[X^2 + \left(Y + \varepsilon \sin\left(2\pi X / R_\lambda\right)\right)^2\right]^{1/2}\right\}^{1/2}$$
$$\eta = \left\{-X + \left[X^2 + \left(Y + \varepsilon \sin\left(2\pi / R_\lambda\right)\right)^2\right]^{1/2}\right\}^{1/2} \tag{8}$$

since η is positive, the positive and negative values of σ correspond to the positive and negative Y–plane, respectively. In the parabolic co-ordinates the vorticity equation can be solved in either positive or negative half plane alone. Since the sinusoidal function encompasses both positive and negative y planes in (x, y) co-ordinates, one might think that the parabolic co-ordinates (σ, η) are not appropriate in such situation. But then it must be remembered that due to the transformations (5), the present problem has been transferred to the positive Y-plane ($0 \le Y < \infty$). As such, the problem of positive or negative y plane does not arise and the use of these co-ordinates are appropriate. The vorticity eqn. (6) in (σ, η) co-ordinates is

$$W_{\sigma\sigma} + W_{\eta\eta} + \varphi_\sigma W_\eta - \varphi_\eta W_\sigma = 0 \tag{9}$$

where $W = \left(\varphi_{\sigma\sigma} + \varphi_{\eta\eta}\right) / \left(\sigma^2 + \eta^2\right)$

It is interesting to note that the complicated vorticity eqn. (6) has been reduced to a very simple form (*via* a lengthy process involving differentiation and large algebra), similar to that of Davis[7] for flat plate. However, in the present case, the lower limit of η(by setting $Y = 0$) being

$$\eta_0 = \left\{-X + \left[X^2 + \left(\varepsilon \sin\left(2\pi X / R_\lambda\right)\right)^2\right]^{1/2}\right\}^{1/2} \tag{10}$$

is non-zero unlike that for flat plate where η_0=0. It may be noted that the present approach is a departure from the widely used approach of using a linearized wall[3,4,6].

The corresponding boundary conditions are

$$\begin{aligned} &\varphi = \varphi_\eta = 0 \qquad \text{at} \quad \eta = \eta_0 \\ &\varphi \to \sigma\eta; \ \varphi_\eta \to \sigma \quad \text{as} \quad \eta \to \infty \end{aligned} \tag{11}$$

These are dictated by the conditions that $u = v = 0$ at Y=0 and $u \to 1$ as $Y \to \infty$. The boundary conditions (11) dictate that the form of φ be

$$\varphi = \sigma f(\eta) \tag{12}$$

This is equivalent to say that φ has been expanded about σ_0 (by setting $Y = 0$ in (8)) on the surface, similar to that of Davis[7], and that only the first term of the series has been retained. The vorticity eqn. (9) for local similarity at any location becomes

$$f'''' + \left[f - \frac{4\eta}{\sigma_0^2 + \eta^2}\right] f''' + \frac{1}{\sigma_0^2 + \eta^2}\left[\left(\sigma_0^2 - \eta^2\right) f' - 2\eta f\right] f'' = 0 \tag{13}$$

where prime denotes differentiation with respect to η.

The corresponding boundary conditions are

$$\begin{aligned} &f = f' = 0 \ \text{ at } \ \eta = \eta_0 \\ &f \to \eta \ ; \ f' \to 1 \ \text{ as } \ \eta \to \infty \end{aligned} \tag{14}$$

It may be noted that the eqn. (13) is similar to that for flat plate[7,8] except that the lower limit of η is non-zero in the present case and that σ_0 is not equal to $(2X)^{1/2}$. For large σ_0, i.e, $X \to \infty$, representing the boundary-layer approximation, one can obtain the local similarity solutions. Unfortunately, the local similarity transformations for the boundary-layer equation are not known though the equation can be obtained from (13) for $\sigma_0 \to \infty$. It appears that a separate search for the local similarity transformations for boundary-layer equation needs to be made.

The numerical solution of the vorticity eqn. (13) under boundary conditions (14) can be obtained provided that η_0 and σ_0 are prescribed at each axial location on the wavy surface. In other words, the flow field can be obtained following the wall waviness.

Results and Discussion

Quasi-linearization and interation technique[9] were used to solve (13) for given η_0 and σ_0 and for $\varepsilon = 0.3$; $10 \leq X \leq 41$ and $R_\lambda = 1$. This range of X covers low to moderately large Reynolds numbers. The solution was built-up with one particular solution and two complementary solutions satisfying the two conditions at infinity. The forward integration was carried out using Hemming's predictor-corrector method on DEC 1090 computer. The integration step size was optimized to obtain accuracy up to 4 decimal places. A large number of computation is involved for unit wave length and unit change in X. This involves very large number of computations for a wide range of Reynolds numbers (X). As such, detailed computations were carried out for $40 \leq X \leq 41$. Though computations were carried out for $X = 10$ also, results are presented for $40 \leq X \leq 41$ for the sake of simplicity. From the flat plate results[7,8], we notice that the variation of shear stress for unit change of Reynolds number is very small. As such, in the intermediate range any noticeable variation will occur in third or fourth decimal place.

Representative axial velocity (u) profile has been shown in Fig. 2 for $X = 40.6$. This has been selected because $X = 40.6$ corresponds to negative value of $\varepsilon \sin(2\pi X)$. Comparison with the flat plate velocity profile is also shown in Fig. 2 (To show the velocity difference clearly, a part of the velocity profile has been shown. It is understood that the velocity profile attains the free-stream value as $\eta \to \infty$, not shown in Fig. 2). For other X, representing positive value of $\varepsilon \sin(2\pi X)$, similar trend is observed. It may be noticed that though η_0 values are different the axial velocity is less than the flat plate axial velocity. Reduction in the mean velocity due to waviness was also observed by Singh and Lumley[3], and Lessen and Gangwani[4]. In the present case, we find that the local velocity is also reduced due to waviness. For Stoke's flow through a pipe having sinusoidal corrugation, Phan-Thien[10] observed decrease in flow rate and increased pressure drop compared to non-corrugated pipe. The decrease in flow rate could be attributed to the decrease in velocity since the average areas are same in these two geometries. These suggest that the present analysis is appropriate and that the flow field can be defined for both low and high Reynolds numbers flow over a wavy wall.

The non-dimensional wall shear stress can be expressed as

$$\tau = \tau_w (X/2)^{1/2} = 2\upsilon\left(v^*_{x^*} + u^*_{y^*}\right)(X/2)^{1/2} / U^2$$
$$= 2f''(\eta_0)(X/2)^{1/2}\sigma_0\left(\sigma_0^2 - \eta_0^2\right) / \left(\sigma_0^2 + \eta_0^2\right)^2 \qquad (15)$$

where suffixes x^* and y^* denote partial derivatives with respect to x^* and y^*, respectively, and it is shown in Fig. 3. Factor $(X/2)^{1/2}$ has been introduced for comparison with flat plate geometry. As mentioned earlier, any significant change in the wall shear values occurs in third or fourth decimal place (to find the shear stress at any point, 0.5 needs to be added to the values given in Fig. 3). Fig. 3 shows that the shear stress attains maximum and then decreases to the flat plate value. This pattern is expected for the positive y-plane. In the negative y-plane i.e., for negative $\varepsilon \sin(2\pi X)$ ($40.5 < X < 41.0$) we do not expect negative shear stress, as this will mean a flow reversal. Also, physically we find that the fluid contact surface in this region ($\varepsilon \sin(2\pi X) < 0$) is more than the flat plate and hence a higher friction is expected. Hence, the positive higher wall shear in this region is justified.

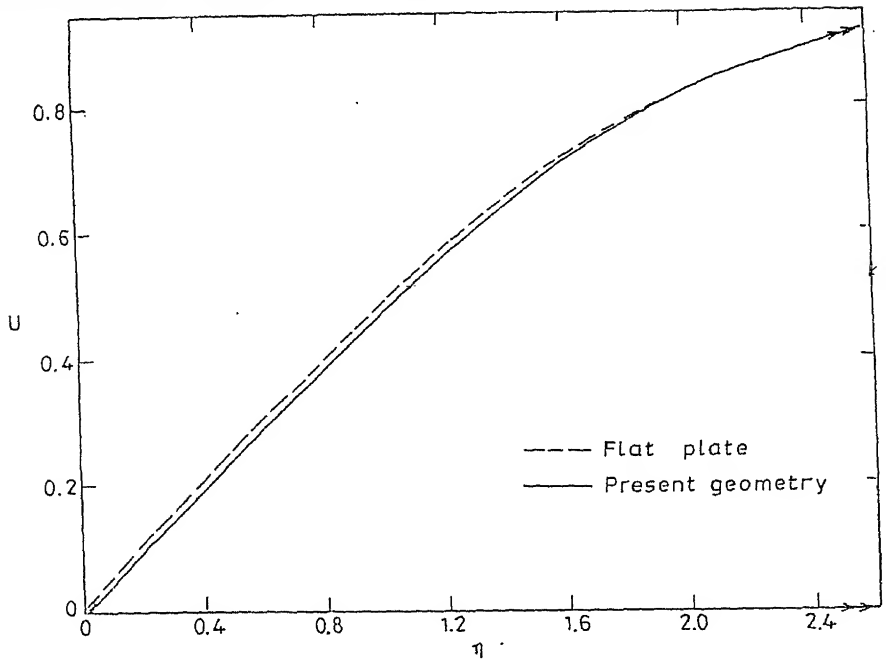

Fig. 2 – Non-dimensional axial velocity profiles.

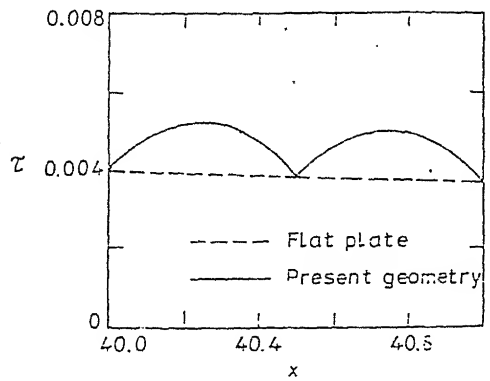

Fig. 3 – Non-dimensional wall shear stress variation with the axial distance.

From the above discussion, we find that the local similarity solution of the vorticity equation for wavy wall, under consideration, is possible and that such solution gives more accurate results than that of the perturbation method. Also, it is expected that the local similarity solution for flow over wavy walls (see Fig. 1b and 1c) in which the waviness is confined to half the wave length should be possible *via* transformations (5) and (8).

Conclusions

To sum up, we find that (i) the local similarity solution of the two-dimensional vorticity equation is possible for flow over a wavy wall and for a wide range of Reynolds numbers without using the perturbation method, (ii) the local axial velocity is less than that for flat plate, (iii) the wall shear is more than the flat plate geometry, (iv) the local similarity solution of the boundary-layer equation is also possible, but the similarity transformations have to be found out.

References

1. Demekhin, F. A. & Shkadov, V. Ya (1989) *Fluid Dynamics* **23** : 811.
2. Benjamin, T. B. (1959) *J. Fluid Mech.* **6** : 61.
3. Singh, K. & Lumley, J.L. (1971) *Appl. Sci. Res.* **24** : 168.
4. Lessen, M & Gangwani, S.T. (1976) *Phys. Fluids* **19** : 510.
5. Shankar, P.N. & Sinha, U.N. (1976) *J. Fluid Mech.* **77** : 243.
6. Vajravelu, K & Sastri, K.S. (1978) *J. Fluid Mech.* **86** : 365.
7. Davis, R.T. (1967) *J. Fluid Mech.* **27** : 691.
8. Afzal, N. & Banthiya, N.K. (1977) *Z.A.M.P.* **28** : 993.
9. Bellman, R.E. & Kalaba, R.E. (1965) *Quasi-linearization and Nonlinear Boundary Value Problem*, Elsevier Publishing Company, New York.
10. Phan-Thien, N. (1981) *Phys. Fluids* **24** : 579.

PROC. NAT. ACAD. SCI. INDIA, 61 (A), II, 1991

Bending vibrations of a beam including effects of rotatory inertia and shear force on Pasterank foundation

(Key words : rotatory inertia/shear force/Pasterank foundation)

JAYOTI KUMAR

Lal Bahadur Shastri Degree College, Sarsawati Nagar-171 205, Distt. Shimla, India.

Received February 18, 1989; Accepted August 14, 1990.

Abstract

The differential equation for bending vibration of a slender beam including the effects of rotatory inertia and shear force in a centrifugal force field on Pasternak foundation has been obtained. A method based on Galerkin's principle has been employed to find the upper bound of fundamental mode of vibration. The accuracy of this upper bound is investigated by comparing the results when the effect of Pasternak foundation is not taken in consideration.

Introduction

The analysis presented in this paper considers vibrations of a slender beam including the effects of rotatory inertia and shear force that could represent a turbine blade of simple geometry. The beam is attached to a disc of radius r_0 and disc rotates with angular velocity Ω. It is assumed that the shear centre of each cross-section coincides with the centre of gravity; consequently only transverse bending vibrations will occur.

For the analysis, it is assumed that S and I which are respectively the area of the cross-section of beam and moment of inertia of the cross-section about the axis perpendicular to the plane of bending are constant. This, however, is not an essential assumption. If S and I are functions of x, the amount of computing work is greater than when S and I are independent of x.

The Differential Equations

The differential equation[1] for transverse vibration of a beam including the effects of rotatory inertia and shear forces is

$$EI\frac{\partial^4 y}{\partial x^4}+\rho S\frac{\partial^2 y}{\partial t^2}-\rho\left(1+\frac{E}{K'G}\right)I\frac{\partial^4 y}{\partial x^2\partial t^2}+\frac{\rho^2 I}{K'G}\frac{\partial^4 y}{\partial t^4}=0 \tag{1}$$

where E is the Young's modulus of elasticity, ρ the density of material, G the modulus of rigidity for the material of bar and K' is the ratio of average shear stress to maximum shear stress over a cross-section.

The differential eqn. (1) on elastic foundation takes the form

$$EI\frac{\partial^4 y}{\partial x^4}+\rho S\frac{\partial^2 y}{\partial t^2}-\rho I\left(1+\frac{E}{K'G}\right)\frac{\partial^4 y}{\partial x^2\partial t^2}+\frac{\rho^2 I}{K'G}\frac{\partial^4 y}{\partial t^4}+q=0 \tag{2}$$

where q is foundation reaction.

The general form for a Pasternak foundation[2] in two dimensional case may be written as

$$q(x,t) = Ky - G_0 \frac{\partial^2 y}{\partial x^2} \tag{3}$$

where K is Winkler foundation modulus and G_0 is shear foundation modulus.

The eqn. (2) represents flexural vibrations of a beam including the effects of rotatory inertia and shear force on Pasternak foundation. This equation is modified by adding the lateral load, $\frac{\partial^2 M}{\partial x^2}$, if the centrifugal force effect is to be considered and then it becomes

$$EI\frac{\partial^4 y}{\partial x^4} + \rho S\frac{\partial^2 y}{\partial t^2} - \rho I\left(1+\frac{E}{K'G}\right)\frac{\partial^4 y}{\partial x^2 \partial t^2} + \frac{\rho^2 I}{K'G}\frac{\partial^4 y}{\partial t^4} + Ky - G_0\frac{\partial^2 y}{\partial x^2} - \frac{\partial^2 M}{\partial x^2} = 0 \tag{4}$$

where

$$\frac{\partial^2 M}{\partial x^2} = \rho S\Omega^2\left[\left\{r_0(l-x) + \frac{1}{2}\left(l^2 - x^2\right)\right\}\frac{\partial^2 y}{\partial x^2} - (r_0 + x)\frac{\partial y}{\partial x}\right] \tag{5}$$

Determination of Natural Frequencies

We now put eqn. (4) in terms of a dimensionless variable by introducing $\bar{\xi}=x/l$. It takes the form

$$\frac{\partial^4 y}{\partial \bar{\xi}^4} - \frac{r^2 l^2}{E/\rho}\frac{l^2}{I/S}\left[\left\{\frac{r_0}{l} + \frac{1}{2} - \left(\frac{r_0}{l}\bar{\xi} + \frac{1}{2}\bar{\xi}^2\right)\right\}\frac{\partial^2 y}{\partial \bar{\xi}^2} - \left(\frac{r_0}{l} + \bar{\xi}\right)\frac{\partial y}{\partial \bar{\xi}}\right]$$

$$-\frac{l^2}{E/\rho}\left(1+\frac{E}{K'G}\right)\frac{\partial^4 y}{\partial \bar{\xi}^2 \partial t^2} + \frac{l^2}{E/\rho}\cdot\frac{l^2}{I/S}\cdot\frac{\partial^2 y}{\partial t^2} + \left(\frac{l^2}{E/\rho}\right)^2\frac{E}{K'G}\frac{\partial^4 y}{\partial t^4} + \frac{Kl^4}{EI}y$$

$$-\frac{G_0}{EI}l^2\frac{\partial^2 y}{\partial \bar{\xi}^2} = 0 \tag{6}$$

The solution of eqn. (6) is of the form

$$y = Y \sin \omega t \tag{7}$$

where ω is the natural frequency of vibration. The function Y satisfies all the boundary conditions of the beam which are as follows.

At the fixed end i.e. at $\bar{\xi} = 0$

(i) deflection due to lateral bending and lateral shear are zero i.e. $Y = 0$.

(ii) $\phi = \dfrac{dy_b}{dx} = \dfrac{dy}{dx} = 0$ where y_b is the lateral bending deflection. At the free end i.e. at $\bar{\xi} = 1$

(a) bending moment = 0 i.e. $\dfrac{d\phi}{dx} = 0$. This implies that $\rho S \dfrac{\partial^2 y}{\partial t^2} - K'GS \dfrac{\partial^2 y}{\partial x^2} = 0$

(b) shear force is zero i.e. $\dfrac{\partial y}{dx} - \phi = C$. This implies that $EI \dfrac{\partial^3 y}{\partial x^3} - \rho I \dfrac{\partial^3 y}{\partial t^2 \partial x} = 0$

Making the substitution of the solution (7) and introducing $\bar{\xi} = x/l$, we get the four conditions which are

$$\left.\begin{aligned} &(i) \quad y = 0 \\ &(ii) \quad \frac{dy}{d\bar{\xi}} = 0 \end{aligned}\right\} \text{at } \bar{\xi} = 0$$

$$\left.\begin{aligned} &(iii) \quad \omega^2 y + \frac{K'G}{\rho l^2} \frac{d^2 y}{d\bar{\xi}^2} = 0 \\ &(iv) \quad \omega^2 \frac{dy}{d\bar{\xi}} + \frac{EI}{\rho l^2} \frac{d^3 y}{d\bar{\xi}^3} = 0 \end{aligned}\right\} \text{at } \bar{\xi} = 1 \tag{8}$$

Substitution of (7) in (6) gives

$$\begin{aligned} &\frac{d^4 y}{d\bar{\xi}^4} - \frac{\Omega^2 l^2}{E/\rho} \cdot \frac{l^2}{I/S} \left[\left\{ \frac{r_0}{l} + \frac{1}{2} - \left(\frac{r_0}{l} \bar{\xi} + \frac{1}{2} \bar{\xi}^2 \right) \right\} \frac{d^2 y}{d\bar{\xi}^2} - \left(\frac{r_0}{l} + \bar{\xi} \right) \frac{dy}{d\bar{\xi}} \right] \\ &+ \frac{\omega^2 l^2}{E/\rho} \left(1 + \frac{E}{K'G} \right) \frac{d^2 y}{d\bar{\xi}^2} - \frac{\omega^2 l^2}{E/\rho} \cdot \frac{l^2}{I/S} \left(1 - \frac{\omega^2 l^2}{E/\rho} \cdot \frac{E}{K'G} \cdot \frac{I/S}{l^2} \right) y \\ &+ \frac{Kl^4}{EI} y - \frac{G_0 l^2}{EI} \frac{d^2 y}{d\bar{\xi}^2} = 0 \end{aligned} \tag{9}$$

Now we make use of the following substitutions

$$\lambda=\frac{\omega^2 l^2}{E/\rho}, K_1=\frac{E}{K'G}, K_2=\frac{l^2}{I/S}, K_3=\frac{\Omega^2 l^2}{E/\rho}, K_4=\frac{\Omega^2 l^2}{E/\rho}, K_5=\frac{G_0 l^2}{EI} \tag{10}$$

Then the eqn. (9) becomes

$$\frac{d^4y}{d\bar{\xi}^4}-K_3K_2\left[\left\{\frac{r_0}{l}+\frac{1}{2}-\left(\frac{r_0}{l}\bar{\xi}+\frac{1}{2}\bar{\xi}^2\right)\right\}\frac{d^2y}{d\bar{\xi}^2}-\left(\frac{r_0}{l}+\bar{\xi}\right)\frac{dy}{d\bar{\xi}}\right]$$
$$+\lambda(1+K_1)\frac{d^2y}{d\bar{\xi}^2}-\lambda K_2\left(1-\frac{K_1}{K_2}\lambda\right)y+K_4y-K_5\frac{d^2y}{d\bar{\xi}^2}=0 \tag{11}$$

For an approximate determination of the fundamental frequency y is chosen as the shape function in a series form. This function satisfies the boundary condition (8) and is given by

$$y=\bar{\xi}^2+C\bar{\xi}^3+D\bar{\xi}^4 \tag{12}$$

From the boundary conditions at $\bar{\xi}=1$, we have

$$\left(1+\frac{2K'G}{\omega^2\rho l^2}\right)+\left(1+\frac{6K'G}{\omega^2\rho l^2}\right)C+\left(1+\frac{12K'G}{\omega^2\rho l^2}\right)D=0 \tag{13}$$

$$2+\left(3+\frac{6E}{\omega^2\rho l^2}\right)C+\left(4+\frac{24E}{\omega^2\rho l^2}\right)D=0 \tag{14}$$

Solving eqn. (13) and (14) for D, we get

$$D=\frac{1}{6}+\left\{-\frac{1}{18}+\frac{1}{12}\frac{E}{K'G}\right\}\frac{\omega^2 l^2}{E/\rho}+\left\{-\frac{1}{54}+\frac{13}{216}\frac{E}{K'G}-\frac{1}{32}\left(\frac{E}{K'G}\right)^2\right\}\left(\frac{\omega^2 l^2}{E/\rho}\right)^2 \tag{15}$$

From eqn. (14), we get

$$C=-\frac{2}{3}+\left\{\frac{1}{9}-\frac{1}{3}\frac{E}{K'G}\right\}\frac{\omega^2 l^2}{E/\rho}+\left\{\frac{1}{18}-\frac{7}{54}\frac{E}{K'G}+\frac{1}{18}\left(\frac{E}{K'G}\right)^2\right\}\left(\frac{\omega^2 l^2}{E/\rho}\right)^2 \tag{16}$$

On substitution, C and D become

$$\left.\begin{aligned} C &= -\frac{2}{3}+\left\{\frac{1}{9}-\frac{1}{3}K_1\right\}\lambda+\left\{\frac{1}{18}-\frac{7}{54}K_1+\frac{1}{8}K_1^2\right\}\lambda^2 \\ D &= \frac{1}{6}+\left\{-\frac{1}{18}+\frac{1}{12}K_1\right\}\lambda+\left\{-\frac{1}{54}+\frac{13}{216}K_1-\frac{1}{32}K_1^2\right\}\lambda^2 \end{aligned}\right\} \tag{17}$$

The terms only upto λ^2 have been retained in (17).

If we are satisfied with the trial solution (12), which is sufficient in most of the cases, we must form the Stieltjes integrals from Galerkin's rule i.e.

$$\int_0^1 \left\langle \frac{d^4y}{d\bar{\xi}^4} - K_1K_2\left[\left\{\frac{r_0}{l}+\frac{1}{2}-\left(\frac{r_0}{l}\bar{\xi}+\frac{1}{2}\bar{\xi}^2\right)\right\}\frac{d^2y}{d\bar{\xi}^2}-\left(\frac{r_0}{l}+\bar{\xi}\right)\frac{dy}{d\bar{\xi}}\right]\right.$$
$$\left. +\left(\lambda+\lambda K_1-K_5\right)\frac{d^2y}{d\bar{\xi}^2}+\left(-\lambda K_2+K_1\lambda^2+K_4\right)y > y d\bar{\xi} \tag{18}$$

Now using (12), the Stieltjes integrals are evaluated as follows

$$J_1 = \int_0^1 \frac{d^4y}{d\bar{\xi}^4} y d\bar{\xi} = 24D\left(\frac{1}{3}+\frac{C}{4}+\frac{D}{5}\right)$$

$$J_2 = \int_0^1 \left[\frac{r_0}{l}+\frac{1}{2}-\left(\frac{r_0}{l}\bar{\xi}+\frac{1}{2}\bar{\xi}^2\right)\right]\frac{d^2y}{d\bar{\xi}^2} y d\bar{\xi}$$
$$= \frac{r_0}{l}\left\{\frac{1}{6}+\frac{2}{5}C+\frac{7}{15}D+\frac{1}{5}C^2+\frac{3}{7}CD+\frac{3}{14}D^2\right\}$$
$$+\left\{\frac{2}{15}+\frac{1}{3}C+\frac{2}{5}D+\frac{6}{35}C^2+\frac{3}{8}CD+\frac{4}{21}D^2\right\}$$

$$J_3 = \int_0^1 \left(\frac{r_0}{l}+\bar{\xi}\right)\frac{dy}{d\bar{\xi}} y d\bar{\xi} = \frac{r_0}{l}\left\{\frac{1}{2}+C+D+\frac{1}{2}C^2+CD+\frac{1}{2}D^2\right\}$$
$$+\left\{\frac{2}{5}+\frac{5}{6}C+\frac{6}{7}D+\frac{3}{7}C^2+\frac{7}{5}CD+\frac{4}{9}D^2\right\} \tag{19}$$

$$J_4 = \int_0^1 \frac{d^2y}{d\bar{\xi}^2} y d\bar{\xi} = \frac{2}{3}+2C+\frac{14}{5}D+\frac{6}{5}C^2+3CD+\frac{12}{7}D^2$$

$$J_5 = \int_0^1 y^2 d\bar{\xi} = \frac{1}{5}+\frac{1}{7}C^2+\frac{1}{9}D^2+\frac{1}{3}C+\frac{2}{7}D+\frac{1}{4}CD$$

Since in these expressions C^2, D^2 and CD are occurring, we evaluate them as given below

$$C^2 = \frac{4}{9} - \frac{4}{9}\left(\frac{1}{3} - K_1\right)\lambda + \left(-\frac{5}{81} + \frac{8}{81}K_1 - \frac{1}{18}K_1^2\right)\lambda^2$$

$$D^2 = \frac{1}{36} + \frac{1}{18}\left(-\frac{1}{3} + \frac{1}{2}K_1\right)\lambda + \left(-\frac{1}{324} + \frac{7}{648}K_1 - \frac{1}{288}K_1^2\right)\lambda^2$$

$$CD = -\frac{1}{9} + \left(\frac{1}{18} - \frac{1}{9}K_1\right)\lambda + \left(\frac{5}{324} - \frac{11}{324}K_1 + \frac{1}{72}K_1^2\right)\lambda^2$$

Eqn. (18) takes the form

$$J_1 - K_3K_2(J_2 - J_3) + (\lambda + \lambda K_1 - K_5)J_4 + \left(-\lambda K_2 + K_1\lambda^2 + K_1\right)J_5 = 0$$

or

$$J_1 - K_3K_2(J_2 - J_3) - K_5J_4 + K_4J_5 + \lambda\{(1 + K_1)J_4 - K_2J_5\} + K_1J_5\lambda^2 = 0 \tag{20}$$

Since all J's given by (19) are functions of C and D, they can be expressed in terms of λ with the help of expressions (17). Substitution of all J's in terms of λ in (20) and retaining terms only upto λ^2 one gets an equation of the form

$$R = Q\lambda + P\lambda^2 = 0 \tag{21}$$

where P, Q and R are constants.

The solution of eqn. (21) is

$$\lambda = \frac{Q \pm \sqrt{Q^2 - 4PR}}{2P} \tag{22}$$

The right hand side of (22) is positive since it may be shown that $Q^2 - 4PR > 0$.

The smaller of two values of λ given by (22) is an upper bound for the frequency of the fundamental mode of vibration, while the larger of the two values of λ corresponds to the next higher mode of vibration. The value of λ so obtained from (22) includes the Pasternak foundation effect. If this effect is ignored the values of λ can be computed by omitting these terms contained in eqn. (20).

Numerical Example

A numerical example for vibrations of a slender rotating beam including effects of rotatory inertia and shear force is now presented. The frequencies are computed from eqn. (22). The physical constants of the blade are taken as follows

$E/G = \frac{8}{3}$, $\Omega = 314 s^{-1}$, $K' = \frac{2}{3}$, $E = 30x10^6 \text{lbs/in}^2$, $l = 10\text{in}$,

$\rho = 0.28 \text{ lbs/in}^3$, $l/\Omega = 10$, $\frac{r_0}{l} = 3$, $\sqrt{K_4} = \sqrt{K_5} = 5$,

These values of $\sqrt{K_4}$ and $\sqrt{K_5}$ were taken from Wang[3]. With these values, the various parameters and the constants used in the frequency equation are as follows:

$I = Sr^2$ (r is the radius of gyration).

$K_1 = 4, K_2 = 100, K_3 = .0920229, K_4 = K_5 = 25$

$C = -.66667 - 1.22222\ \lambda + 1.53704\ \lambda^2$, $D = .16667 + .27778\ \lambda - .27778\ \lambda^2$

$C^2 = 0.44444 - 1.62163\ \lambda - .55556\ \lambda^2$, $D^2 = 0.027778 + .09259\ \lambda - .01543\ \lambda^2$

$CD = -0.11111 - .38889\ \lambda + .10185\ \lambda^2$, $J_1 = 0.80001 + .33333\ \lambda - 1.68520\ \lambda^2$

$J_2 = 0.09259 - 3.19372\ \lambda + 1.58450\ \lambda^2$, $J_3 = 0.46790 - 8.08350\ \lambda + 4.11377\lambda^2$

$J_4 = 0.04762 - 4.63015\ \lambda + 1.90872\ \lambda^2$, $J_5 = 0.06421 - .64777\ \lambda + .37736\ \lambda^2$

$K_1 J_5 = 0.25684 - 2.59108\ \lambda + 1.50944\ \lambda^2$,

$K_2 J_5 - (1+K_1) J_4 = 6.18290 - 41.62625\ \lambda + 28.19240\ \lambda^2$, $J_1 - K_2 K_3 (J_2 - J_3) - K_5 J_4 + K_4 J_5 = 4.66847 - 82.94784\ \lambda - 16.69412\ \lambda^2$

Substituting these values in (20), retaining only up to second order terms of λ, we get

$$4.66847 - 89.13074\ \lambda + 25.18897\ \lambda^2 = 0 \tag{23}$$

The two values of λ for this equation are

$$\lambda_1 = .05318,\ \lambda_2 = 3.48531 \tag{24}$$

which are the upper bounds of the frequencies corresponding to the first two modes of vibrations of rotating blade including the effects of Pasternak foundation. If the effect of Pasternak foundation is not taken into consideration, the equation in λ is

$$4.25372 - 50.79006\ \lambda + 63.47306\ \lambda^2 = 0 \tag{25}$$

which gives the smaller value of λ i.e. corresponding to the fundamental mode of vibration as

$$\lambda_1 = .09505 \tag{26}$$

Concluding Remarks

On comparing the values of λ_1 from (24) and (26) it can be easily stated that the fundamental frequency of rotating beam is considerably decreased, when it is placed on Pasternak foundation.

References

1. Timoshenko, S.P. (1921) *Phil. Mag* 6(41) : 744.
2. Kerr, A.D. (1964) *Jour. Appld. Mech.* 491.
3. Wang, T.M. (1977) *Jour. Sound & Vibrations* 51 : 149.

PROC. NAT. ACAD. SCI. INDIA, 61(A), II, 1991

Flow of a dusty visco-elastic (Kuvshiniski model) liquid down an inclined plane

(Key words : fluid mechanics/Kuvshiniski model/dusty visco-elastic liquid/visco-elastic parameter/dusty gas/laminar flow)

R. K. S. CHAUDHARY and K.K. SINGH

Department of Mathematics, Agra College, Agra-282 002, India.

Received June 8, 1989; Revised May 4, 1990; Accepted August 14, 1990.

Abstract

The motion of visco-elastic liquid (Kuvshiniski type) with uniform distribution of dust particles down an inclined plane under the influence of exponential pressure gradient has been studied. The velocities of liquid and dust particles are obtained in elegant forms. The velocity profiles of liquid and dust particles have also been plotted to visualize the physical situations of the motion.

Introduction

The attention of many research workers in fluid mechanics has been diverted to the study of the influence of dust particles on the motion of fluids in the past few years. A model equation describing the motion of such mixed system has been given by Saffman[1]. Based upon Saffman's model several authors[2-5] have investigated a number of dusty gas flow problems in different situations.

There is another class of problems of the flow of dusty visco-elastic fluids such as latex particles emulsion paints, reinforcing particles in polymer melts and rock crystals in molten lava. The study of these problems and rheological aspects of such flows have not received much attention although this has some bearing on the problems of petroleum industry and chemical engineering. Several authors[6-9] have contributed in this field. Mandal *et al.*[10] have considered unsteady flow of dusty visco-elastic (Kuvshiniski type) liquid between two oscillating plates.

Motivation for studying the problem is likely to have some industrial and chemical engineering application on the problems of transport of solid particles suspended in visco-elastic fluids through channels.

Formulation and Solution of the Problem

In the present investigation, we consider the laminar flow of an unsteady visco-elastic Kuvshiniski type liquid[11] with uniform distribution of dust particles down an inclined plane of inclination θ to the horizointal. The liquid is bounded by a parallel upper surface at a distance h from the plane.

Let us choose the origin of coordinate system at the bottom of the inclined plane x-axis opposite to the direction of the flow and along the greatest slope of the plane and y-axis perpendicular to the plane. Since both the dust and liquid particles move along the greatest slope of the plane and the flow is laminar the velocity of both liquid and dust particles can be defined by the following relations :

$$\left.\begin{aligned} u_1 &= u_1(y,t), \quad u_2 = 0, \quad u_3 = 0 \\ v_1 &= v_1(y,t), \quad v_2 = 0, \quad v_3 = 0 \end{aligned}\right\} \tag{1}$$

where (u_1, u_2, u_3) and (v_1, v_2, v_3) are the velocity components of liquid and dust particles, respectively.

Following Saffman[1], the equations of motion for the flow of dusty visco-elastic liquid (Kuvshiniski) type) are given by

$$\left(1+\alpha\frac{\partial}{\partial t}\right)\frac{\partial u_1}{\partial t} = -\frac{1}{\rho}\left(1+\alpha\frac{\partial}{\partial t}\right)\frac{\partial p}{\partial x} + \upsilon\frac{\partial^2 u_1}{\partial y^2} + \frac{KN_0}{\rho}\left(1+\alpha\frac{\partial}{\partial t}\right)(v_1 - u_1) - g\sin\theta \tag{2}$$

$$\frac{1}{\rho}\frac{\partial p}{\partial Y} + g\cos\theta = 0 \tag{3}$$

$$-\frac{1}{\rho}\frac{\partial p}{\partial z} = 0 \tag{4}$$

$$\frac{\partial v_1}{\partial t} = \frac{K}{m}(u_1 - v_1) \tag{5}$$

where α is elastic parameters of the liquid particle, $\upsilon(=\mu/\rho)$ the kinematic viscosity, p the pressure, K the Stoke's resistance coefficient, m the mass of dust particles, N_0 the number density of dust particles and t the time.

The initial and boundary conditions are

$$t \le 0 \qquad u_1 = 0 = v_1$$
$$t > 0 \qquad u_1 = 0 = v_1 \quad \text{at} \quad y = 0$$

We express the pressure p as

$$p = -\rho g(x\sin\theta + y\cos\theta) - x\rho\phi(t) \tag{6}$$

Using eqn. (6) in (2) – (5), we get

$$\left(1+\alpha\frac{\partial}{\partial t}\right)\frac{\partial u_1}{\partial t} = F(t) + \upsilon\frac{\partial^2 u_1}{\partial y^2} + \frac{KN_0}{\rho}\left(1+\alpha\frac{\partial}{\partial t}\right)(v_1 - u_1) \tag{7}$$

$$\frac{\partial v_1}{\partial t} = \frac{K}{m}(u_1 - v_1) \tag{8}$$

where $F(t) = \phi(t) + \alpha\phi'(t)$

Let us choose u, v and $F(t)$ as

$$\left.\begin{aligned} u_1(y,t) &= u(y)\, e^{-\lambda^2 t} \\ v_1(y,t) &= v(y) e^{-\lambda^2 t} \\ F(t) &= c\, e^{-\lambda^2 t} \end{aligned}\right\} \tag{9}$$

where c and λ are the real constants.

Substituting the values of u_1, v_1 and $F(t)$ in eqn. (7) and (8), we get

$$\frac{d^2 f}{dy^2} + A^2 f = 0 \tag{10}$$

$$v = \frac{K}{K - m\lambda^2} u \tag{11}$$

where

$$f = A^2 u + d$$

$$A^2 = \frac{\lambda^2}{\upsilon}\left(1 - \alpha\lambda^2\right)\left\{1 + \frac{Mm}{K - m\lambda^2}\right\}$$

$$M = \frac{KN_0}{\rho} \quad \text{and} \quad d = \frac{c}{\upsilon}$$

Here the boundary conditions are :

$$\left.\begin{aligned} f &= d \qquad \text{when} \quad y = 0 \\ f &= -UA^2 + d \qquad \text{when} \quad y = h \end{aligned}\right\} \tag{12}$$

The solution of eqn. (9) subject to the boundary conditions (12) is given by

$$f = B_1 \cos Ay + c_1 \sin Ay$$

where

$$B_1 = d$$

$$c_1 = \frac{d(1 - \cos Ah) - UA^2}{\sin Ah}$$

The velocities of the liquid and dust particles are expressed as

$$u_1 = \left[\frac{-d(1-\cos Ay)\sin Ah + \{d(1-\cos Ah) - UA^2\}\sin Ay}{A^2 \sin Ah}\right] e^{-\lambda^2 t} \text{ and}$$

$$v_1 = \frac{K}{K - m\lambda^2}\left[\frac{-d(1-\cos Ay)\sin Ah + \{d(1-\cos Ah) - UA^2\}\sin Ay}{A^2 \sin Ah}\right] e^{-\lambda^2 t} \tag{15}$$

The discharge of the flux per second for unit width of the plane is

$$Q = \int_0^h \pi\, y u_1\, dy$$

$$Q = \frac{e^{-\lambda^2 t}}{2A^4 \sin Ah}\Big[2Ah\{-Adh\sin Ah + \sin^2 Ah - d(1-\cos Ah)\cos Ah + UA^2 \cos Ah\}$$
$$+A^2 dh^2 \sin Ah + \sin 2Ah + 2d(1-\cos Ah)\sin Ah - 2UA^2 \sin Ah\Big] \tag{16}$$

The velocities of liquid and dust particles at height h above the inclined plane are respectively given by

$$U_1 = \left[\frac{-d(1-\cos Ah) + d(1-\cos Ah) - UA^2}{A^2}\right] e^{-\lambda^2 t} = -Ue^{-\lambda^2 t} \tag{17}$$

and

$$V_1 = \frac{K}{K - m\lambda^2}\left[\frac{-d(1-\cos Ah) + d(1-\cos Ah) - UA^2}{A^2}\right] e^{-\lambda^2 t} = -\frac{KU}{K - m\lambda^2} e^{-\lambda^2 t} \tag{18}$$

Discussion

Fig. 1 exhibits visco-elastic effects on the flow field. The elastic parameter α is favourable to the velocity for both liquid and dust particles. The velocity profiles are non-linear close to the plate there after they become almost linear. From Fig. 2 it is evident that near the plate the velocity profiles tend to be linear, of course dusty phase being slower than the liquid phase as is expected in the physical situation.

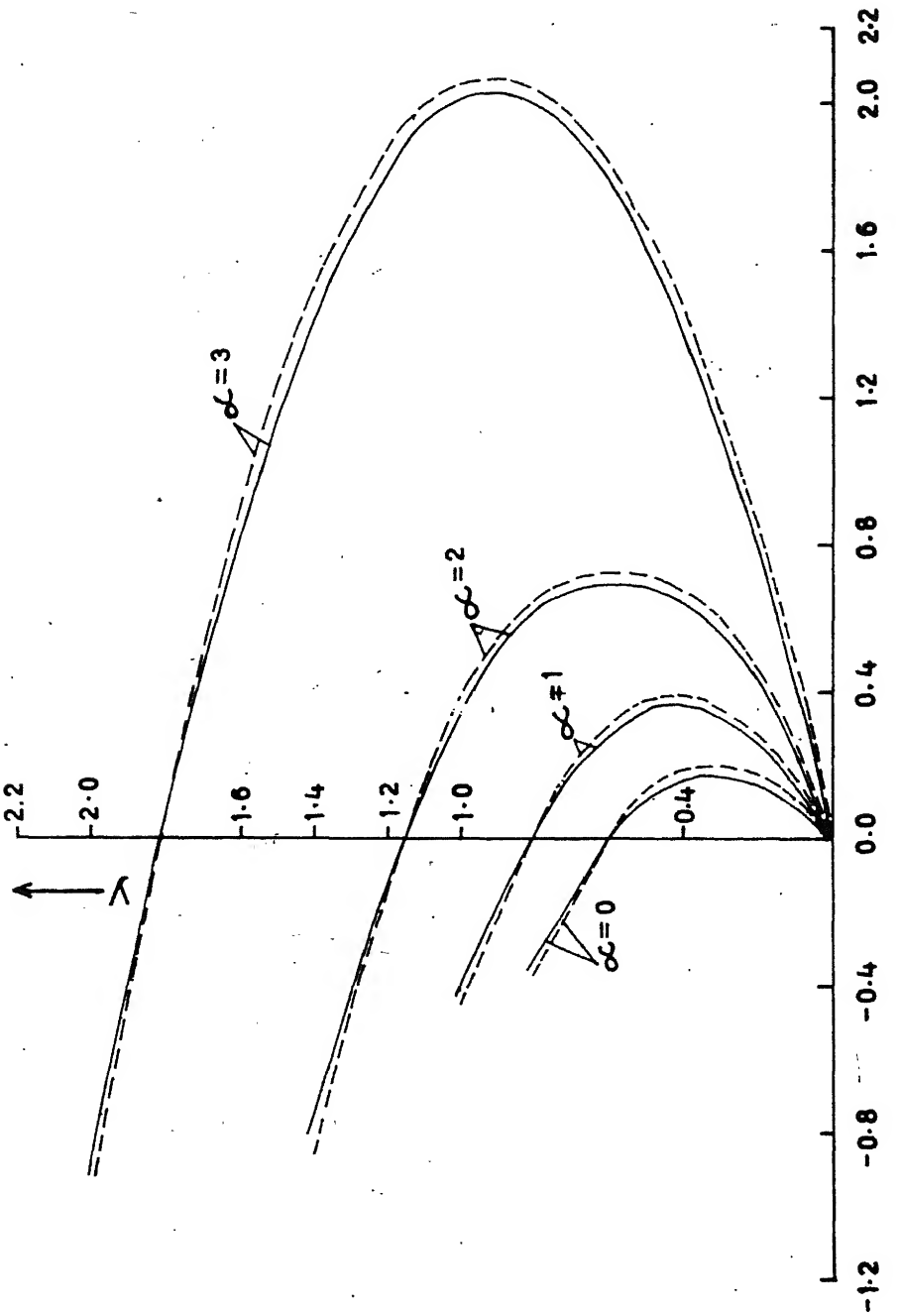

Fig. 1 - Velocity profiles for the liquid and the dust particles, $u = 1$, $t = 0.4$, $\cos AH = 1/2$, $\sin AH = \sqrt{3}/2$, —liquid,---dust.

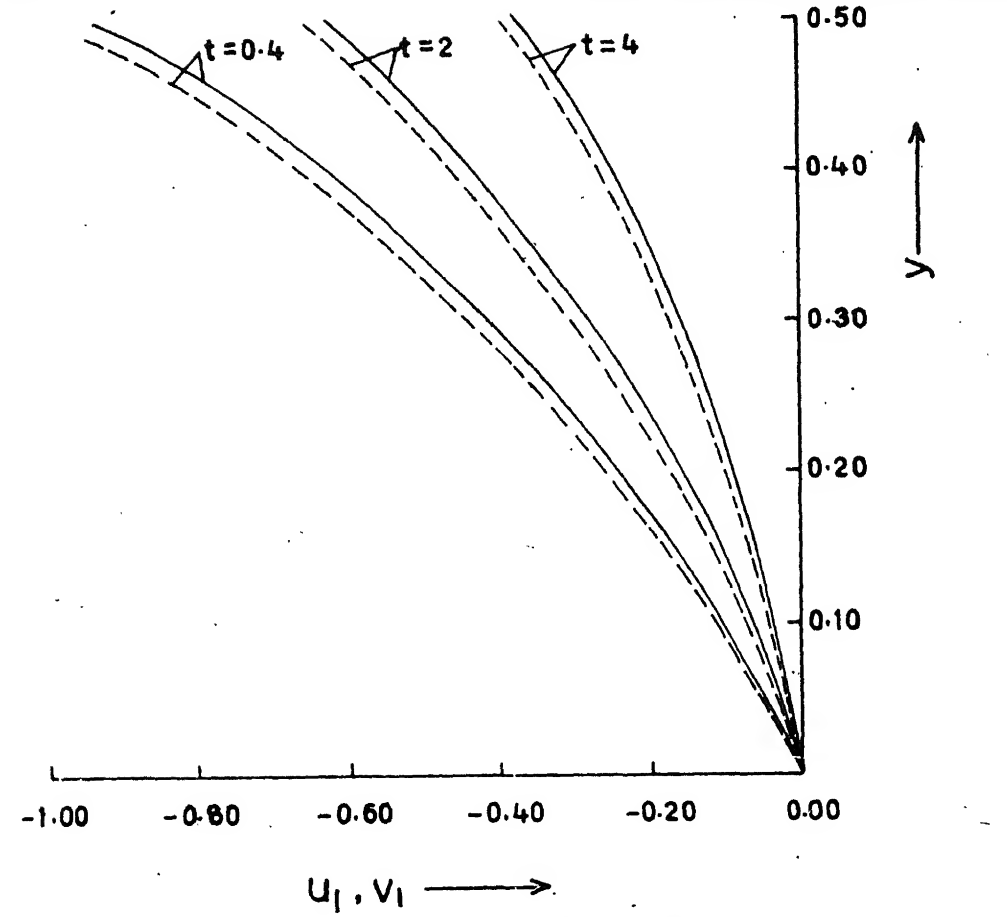

Fig. 2 - Velocity profiles for the liquid and the dust particles, $A = 2$, $u_c = 1$, $\cos Ah = 1/2$, $\sin AH = \sqrt{3}/2$, —liquid, ----dust.

References

1. Saffman, P.G. (1962) *J. Fluid Mech.* 13 : 120.
2. Marble, F.E. (1963) *Fifth AGARD Combustion and Propulsion Coloquim*, Pergamon Press, Oxford, p. 175.
3. Vimala, C.S. (1972) *Def. Sci. J.* 22 : 231.
4. Kishore, N. & Pandey, R.D. (1977) *J. Scient. Res.* 27 : 151.
5. Singh, K.K. (1979) *Agra University J. Res. (Sci.)* 28 : 39.
6. Srivastava, L.P. (1971) *Istanbul Teknik University Bulteni* 24 : 19.
7. Sharma, C.L. & Dubey, S.N. (1976) *Bull. DeL' Acad. Polo des Sci. Series Des. Sci. Teck.* 4 : 145.
8. Bagchi, S. & Maiti, M.K. (1980) *Acta Cienc. Indica* 130.
9. Mukherjee, S. Maiti, M.K. & Mukherjee, S. (1984) *Indian J. Technol.* 22 : 41.
10. Mandal, G.C., Mukherjee, S. & Mukherjee, S. (1986) *J. Indian Inst. Sci.* 66 : 77.
11. Kuvshiniski, E.V. (1951) *J. Expl. Theor. Phys., USSR* 21 : 88.

PROC. NAT. ACAD. SCI. INDIA, 61(A), II, 1991

On functional relations

(Key words : fractional calculus/Rieman-Liouville operator/hypergeometric function/ digamma function)

SHASHI KANT and C. L. KOUL

Department of Mathematics, Malaviya Regional Engineering College, Jaipur-302 017, India.

Received March 14, 1990; Accepted September 22, 1990.

Abstract

Two formulae involving series summation and the diagamma function are established with the help of a generalized Riemann-Liouville operator of fractional calculus.

Introduction

The Riemann-Liouville fractional integral operator of order α of a function $f(x)$ is defined and represented as

$$R^{\alpha}_{0,x}[f(x)] = \frac{1}{\Gamma(\alpha)}\int_0^x (x-t)^{\alpha-1} f(t)\,dt,\ \mathrm{Re}(\alpha)>0$$

$$= \frac{d^n}{dx^n}\left[R^{\alpha+n}_{0,x}[f(x)]\right], 0<\alpha+n\le 1, n=0,1,2,\ldots \tag{1}$$

while the Weyl operator of order α of a function $f(x)$ is given by

$$W^{\alpha}_{x,\infty}[f(x)] = \frac{1}{\Gamma(\alpha)}\int_x^{\infty} (t-x)^{\alpha-1} f(t)\,dt,\ \mathrm{Re}(\alpha)>0$$

$$= (-1)^n \frac{d^n}{dx^n}\left[W^{\alpha+n}_{x,\infty}[f(x)]\right],\ 0<\alpha+n\le 1, n=0,1,2\ldots \tag{2}$$

A generalization of the Riemann-Liouville fractional integral operator defined by (1) was studied recently by Saigo and Raina[1] and represented and defined as follows

Let $\alpha>0$, β and η be real numbers,

$$I^{\alpha,\beta,\eta}_{0,x}[f(x)] = \frac{x^{-\alpha-\beta}}{\Gamma(\alpha)}\int_0^x (x-t)^{\alpha-1}\, {}_2F_1\left[\begin{matrix}\alpha+\beta,-\eta\\ \alpha\end{matrix};\ 1-\frac{t}{x}\right] f(t)dt \tag{3}$$

where ${}_2F_1$ denotes the familiar Gauss Hypergeometric series, *viz.*,

$${}_2F_1\left[\begin{matrix}a,b\\ c\end{matrix};z\right] = \sum_{n=0}^{\infty}\frac{(a)_n(b)_n}{(c)_n n!} z^n,\ |z|<1 \tag{4}$$

For $\alpha \le 0$

$$I_{0,x}^{\alpha,\beta,\eta}[f(x)] = \frac{d^n}{dx^n} I_{0,x}^{\alpha+n,\beta-n,\eta-n}[f(x)] \tag{5}$$

where $0 < \alpha + n \leq 1$, n is a positive integer.

The inverse operator of $I_{0,x}^{\alpha,\beta,\eta}$ is given by (see Saigo[2])

$$\left(I_{0,x}^{\alpha,\beta,\eta}\right)[f(x)]^{-1} = I_{0,x}^{-\alpha,-\beta,\alpha+\eta}[f(x)] \tag{6}$$

The following particular cases are due to Saigo and Raina[1].

$$I_{0,x}^{\alpha,-\alpha,\eta}[f(x)] = R_{0,x}^{\alpha}[f(x)] = \frac{1}{\Gamma(\alpha)} \int_0^x (x-t)^{\alpha-1} f(t)\,dt \tag{7}$$

$$I_{0,x}^{\alpha,0,\eta}[f(x)] = E_{0,x}^{\alpha,\eta}[f(x)] = \frac{x^{-\alpha-\eta}}{\Gamma(\alpha)} \int_0^x (x-t)^{\alpha-1}\ t^{\eta} f(t)\,dt \tag{8}$$

where $E\,[f(x)]$ is the fractional integral operator[1]. The inverse operator for R is given by

$$\left[R_{0,x}^{\alpha}[f(x)]\right]^{-1} = R_{0,x}^{-\alpha}[f(x)] \tag{9}$$

The two functional relations established in this paper are the following :

For $\lambda > \max\{0, -\alpha, -\alpha-\beta, -\alpha-\beta-\eta\}$,

$$\sum_{n=1}^{\infty} \frac{(\alpha)_n}{n\Gamma(\alpha+\beta+\lambda+n)}\ {}_3F_2\left[\begin{matrix}\alpha+\beta, \alpha+n, -\eta \\ \alpha, \alpha+\beta+\lambda+n\end{matrix}; 1\right]$$

$$= \frac{\Gamma(\lambda+\eta)}{\Gamma(\lambda)\Gamma(\alpha+\beta+\lambda+\eta)}\left[\Psi(\lambda) + \Psi(\alpha+\beta+\lambda+\eta) - \Psi(\beta+\lambda) - \Psi(\lambda+\eta)\right], \tag{10}$$

and for $\lambda > \max\{0, \alpha\}$,

$$\sum_{n=1}^{\infty} \frac{(\alpha)_n}{n(\lambda)_n}\ {}_{p+1}F_{q+1}\left[\begin{matrix}(a_p), \lambda \\ (b_q), \lambda+n\end{matrix}; \frac{x}{a}\right]$$

$$= \sum_{r=0}^{\infty} \frac{\prod_{j=1}^{p}(a_j)_r}{\prod_{j=1}^{q}(b_j)_r\, r!}\left(\frac{x}{a}\right)^r \left\{\Psi(\lambda+r) - \Psi(-\alpha+\lambda+r)\right\} \tag{11}$$

Results Required

(1) If $K > \max(0, \beta-\eta)-1$, then (see Saigo and Raina[1])

$$I_{0,x}^{\alpha,\beta,\eta}\left[x^K\right]=\frac{\Gamma(K+1)\Gamma(-\beta+\eta+K+1)}{\Gamma(-\beta+K+1)\Gamma(\alpha+\eta+K+1)}x^{K-\beta} \tag{12}$$

(2) From Gradshteyn and Ryzhik[3], if $\mathrm{Re}(n+\alpha) > 0$ and $\mathrm{Re}(\beta+\lambda) > 0$,

$$\int_0^x (x-t)^{n+\alpha-1}t^{\beta+\lambda-1}\,{}_2F_1\left[\begin{matrix}\alpha+\beta,-\eta\\ \alpha\end{matrix};1-\frac{t}{x}\right]dt$$

$$=x^{\alpha+\beta+\lambda+n-1}\frac{\Gamma(\beta+\lambda)\Gamma(\alpha+n)}{\Gamma(\alpha+\beta+\lambda+n)}\,{}_3F_2\left[\begin{matrix}\alpha+\beta,\alpha+n,-\eta\\ \alpha,\alpha+\beta+\lambda+n\end{matrix};1\right] \tag{13}$$

Proofs of the Formulae

To establish the result given in (10), we start with the formula[1]

$$I_{0,x}^{-\alpha,-\beta,\alpha+\eta}\left[x^{\lambda-1}\right]=\frac{\Gamma(\lambda)\Gamma(\alpha+\beta+\lambda+\eta)}{\Gamma(\beta+\lambda)\Gamma(\lambda+\eta)}x^{\beta+\lambda-1} \tag{14}$$

valid for $\lambda > \max(0, -\alpha-\beta-\eta)$, which with the help of (5), can be put as

$$\frac{d^n}{dx^n}\left\{\frac{x^{\alpha+\beta}}{\Gamma(\eta-\alpha)}\left[\int_0^x (x-t)^{-\alpha+n-1}\,{}_2F_1\left[\begin{matrix}-\alpha-\beta,\ -\alpha-\eta+n\\ -\alpha+n\end{matrix};1-\frac{t}{x}\right]t^{\lambda-1}\,dt\right.\right.$$

$$\left.\left.=\frac{\Gamma(\lambda)\Gamma(\alpha+\beta+\lambda+\eta)}{\Gamma(\beta+\lambda)\Gamma(\lambda+\eta)}x^{\beta+\lambda-1}\right.\right. \tag{15}$$

provided that $\lambda > \max(0, -\alpha-\beta-\eta)$ and $0 < -\alpha+n \le 1$, n is a positive integer.

Differentiating both sides of (15) with respect to λ, we have

$$\frac{d^n}{dx^n}\left\{\frac{x^{\alpha+\beta}}{\Gamma(-\alpha+n)}\int_0^x (x-t)^{-\alpha+n-1}\,{}_2F_1\left[\begin{matrix}-\alpha-\beta,\ -\alpha-\eta+n\\ -\alpha+n\end{matrix};1-\frac{t}{x}\right]t^{\lambda-1}\log t\,dt\right\}$$

$$=\left\{\log x+g(\alpha,\beta,\lambda,\eta)\right\}K(\alpha,\beta,\lambda,\eta)\,x^{\beta+\lambda-1} \tag{16}$$

which, in view of the definition of operator I in (5), gives

$$I_{0,x}^{-\alpha,-\beta,\alpha+\eta}\left[x^{\lambda-1}\log x\right]=\left\{\log x+g(\alpha,\beta,\lambda,\eta)\right\}K(\alpha,\beta,\lambda,\eta)x^{\beta+\lambda-1} \tag{17}$$

for $\lambda > \max[0, -\alpha-\beta-\eta)$, where we assume that

$$g(\alpha,\beta,\lambda,\eta)=\Psi(\lambda)+\Psi(\alpha+\beta+\lambda+\eta)-\Psi(\beta+\lambda)-\Psi(\lambda+\eta) \tag{18}$$

and

$$K(\alpha,\beta,\lambda,\eta)=\frac{\Gamma(\lambda)\Gamma(\alpha+\beta+\lambda+\eta)}{\Gamma(\beta+\lambda)\Gamma(\lambda+\eta)}. \tag{19}$$

Next, consider the following Volterra type integral equation

$$\int_0^x (x-t)^{\alpha-1}\,{}_2F_1\left[\begin{matrix}\alpha+\beta,-\eta\\ \alpha\end{matrix};1-\frac{t}{x}\right] f(t)\,dt=\Gamma(\alpha)x^{\alpha+\beta+\lambda-1}\log x \tag{20}$$

which, in view of(3), can be re-written as

$$I_{0,x}^{\alpha,\beta,\eta}[f(x)]=x^{\lambda-1}\log x \tag{21}$$

With the help of the inverse operator given by (6), (21) yields

$$f(x)=I_{0,x}^{-\alpha,-\beta,\alpha+\eta}\left[x^{\lambda-1}\log x\right] \tag{22}$$

This yields the solution of the integral equation in (20). Also from (17), we have

$$f(x)=\left\{\log x+g(\alpha,\beta,\lambda,\eta)\right\}K(\alpha,\beta,\lambda,\eta)\,x^{\beta+\lambda-1} \tag{23}$$

We next substitute the value of $f(x)$ from (23) in (21) to get

$$I_{0,x}^{\alpha,\beta,\eta}\left[x^{\beta+\lambda-1}\log x\right]+g(\alpha,\beta,\lambda,\eta)\,I_{0,x}^{\alpha,\beta,\eta}\left[x^{\beta+\lambda-1}\right]=\frac{x^{\lambda-1}\log x}{K(\alpha,\beta,\lambda,\eta)} \tag{24}$$

We now evaluate the two fractional integrals occurring on the L.H.S. of(24). We have by definition (3),

$$I_1=I_{0,x}^{\alpha,\beta,\eta}\left[x^{\beta+\lambda-1}\log x\right]=\frac{x^{-\alpha-\beta}}{\Gamma(\alpha)}\int_0^x (x-t)^{\alpha-1}\,{}_2F_1\left[\begin{matrix}\alpha+\beta,-\eta\\ \alpha\end{matrix};1-\frac{t}{x}\right]t^{\beta+\lambda-1}\log t\,dt \tag{25}$$

and since $$\log t=\log x-\sum_{n=1}^{\infty}\frac{(x-t)^n}{nx^n} \tag{26}$$

by Taylor's expansion, (25) now gives on integrating term by term (which is valid due to absolute convergence of the involved integrals)

$$I_1=\log x\;I_{0,x}^{\alpha,\beta,\eta}\left[x^{\beta+\lambda-1}\right]-\sum_{n=1}^{\infty}\frac{x^{-\alpha-\beta-n}}{n\Gamma(\alpha)}\int_0^x (x-t)^{n+\alpha-1}\,{}_2F_1\left[\begin{matrix}\alpha+\beta,-\eta\\ \alpha\end{matrix};1-\frac{t}{x}\right]t^{\beta+\lambda-1}.dt \tag{27}$$

and on further using (12) and (13) in (27), we get

$$I_1=\frac{x^{\lambda-1}\log x}{K(\alpha,\beta,\lambda,\eta)}-\sum_{n=1}^{\infty}\frac{x^{\lambda-1}}{n\,\Gamma(\alpha)}\frac{\Gamma(\beta+\lambda)\Gamma(\alpha+n)}{\Gamma(\alpha+\beta+\lambda+n)}\,{}_3F_2\left[\begin{matrix}\alpha+\beta,\ \alpha+n,\ -\eta\\ \alpha,\alpha+\beta+\lambda+n\end{matrix};1\right] \tag{28}$$

Again from (12),

$$I_2=I_{0,x}^{\alpha,\beta,\eta}\left[x^{\beta+\lambda-1}\right]=\frac{\Gamma(\beta+\lambda)\Gamma(\lambda+\eta)}{\Gamma(\lambda)\Gamma(\alpha+\beta+\lambda+\eta)}\,x^{\lambda-1},\ \text{for}\ \lambda>\max(-\beta,-\eta) \tag{29}$$

Putting the values of I_1 and I_2 in (24) and then simplifying the resultant expression, we arrive at the following result given in (10)

$$\sum_{n=1}^{\infty}\frac{(\alpha)_n}{n\,\Gamma(\alpha+\beta+\lambda+n)}\,{}_3F_2\left[\begin{matrix}\alpha+\beta,\ \alpha+n,\ -\eta\\ \alpha,\alpha+\beta+\lambda+n\end{matrix};1\right]$$

$$=\frac{\Gamma(\lambda+\eta)}{\Gamma(\lambda)\Gamma(\alpha+\beta+\lambda+\eta)}\left[\Psi(\lambda)+\Psi(\alpha+\beta+\lambda+\eta)-\Psi(\beta+\lambda)-\Psi(\lambda+\eta)\right] \tag{30}$$

provided $\lambda>\max(0,-\beta,-\eta,-\alpha-\beta-\eta)$.

To obtain the second result given in eqn. (11) above, we start with the formula[4]

$$I_{0,x}^{-\alpha,\alpha,\eta+\alpha}\left\{x^{\lambda-1}\,{}_pF_q\left[(a_p);(b_q);\frac{x}{a}\right]\right\}=\frac{x^{-\alpha+\lambda-1}\,\Gamma(\lambda)}{\Gamma(-\alpha+\lambda)}\,{}_{p+1}F_{q+1}\left[\begin{matrix}(a_p),\lambda\\ (b_q),-\alpha+\lambda\end{matrix};\frac{x}{a}\right] \tag{31}$$

which, with the help of (5), can be put as

$$\frac{d^n}{dx^n}\left[\frac{1}{\Gamma(n-\alpha)}\int_0^x(x-t)^{-\alpha+n-1}\,t^{\lambda-1}\,{}_pF_q\left[(a_p);(b_q);\frac{t}{a}\right]dt\right]$$

$$=\frac{x^{-\alpha+\lambda-1}}{\Gamma(-\alpha+\lambda)}\,{}_{p+1}F_{q+1}\left[\begin{matrix}(a_p),\lambda\\ (b_q),-\alpha+\lambda\end{matrix};\frac{x}{a}\right] \tag{32}$$

where $0<-\alpha+n\le 1$, n is a positive integer.

Differentiating both sides of (32) with respect to λ, it gives, in view of the definition given in (5),

$$\frac{d^n}{dx^n}\left[\frac{1}{\Gamma(-\alpha+n)}\int_0^x(x-t)^{-\alpha+n-1}\,t^{\lambda-1}\log t\,{}_pF_q\left[\begin{matrix}(a_p)\\ (b_q)\end{matrix};\frac{t}{a}\right]dt\right]$$

$$=I_{0,x}^{-\alpha,\alpha,\eta+\alpha}\left[x^{\lambda-1}\,{}_pF_q\left[\begin{matrix}(a_p)\\ (b_q)\end{matrix};\frac{x}{a}\right]\log x\right]$$

$$=\frac{x^{-\alpha-1}}{\Gamma(-\alpha+\lambda)}\Gamma(\lambda)\left[\log x\,{}_{b+1}F_{q+1}\left[\begin{matrix}(a_p),\lambda\\ (b_q),-\alpha+\lambda\end{matrix};\frac{x}{a}\right]\right.$$

$$+\sum_{r=0}^{\infty} \frac{\prod_{j=1}^{p}(a_j)_r(\lambda)_r}{\prod_{j=1}^{q}(b_j)_r(-\alpha+\lambda)_r\, r!}\left(\frac{x}{a}\right)^r\{\psi(\lambda+r)-\psi(-\alpha+\lambda+r)\}\Bigg] \tag{33}$$

since term by term differentiating is valid due to absolute convergence of the involved series.

We now again consider the following integral equation

$$\int_0^x (x-t)^{\alpha-1} f(t)dt = \Gamma(\alpha)x^{\lambda-1}\, {}_pF_q\left[\begin{matrix}(a_p)\\(b_q)\end{matrix};\frac{x}{a}\right]\log x \tag{34}$$

The L.H.S. of which, in terms of the I-operator, can be put as $I_{0,x}^{\alpha,-\alpha,\eta}[f(x)]$ and which on inverting with the help of (6) gives the solution of (34) in the following form

$$f(x) = I_{0,x}^{-\alpha,\alpha,\eta+\alpha}\left[x^{\lambda-1}\, {}_pF_q\left[\begin{matrix}(a_p)\\(b_q)\end{matrix};\frac{x}{a}\right]\log x\right] \tag{35}$$

Now on substituting from eqn. (33) and (26) in eqn. (35), we get the desired result mentioned in (11) above. The method given above is essentially due to Kalla[5].

Particular cases

If, in eqn. (10), we take $\beta = 0$ and use the result

$${}_2F_1\left[\begin{matrix}a,b\\c\end{matrix};1\right] = \frac{\Gamma(c)\Gamma(c-a-b)}{\Gamma(c-a)\Gamma(c-b)},\ \mathrm{Re}(c-a-b)>0 \text{ and } c \neq 0,-1,-2,\ldots$$

it reduces to the following result due to Kalla and Ross[6]

$$\frac{\Gamma(\mu)}{\Gamma(\alpha)}\sum_{n=1}^{\infty}\frac{\Gamma(\alpha+n)}{n\,\Gamma(\mu+n)} = \psi(\mu)-\psi(\mu-\alpha) \tag{36}$$

where $\mu = \alpha + \lambda + \eta$.

In in eqn. (11), we take $p = 2$ and $q = 1$, it reduces to another known result due to Kalla[5], which in turn is a generalization of many known results as indicated therein. It may be pointed out that (11) agrees with a result given by Nishimoto and Srivastava[7].

By specialising the various parameters appearing in our main results given in (10) and (11) above, a number of results can be derived.

References

1. Saigo, M. & Raina, R.K. (1988) *Fukuoka Univ. Sc. Rep.* **18**(1) : 15.
2. Saigo, M. (1979) *Math Japan* **24** : 379.
3. Gradshteyn, I.S. & Ryzhik, I.M. (1980) *Table of Integrals, Series and Products*, Academic Press, New York, p. 285.
4. Erde'lyi, A. (1954) *Tables of Integral Transforms*, Vol. II, McGraw Hill, New York, p. 200.
5. Kalla, S.L. (1987) *SERDICA Bulg. Math. Pub.* **13** : 170.
6. Kalla, S.L. & Ross, B. (1985) *Fractional Calculus*, Pitman Advanced Publishing Program, p. 32.
7. Nishimoto, K. & Srivastava, H.M. (1989) *The J. College Engg. Nihon Univ.* **30**(B) : 105.

PROC. NAT. ACAD. SCI. INDIA, 61 (A), II, 1991

An analogue of Caristi-fixed point theorem in a quasi-metric space

(Key words : quasi-metric space/Caristi-fixed point theorem/p-orbital continuity)

RAGHU CHIKKALA and A. P. BAISNAB

Mathematics Department, University of Burdwan, Burdwan-713 104, India.

Received August 2, 1990; Accepted September 22, 1990.

Abstract

Two fixed point theorems have been presented over a quasi-metric space. In consequence, an analogue of Caristi-fixed point theorem has been obtained.

Introduction

In this paper, fixed point theorems over a quasi-metric space have been proved for a mapping satisfying certain contraction condition. For quasi-metric topology and allied topics, specially in setting of bi-topological spaces one must see Kelly[1]. In proving theorem 1.1, we have used the notion of orbital continuity of the mapping. Theorem 1.1 also leads to Theorem 1.2 which is an analogue of Caristi-fixed point theorem[2] in a quasi-metric space. Necessity of conditions in Theorem 1.2 has been examined by giving suitable examples. Continuity of fixed points has also been discussed.

Definitions

We start with necessary definitions :

Definition 1.1 : A quasi-metric p on a nonempty set X is a non-negative real valued function $p(,)$ on $X \times X$ satisfying

(i) $p(x, y) = 0$ if and only if $x = y (x, y \in X)$

(ii) $p(x, z) \leq p(x, y) + p(y, z)$; $(x, y, z \in X)$.

Let $p(,)$ be a quasi-metric on X, then in a natural way there arises another quasi-metric $q(,)$ on X called conjugate of $p(,)$, defined by $q(x, y) = p(y, x) : (x, y \in X)$. Sets of the form $\{y : p(x, y) < r\}$ $(r > 0)$ as $x \in X$ give rise to topology τ_p over X. Similarly, q gives rise to a topology on X. The topology on (X, p) is defined by τ_p.

Definition 1.2 : A sequence $\{x_n\}$ of X is said to be p-cauchy if and only if for $\varepsilon > 0$, $\exists\, m$ such that

$$p(x_r, x_s) < \varepsilon \quad \text{whenever} \quad r > s \geq m$$

A sequence $\{x_n\}$ in X is said to p-converge to a limit ξ in X if and only if $p(\xi, x_n) \to 0$ as $n \to \infty$ and in this case $\{x_n\}$ is called p-convergent.

Definition 1.3 : (X, p) is said to be complete if and only if every p-cauchy sequence in X is p-convergent in X.

Definition 1.4 : In a quasi-metric space (x, p), a mapping $T : (X, p) \to$ itself is said to be orbital continuous at $x_0 \in X$ if for some $u \in X$, $p(U, x_{n_i}) \to 0$ gives $p\,(T(u), T(x_{n_i})) \to 0$.

where $\{x_{n_i}\}$ is a sequence of $\{x_n\}$ such that $x_1 = T(x_0), x_2 = T(x_1),\ldots\ldots, x_n = T(_{x_{n-1}}),\ldots\ldots\ldots\ldots,$

T is said to be orbitally continuous if T is so at all points of X.

Theorems

Theorem 1.1 : Let (X, p) be a complete quasi-metric space. Let $T : X \to X$ satisfy

(i) $p(tx, ty) \le \alpha[q(x,Tx) + q(y,Ty)] + \beta p(x, y)$

where $\alpha \ge 0, \quad \beta \ge 0$ and $Z\alpha + \beta < 1$

(ii) T is p-orbitally continuous at some point x_0 of X.

Then there is a unique fixed point of T in X.

Proof : Define $\{x_n\}$ in X where $x_n = T^n x_0, x_{n+1} = Tx_n, \; n = 0, 1,2,\ldots\ldots$

without loss of generality, assume $x_n \neq x_{n+1}$; then

$$p(x_2, x_1) = p(Tx_1, Tx_0)$$
$$\le \alpha[q(x_1, Tx_1) + q(x_0, Tx_0)] + \beta\, p(x_1, x_0)$$
$$= \alpha p(x_2, x_1) + \alpha q(x_0, x_1) + \beta\, q(x_0, x_1)$$

or $\quad p(x_2, x_1) \le \dfrac{\alpha+\beta}{1-\alpha}\; q(x_0, x_1)$

$$p(x_3, x_2) = p(Tx_2, Tx_1)$$
$$\le \alpha[q(x_2, Tx_2) + q(x_1, Tx_1)] + \beta\, p(x_2, x_1)$$
$$= \alpha\, p(x_3, x_2) + \alpha\, q(x_1, x_2) + \beta\, q(x_1, x_2)$$

or $\quad p(x_3, x_2) \le \left(\dfrac{\alpha+\beta}{1-\alpha}\right) q(x_1, x_2)$

$$= \left(\frac{\alpha+\beta}{(1-\alpha)}\right) p\;(x_2, x_1)$$
$$\le \left(\frac{\alpha+\beta}{1-\alpha}\right)^2 q\;(x_0, x_1)$$

and proceeding this way we have

$$p(x_{n+1}, x_n) \leq \left(\frac{\alpha+\beta}{1-\alpha}\right)^n q(x_0, x_1) = r^n q(x_0, x_1) \tag{1}$$

where $r = \dfrac{\alpha+\beta}{1-\alpha} < 1.$

$$\therefore p(x_{n+p}, x_n) \leq p(x_{n+p}, x_{n+p-1}) + \ldots\ldots + p(x_{n+1}, x_n) \leq \left[r^{n+p-1} + \ldots\ldots + r^n\right] q(x_0, x_1)$$

$$< \frac{r^n}{1-r} q(x_0, x_1) \to 0 \quad \text{as} \quad n \to \infty$$

which implies that $\{x_n\}$ is a p-cauchy sequence in X. By completeness of X, there exists $U \in X$ such that p-lim $x_n = u$. By orbital continuity of T,

$$p - \lim T x_n = Tu \text{ i.e. } p - \lim x_{n+1} = Tu, \text{ i.e. } u = Tu$$

which shows that u is a fixed point of T. To prove uniqueness, let $v \in X$ be another fixed point of T.

Thus, $p(u, v) = p(Tu, Tv) \leq \alpha[q(u, Tu) + q(v, Tv)] + \beta p(u, v)$

i.e. $p(u, v) \leq \beta(u, v)$; a contradiction. Hence $u = v$.

Remark : In case p is a metric $= d$ over X, we observe that condition (ii) of Theorem 1.1 is redundant. Because, from (1) we have

$$\sum_{n=0}^{\infty} d\left(T^{n+1}x, T^n x\right) < \infty$$

and, hence Theorem 2 of Bollenbacher and Hicks[3] applies to ensure existence of a lower semi continuous (l.s.c.) function φ over X to satisfy

$$d(Tx, x) \leq \varphi(x) - \varphi(T(x)), \text{ for } x \in X.$$

Thus we arrive at Caristi-fixed point theorem[2], an application of which ends with fixed point of T :

However, over a quasi-metric space we now prove Theorem 1.2 which is an analogue of Caristi-fixed point theorem.

Theorem 1.2 : Let (X, p) be a complete quasi-metric space and let T be a mapping of X into itself. Let $\varphi : X \to R^+$ satisfy

$$p(Tx, x) \leq \varphi(x) - \varphi(T(x)), \quad x \in X \tag{2}$$

If T is orbitally continuous at $x = x_0$ then p-lim $T^n x = u$ exists and $Tu = u$.

Proof : Define $\{x_n\}$ in X where $x_n = T^n x_0$, i.e. $x_{n+1} = Tx_n$, $n = 0, 1,2,\ldots\ldots$, without loss of generality let, $x_n \neq x_{n+1}$. Then

$$p(x_{n+1}, x_n) = p(Tx_n, x_n) \leq \varphi(x_n) - \varphi(x_{n+1})$$

$$\therefore \sum_{v=1}^{n} p(x_{v+1}, x_v) \leq \varphi(x_1) - \varphi(x_{v+1}) \leq \varphi(x_1).$$

Hence,

$$\sum_{v=1}^{\infty} p(x_{v+1}, x_v) < \infty.$$

This implies that $\{x_n\}$ is a p-cauchy sequence in X. By completeness of X, there exists $u \in X$ such that p-lim $x_n = u$. By orbital continuity of T at x_0, we have p-lim $Tx_n = u$.

i.e. $p - \lim x_{n+1} = Tu$

$\therefore \quad u = Tu$

which shows that u is a fixed point of T.

We now examine necessity of conditions of Theorem 1.2.

Example 1.1 beow shows that one cannot dispense with condition (2) of Theorem 1.2.

Example 1.1 : Let us consider that complete metric space $X = \{0\} \cup [1, \infty]$ with usual metric of reals; and let $T : X \to X$ be defined by

$T(x) = 0$, $1 \leq x < \infty$ and $T(0) = 1$.

T has no fixed point inspite of it being orbitally continuous at $x = 0$. However, we show that there does not exist such a function φ as to satisfy condition (2) of Theorem 1.2. Because, assuming the contrary, we have

$$d(T0, 0) = d(1,0) = 1 \leq \varphi(0) - \varphi(1).$$

and

$$d(T1,1) = d(0,1) = 1 \leq \varphi(1) - \varphi(0).$$

This is impossible.

On the other hand one cannot delete condition of orbital continuity of T from Theorem 1.2 either. Example 1.2 below supports this contention.

Example 1.2 : Consider the complete metric space $X = \left\{\frac{1}{n}\right\} \cup \{0\}$ with usual metric of reals and let $T : X \to X$ be defined by

$$T\left(\frac{1}{n}\right)=\frac{1}{n+1},\ n\geq 1 \text{ and } T(0)=1.$$

Here T has no fixed point. It is a routine exercise to see that T is nowhere orbitally continuous over X.

We now construct a function $\varphi : X \to R^+$ to satisfy condition (2) of Theorem 1.2.

Take $\varphi(0)=3$ and $\varphi\left(\frac{1}{n}\right)=\frac{2}{n}$ for $n\geq 1$.

Here, we have

$$d\left(\frac{1}{n},T\left(\frac{1}{n}\right)\right)=\frac{1}{n(n+1)}<\frac{2}{n(n+1)}=\varphi\left(\frac{1}{n}\right)-\varphi\left(T\left(\frac{1}{n}\right)\right);$$

Further $d(0,T(0))=1=\varphi(0)-\varphi(T(0))$

and $d(1,T(1))=\frac{1}{2}<1=\varphi(1)-\varphi(T(1))$

Thus φ satisfies condition (2) of Theorem 1.2.

Continuity of Fixed Points

We give Theorems 2.1 and 2.2 below in respect of continuity of fixed points in the setting of quasi-metric space. Their proofs run close to those of analogous theorems involving a restricted class of mappings in metric spaces as proved by Ray[4]. We include proof of Theorem 2.1 only to show the difference; and proof of Theorem 2.2 is left out by making reference to Ray[4].

Theorem 2.1 : Let (X, p) be a complete quasi-metric space, let $T_i : X \to X$ be a mapping with a fixed point u_i for $i = 0, 1,2,\ldots\ldots$ and let $\{T_i\}_{i=1}^{\infty}$ converge uniformly to T_0. If

$$p(T_0(x), T_0(y)) \leq \alpha\left[p(x,T_0(x))+q(y,T_0(y))\right]+\beta\, p(x,y)$$

for $x, y \in X$ and α is positive and $0 \leq \beta < 1$; Then $\{u_i\}$ p–converges to u_0.

Proof : Let $\varepsilon > 0$ be given. By uniform convergence of $\{T_i\}$ to T_0, there is an index N such that

$p(T_0x, T_ix) < \varepsilon\left(\frac{1-\beta}{1+\alpha}\right)$ for all $x \in X$ and $i \geq N$. Then

$$p(u_0,u_i) = p\big(T_0(u_0), T_i(u_i)\big)$$
$$\leq p\big(T_0(u_o)T_0(u_i)\big) + p\big(T_0(u_i), T_i(u_i)\big)$$
$$\leq \alpha\Big[p\big(u_0,T_0(u_0)\big) + q\big(u_i,T_0(u_i)\big)\Big] + \beta\ p(u_0,u_i) + p\big(T_0(u_i),T_i(u_i)\big)$$
$$\leq \alpha\ p\big(T_0(u_i),T_i(u_i)\big) + \beta P(u_0,u_i) + p\big(T_0(u_i),T_i(u_i)\big)$$

or $p(u_0,u_i) \leq \left(\frac{1+\alpha}{1-\beta}\right) p\big(T_0(u_i),T_i(u_i)\big) < \varepsilon\left(\frac{1+\alpha}{1-\beta}\right)\left(\frac{1-\beta}{1+\alpha}\right) = \varepsilon$

i.e. $p(u_0,u_i) < \varepsilon$ whenever $i \geq N$.

Theorem 2.2 : Let (X, p_0) be a complete quasi-metric space and let $\{p_n\}$ be a sequence of quasi-metrics on X converging uniformly to $\{p_0\}$. Let $\{T_n\}$ be a sequence of mappings converging to p_0-pointwise to a mapping T_0 with fixed point u_0, and let each T_n having fixed point u_n satisfy

$$p_n(T_n x, T_n y) \leq \alpha\big[p_n(x, T_n x) + q_n(y, T_n y)\big] + \beta\ p_n(x, y),$$

where $x, y \in X$ and α is positive and $0 \leq \beta < 1$.

Then $\{u_n\}$ p_0-converges to u_0. The proof is similar to that of Theorem 3.2 of Ray[4] and is left out.

Theorems 2.1 and 2.2 at once generalise Theorems 3.1 and 3.2 of Ray[4] respectively and we remark that uniform convergence of $\{p_n\}$ in Theorem 2.2 cannot be relaxed by pointwise convergence. This is evident from the example constructed by Ray[4] in the setting of metric spaces. Also one cannot weaken uniform convergence of $\{T_n\}$ to pointwise convergence in Theorem 2.1. This is supported by Example given below :

Example : Take $X = \{0\} \cup \left\{\frac{1}{2^i}\right\} \cup \{1\}$,

with usual metric of reals. Then X is a complete metric space.

Define $T_n : X \to X$, as follows :

$$T_n(0) = T_n(1) = 1, \text{ for all } n \text{ ; and } T_n\left(\frac{1}{2^i}\right) = \frac{1}{2^n}, \text{ if } i = n$$
$$= 1, \text{ if } i \neq n.$$

Then $\{T_n\}$ converges pointwise to T_0 over X where $T_0 : X \to X$, is given by $T_0(x) = 1$ for all $x \in X$. Here T_0 satisfies requirement of Theorem 2.1 with fixed point = 1. Also T_n has fixed point = $1/2^n$; but $1/2^n$ does not converge to fixed point of T_0.

References

1. Kelly, J.C. (1963) *Proc. Lond. Math. Soc.* **13** : 71.
2. Caristi, J. (1976) *Trans. Amer. Math. Soc.* **215** : 241.
3. Bollenbacher, A. & Hicks, T.L. (1988) *Proc. Amer. Math. Soc.* **102** : 898.
4. Ray, B. (1973) *Colloquium Mathematicum* **27** : 41.

PROC. NAT. ACAD. SCI. INDIA, 61 (A), II, 1991

Photoacoustic spectra of some nitrobenzene derivatives

(Key words : photoacoustic spectra/electronic absorption spectra/1-chloro-2, 4-dinitro, 2,5-dibromo & 3,4-dichloro nitrobenzenes/C_s symmetry)

L. N. TRIPATHI and A. P. UPADHYAY*

Department of Physics, University of Gorakhpur, Gorakhpur-273 009, India.

**Department of Physics, National P.G. College, Barhalganj, Gorakhpur-273 402, India.*

Received November 11, 1989; Revised April 10, 1990; Accepted June 6, 1990

Abstract

The photoacoustic spectra (PAS) of solid samples of 1-chloro-2, 4-dinitro, 2,5-dibromo and 3,4-dichloro nitrobenzenes have been recorded and analysed in the light of their solution absorption spectra. The PAS of all the samples show three band systems. The longest wavelength band system III, attributed to n-π^* transitions, has been found to develop sharply in PAS whereas it developed weakly in their U.V. solution phase spectra.

Introduction

The photoacoustic spectroscopy is a technique to study spectra of solids and semi-solids[1-9]. In this technique, heat is generated in a sample through non-radiative processes following the periodic illumination and consequent absorption of light by the sample. This technique measures the amount of absorbed optical energy de-excited through non-radiative processes and, therefore, the PAS corresponds qualitatively to optical spectrum and this has been used in identification[10] of the substances. In this work, we report PAS of 1-chloro-2, 4-dinitro, 2,5-dibromo and 3,4-dichloro nitrobenzenes along with their solution absorption spectrum. Analysis of the PAS has been proposed in the light of their solution absorption spectrum, because a comparison of PAS with their solution absorption spectra suggests a possible method of identifying different electronic band systems in a PAS[11].

Materials and Methods

The samples investigated *viz.* 1-chloro-2, 4-dinitro, 2, 5-dibromo and 3,4-dichloro nitrobenzenes were obtained from Koch-Light Laboratories, England. The PAS of all the three solid samples were recorded using Princeton applied research model-6001 spectrophotometer with 1 kW xenon arc lamp. The modulation frequency of 40 Hz was used with monochromator slit of slit width 2 mm in frequency region 200-500 nm. The scan rate was set at 200 nm/min. The electronic absorption spectra of these samples in methanol solution were recorded using (i) Carey-14 spectrophotometer in region 200-800 nm and (ii) Cary-2300 spectrophotometer in region 200-300 nm. The prominent features in photoacoustic and solution spectra are given in Table 1. The electronic origin of band systems I, II and III in PAS and the optical electronic spectra of the molecules are given in Table 2.

The PAS of 1-chloro-2, 4-dinitro, 2,5-dibromo and 3,4-dichloro nitrobenzenes show three regions of absorption. Each absorption region comprises of a main peak (most intense peak of the region) and a number of secondary absorption peaks of varying intensities.

Table 1 - Wavelength and prominent features in PAS and optical absorption electronic spectra of 1-chloro-2, 4-dinitro, 2,5-dibromo and 3,4-dichloronitrobenzene

Transition	PAS		Electronic spectrum (A)		(B)	
1	2		3			
1-chloro-2, 4-dinitrobenzene :						
Band system I						
	nm	int.	nm	int.	nm	int.
Spectral region :	200 – 224	nm	200 – 222	nm	200 – 225	nm
Most intense peak :	220	ms	210	s	205	vs
Absorption peaks :	205	m	210	s	206	vs
	–		–		208	s
	–		–		212	s
	214	m	–		215	s
	220	ms	–		218	s
			–		222	s
Band system II						
Spectral region :	230 – 280	nm	230 - 280	nm	230 - 280	nm
Most intense peak :	250	s	240	s	245	vs
Absorption peaks :	231	m	–		232	s
	235	m	–		236	s
			–		238	s
	243	ms	–		242	s
	250	s	240	s	245	vs
	258	ms	260	ms	258	s
	264	ms	–		265	s
	–		–		268	s
	272	m	–		273	s
	276	m	–		275	s
Band system III						
Spectral region :	335 – 380	nm	330 - 380	nm	x	x
Most intense peak :		342	ms	350	w	
Absorption peaks :	360	m	–			
	370	m	–			

(Contd.)

Table 1 (contd.)

1	2		3			
2,5-dibromonitrobenzene						
Band system I						
Spectral region :	200 – 227	nm	200 – 225	nm	200 – 220	nm
Most intense peak :	225	ms	220	s	210	s
Absorption peaks :	205	m	–		206	m
	210	m	–		208	m
	–		220	s	210	s
	–		–		212	ms
	215	m	–		214	ms
	225	ms	–			
Band system II						
Spectral region :	230 – 275	nm	225 – 280	nm	220 – 275	nm
Most intense peak :	265	vs	230	s	232	vs
Absorption peaks :	232	s	230	vs	232	vs
	235	s	–		235	s
	240	s	–		238	s
	250	s	–		–	
	255		–		–	
	265	vs	–		–	
	270	s	–		–	
Band system III						
Spectral region :	280 – 370	nm	280 – 380	nm	–	
Most intense peak :	300	vs	310	w	–	
Absorption peaks :	285	s	–		–	
	300	vs	310		–	
	325	s	–		–	
	345	s	–		–	
	360	s	–		–	
3, 4-dichloronitrobenzene						
Band system I						
Spectral region :	200 – 225	nm	200 – 240	nm	200 – 240	nm
Most intense peak :	214	vs	212	vs	212	s
Absorption peaks :			–		202	m
	205	m	–		204	m
			–		207	ms
	208	m	–		210	ms
			212	vs	212	s

(Contd.)

Table 1 (contd.)

1	2		3			
	214	ms	–		218	ms
	220	m	–		222	ms
Band system II						
Spectral region :	235 – 290	nm	245 – 290	nm	245 – 290	nm
Most intense peak :	250	s	270	s	267	ms
Absorption peaks :	248	ms	–		247	w
	250	s	–		252	w
	–		–		255	m
	–		–		257	m
	–		–		262	m
	265	ms	270	s	267	ms
	–		–		277	m
	277	ms	–		–	
Band system III						
Spectral region :	300 – 360	nm	300 – 360	nm	–	
Most intense peak :	328	ms	350	m	–	
Absorption peaks :	312	m	–		–	
	320	m	–		–	
	328	ms	–		–	
	335	m	–		–	
	345	m	350	m	–	
	355	m	–		–	

Table 2 – Electronic origins of bands of 1-chloro-2, 4-dinitro 2,5-dibromo and 3, 4-dichloronitrobenzene

Transition	1–chloro-2, 4-dinitrobenzene			2,5-dibromonitrobenzene			3,4-dichloronitrobenzene		
	PAS nm	Electronic (A) nm	Spectrum (B) nm	PAS nm	Electronic (A) nm	Spectrum (B) nm	PAS nm	Electronic (A) nm	Spectrum (B) nm
System I	224	222	225	227	225	218	225	240	240
System II	280	280	280	275	280	280	290	290	290
System III	380	380	–	370	380	–	360	360	–

Notations : int. = intensity, nm = nanometer, (A) = solution absorption electronic spectrum recorded on Cary-14 spectrophotometer, (B) = Elecronic spectrum recorded on Cary - 2300 spectrophotometer.

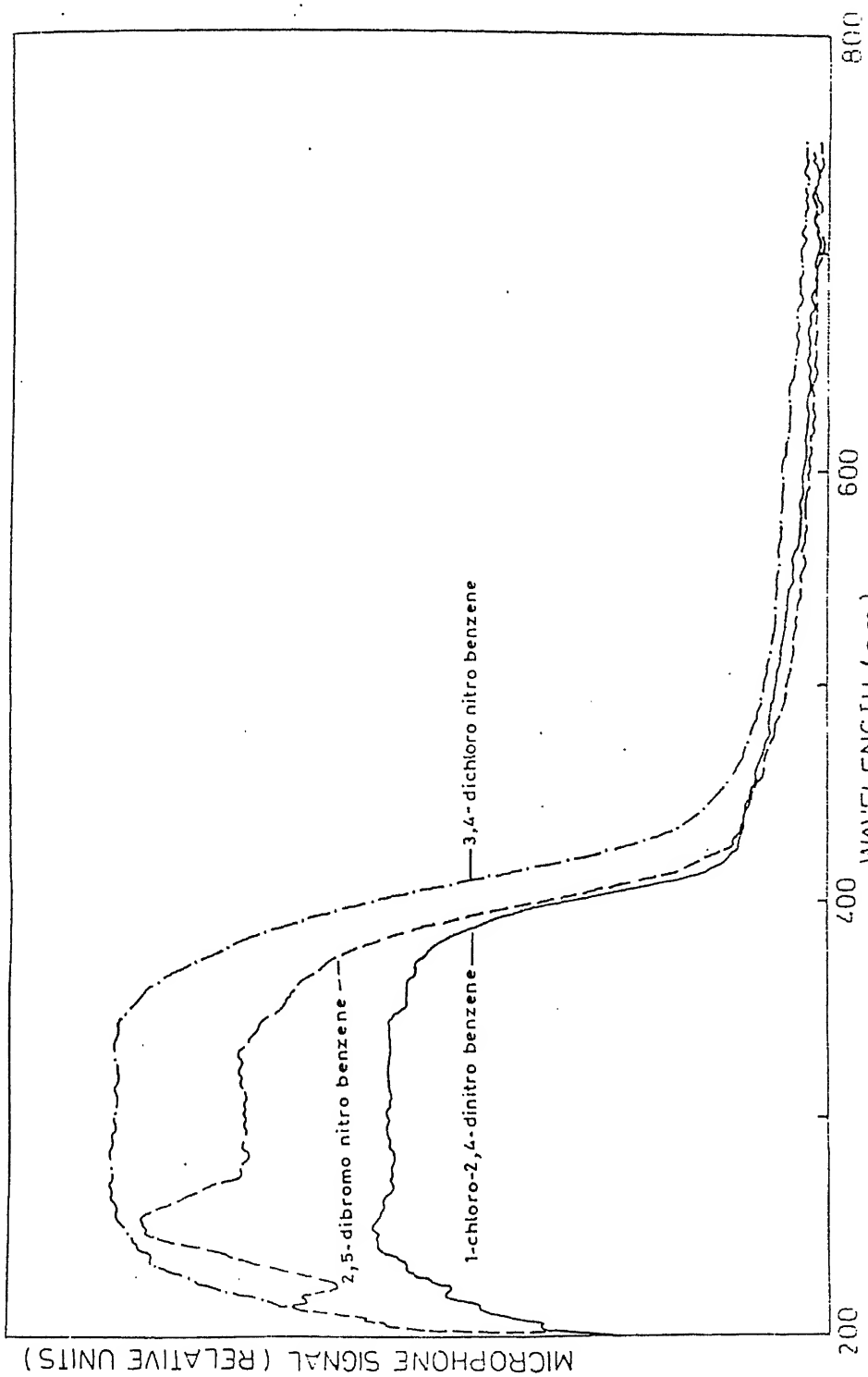

Fig. 1 - Photo acoustic spectra.

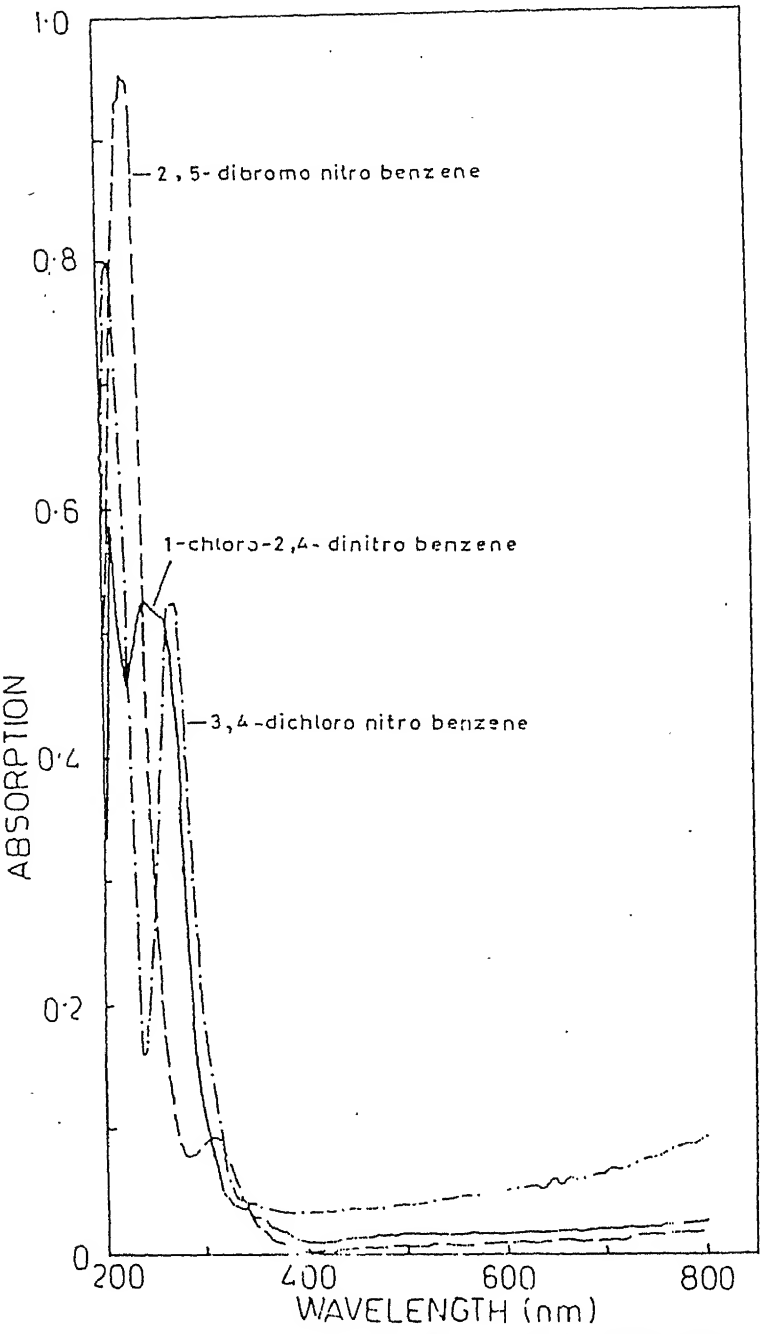

Fig. 2 - Solution absorption spectra on Cary 14, spectrophotometer.

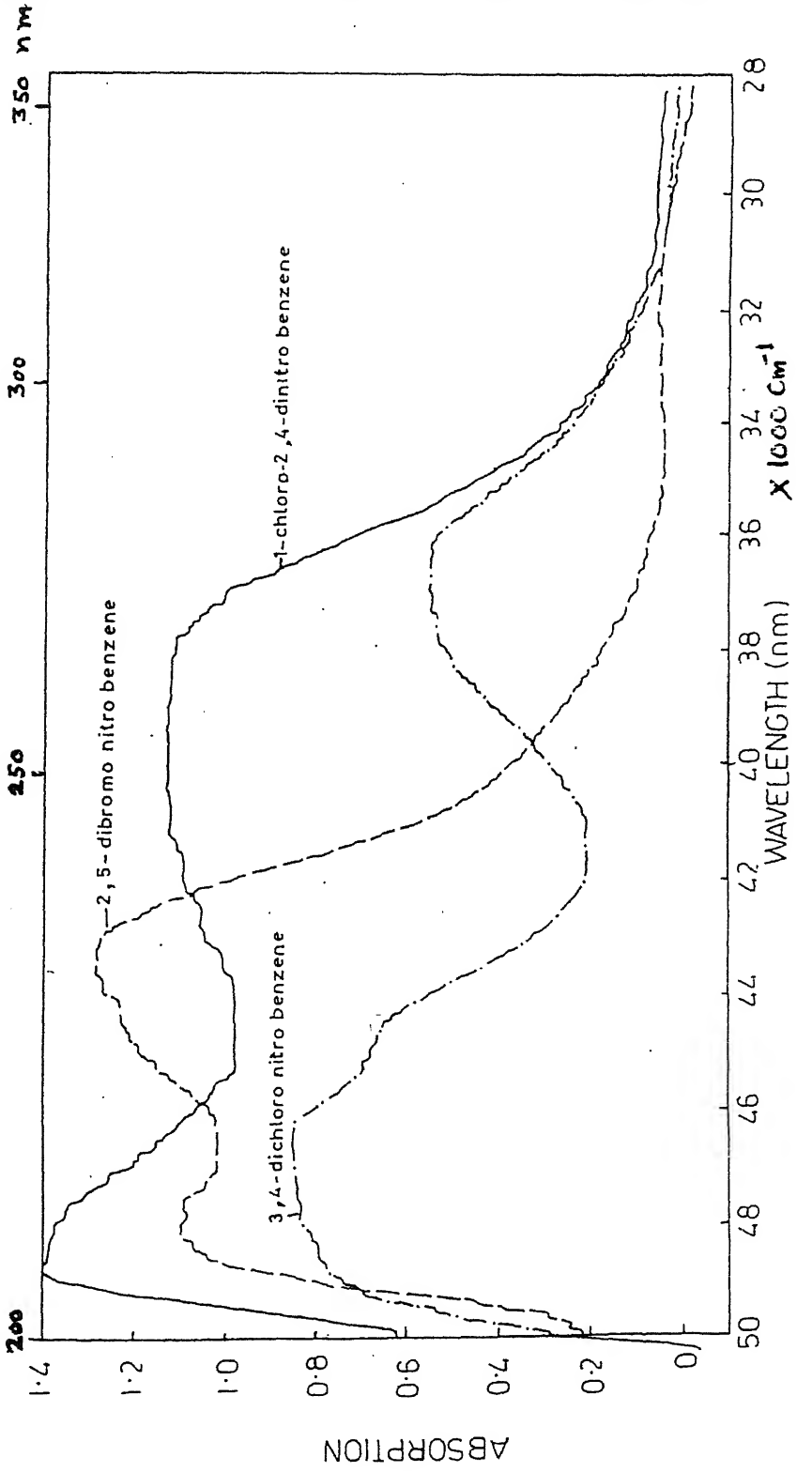

Fig. 3 - Solution absorption spectra on Cary 2300 spectrophotometer.

The PAS of 1-chloro-2, 4-dinitrobenzene (Fig. 1) shows that the distinction between band systems I and II and that between band systems II and III is clearcut. The PAS signals of band system II are stronger as compared to those of systems I and III.

In PAS of 2, 5-dibromonitrobenzene (Fig. 1), the distinction between regions II and III is much confusing. The bands of region II appear to merge into region III. There is no clear cut distinction between systems I and II and between II and III. The band systems II and III are found to develop much sharply compared to the bands of system I.

The PAS of 3, 4-dichloronitrobenzene (Fig. 1) shows that the distinction between band systems I and II is clearcut but it is confusing between band systems II and III. The band system III has been found to develop much sharply as compared to the band systems I and II. The bands of system II appear to merge into region III. The PAS signals of band systems II and III are nearly equally intense. PAS signals of band system I are much weaker as compared to the bands of systems II and III.

The solution absorption spectrum (A) (Fig. 2 & 3) of all the three samples show three band systems in good agreement with the three regions of absorptions in their PAS. The U.V. solution spectrum (B) shows only first two band systems. The band system III is found absent since this spectrophotometer records spectrum in region 200-300 nm. The spectrum (B) exhibits discrete vibrational structure of the first two band systems showing a large number of intense absorption peaks.

Analysis : 1-chloro-2, 4-dinitrobenzene : The PAS shows that the band system I extends the spectral region between 200-224 nm. The main peak lying at 220 nm, the secondary absorption peaks have been measured at 205 and 214 nm with medium intensities. The solution spectra (A) and (B) show this region between 200-225 nm. The spectrum (A) shows only one strong peak at 210 nm whereas the spectrum (B) shows a large number of absorption peaks at 201, 206, 208, 212, 215, 218 and 222 nm with strong intensities. The band observed at 206 nm is the most intense peak of region I. This most intense peak of electronic spectrum (B) at 206 nm which appears at 210 nm in electronic spectrum (A) of the substance may be correlated with the main peak of its PAS at 220 nm. The main peak of PAS of this band system is found to shift to longer wavelength side of the most intense peaks in its electronic optical spectra (A) and (B).

Band system II observed in PAS of this molecule in spectral region 230-280 nm shows main peak at 250 nm with strong intensity. The secondary absorption peaks of this region have been measured at 231, 235, 243, 258, 264, 272 and 276 nm. Both optical spectra (A) and (B) show this spectral region between 230-280 nm which is same as that observed in its PAS. The spectrum (A) shows two absorption peaks at 240 and 260 nm of which the former is more intense. The spectrum (B) shows absorption peaks at 232, 236, 238, 242, 258, 265, 268, 273 and 275 nm. The absorption peak at 245 nm is the most intense peak of band system II in spectrum (B) which appears at 240 nm in spectrum (A) – may be correlated with the main peak of the band system observed in its PAS at 250 nm. The main peak of PAS has been observed to shift to longer wavelength side of the most intense peak of optical spectra (A) and (B).

The longest wavelength band system III attributed to n-π^* transitions has been observed in its PAS in spectral region 335-380 nm with main peak lying at 342 nm and secondary

absorption peaks at 360 and 370 nm. The optical spectrum (A) shows this system in spectral region between 330-380 nm with only one weak absorption maxima at 350 nm. The main peak in its PAS observed at 342 nm may be correlated with the absorption maxima observed at 350 nm in its optical spectrum (A). It is observed that the main peak in its PAS is shifted to lower wavelength side, contrary to the observations of band systems I and II where it shifted to longer wavelength side of the most intense peak of the optical spectra (A) and (B).

Like other substituted benzene derivatives, the first two band systems I and II observed in PAS as well as in optical spectra (A) and (B) of this molecule are attributed to π-π^* transitions of phenyl group corresponding to 2600 A transition $^1B_{2u}$—$^1A_{1g}$ and 2000 A transition $^1B_{1u}$—$^1A_{1g}$ of benzene. The band system III on longest wavelength side is observed by electronic transition localized to a great extent in —NO_2 part of the molecule. This spectra may be explained by considering electrons in n-orbitals as well as in π^*-orbitals giving rise to n–π^* transitions. This electronic transition would correspond to an allowed $^1A''$–$^1A'$ transition of substituted benzenes with C_s symmetry. This molecule shows low vapour pressure at ordinary working condition hence it is very difficult to record its vapour phase absorption spectrum. Thus the PAS studies of n-π^* transition electronic system of this compound may give useful results.

The spectral features of PAS and optical electronic spectra of 2, 5-dibromo and 3, 4-dichloronitrobenzene, showing most intense peak and other absorption peaks of varying intensities, are summarised in Table 1.

Identification of electronic band origin : The identification of electronic origin of bands in PAS is, however, a difficult problem. The electronic origins of each band system in PAS of 1-chloro-2,4-dinitro, 2,5-dibromo and 3,4-dichloronitrobenzenes alongwith the electronic origin of bands in their solution absorption spectra (A) and (B) are given in Table 2.

The region where the slope of PAS contour changes on longer wavelength side of system I around 224, 280 nm in band system II and 380 nm in band system III may be identified as the electronic origins of bands of system I, II and III in PAS of 1-chloro-2, 4-dinitrobenzene.

Likewise, the electronic origins of bands of systems I, II and III in PAS of 2,5-dibromo and 3,4-dichloro nitrobenzens have been identified and listed in Table 2.

Results and Discussion

The PAS and the solution spectra (A) of 1-chloro-2, 4-dinitro, 2,5-dibromo and 3,4-dichloronitrobenzenes show three absorption regions in good agreement with the three spectral regions of their optical solution absorption spectra. Region III is found absent in solution spectra (B) because this records spectrum in region 200-300 nm only.

The non-radiative transitions of system I in PAS of all the molecules become less and less effective as compared to band systems II and III. The photoacoustic signal is directly related to the loss of excitation energy by non-radiative processes. Although it is difficult to draw conclusion about individual molecules, we notice regularity in the present group of molecules. It is found that the non-radiative transitions in region I becomes less and less effective compared to those in regions II and III, the order being 1-chloro-2,4-dinitro<3,4-dichloro- < 2, 5-dibromo-nitrobenzenes. This trend may be correlated with the electro

negativity of the substituents.

Conclusion : The band system III attributed to n–π^* transitions is found to develop much sharply in their PAS compared to that in their U.V. solution phase spectra. The band system III in their PAS shows a large number of absorption bands showing strong intensities. Thus PAS studies of n–π^* transition in 1-chloro-2 4-dinitro, 2,5-dibromo and 3, 4-dichloro-nitrobenzenes, for which it is difficult to record vapour absorption spectrum at ordinary working conditions, may give useful informations.

The three regions of absorptions observed in PAS are found to be in good agreement with those of the spectral regions and other features of their solution absorption spectra. This shows that the PAS and the solution absorption spectra correspond qualitatively to each other.

Acknowledgements

The authors express their grateful thanks to the Incharge of Central Instrumentation Laboratory, Hyderabad University and Regional Sophisticated Instrumentation Centre, I.I.T., Madras for giving permission to record PAS and U.V. solution phase spectra respectively and to Dr. P.K. Tripathi, Scientist, National Chemical Laboratory, Pune for his help in recording U.V. solution phase spectra. They also thank Professor K.N. Upadhyay of B.H.U. for encouragement and cooperation.

References

1. Kirkbright, G.F. & Costlenden, S.L. (1980) *Chemistry in Britain* **16** : 661.
2. Marchetti, A.P. & Keams, D.R. (1967) *J. Amer. Chem. Soc.* **89** : 768.
3. Rosenowaig, A. (1973) *Opt. Commun.* **7** : 305.
4. Rosenowaig, A. (1973) *Science* **181** : 657.
5. Sosenowaig, A. (1975) *Anal. Chem.* **47** : 592.
6. Rosenowaig, A. (1975) *Phys. Today* **28** : 23.
7. Rosenowaig, A. (1978) *Advances in electronics and electron physics*, Academic Press, New York.
8. Rai, V. N. & Thakur, S.N. (1981) *Physics News* **12** : 102.
9. Rai, V.N., Singh, J.P. & Thakur, S.N. (1981) *J. Res. & Industry* **26** : 165.
10. Rosenowaig, A. & Hall, S.S. (1975) *Anal. Chem.* **47** : 548.
11. Pandey, V.N. & Thakur, S.N. (1980) *J. Mol. Struct.* **68** : 67.

PROC. NAT. ACAD. SCI. INDIA, 61(A), II, 1991

Semi-empirical molecular orbital studies on the electronic structure of mono and di amino substituted benzenes

(Key words : MINDO/3 molecular orbital techniques/aniline/isomeric diamino benzenes/oxidation number/ionization potential/dipole moment/bond order index/valence index)

AJAI KUMAR*, J.S. YADAV** and O.P. SINGH

**On academic leave from L.B.S. (P.G.) College, Gonda-271 001, India.*
Department of Physics, M.L.K. (P.G.) College, Balrampur-271 201, India.
***Department of Chemical Engineering and Chemistry, New Jersey Institute of Technology, Newark, NJ 07102, U.S.A.*

Received December 11, 1989; Revised June 11, 1990; Accepted July 14, 1990.

Abstract

MINDO/3 semi-empirical molecular orbital technique has been used to calculate bond order indices, valence indices, oxidation numbers, ionization potentials, dipole moments etc. of aniline and isomeric diamino benzenes. The computed bond orders, the valence indices and ionization potentials are found very close to their corresponding classical values and experimental observations respectively. The reactivities of different atoms in terms of Jug's hyper-, normal- and sub-valences are discussed in terms of their affinities for covalent bond formation.

Introduction

One of the main objectives of the molecular orbital studies on the electronic structure of molecules is to elucidate the nature of the classical chemical bond in terms of quantum chemical parameters. Indices like bond order, valence and atomic charges are such classical concepts which have been not only used to parameterize and distinguish different bonding situations but also they represent useful link between the quantum chemical results and classical concepts. Despite the availability of better computation facilities, the quantum chemical calculations at *ab initio* level are expensive[1] even for small and medium size molecules. Therefore, semi-empirical methods are still employed to get the structural and electronic aspects of organic molecules[2]. Recently modified neglect of differential overlap and final version of modified intermediate neglect of differential overlap (MINDO/3) semi-empirical methods of Dewar's group[3,4] have proven to be alternate to the *ab initio* method[5].

The electronic structure of substituted benzenes are of basic importance for a deeper understanding of their reactivities and spectral properties. The complete neglect of differential overlap (CNDO) and intermediate neglect of differential overlap (INDO) semi-empirical methods have been used to study the electronic structures and geometries of some substituted benzenes[6,7]. A qualitative prediction of molecular geometry, both at MNDO semi-empirical and *ab initio* STO-3G SCF formation, has been carried out for some fluoro benzenes[8-10]. Several papers on bond order concept in semi-empirical formalism have been published which refer to bond quantities[11], bond order[12,13], bond indices[14] or bond overlap[15] but most of them actually mean a property other than the valence multiplicity. Furthermore, Jug in his subsequent papers[16-19], distinguished the bond order from the bond index[20-22]. The former is based on the evaluation of eigen values by diagonalising the inter-atomic part of the density matrix whereas the later is a function of the square of the density matrix elements. In addition

to this, in the same publication, he also provided a definition of valence index which is *ab initio* analogy of Mayer's definition.

Since we have continued interest in the electronic structure of substituted benzenes, we reported our results on these indices for several benzenes derivatives involving – F, – Cl, – OH, – NH_2 and – CH_3 as substituents in *ab initio* SCF theory[8-10,23-27], using Mayer's[28,29] and Giambiagi's[30] definitions for bond orders, valence indices and oxidation numbers, respectively. In above publications we have preferred Mayer's method over Elliott and Richard's method for the computation of bond orders from *ab initio* molecular wave functions based on Dean and Richard's[31] charge partition technique as the later method needs further parameterization for bonds other than C–C.

Another useful concept for describing and interpreting the extent of electron transfer to or from the vicinity of a given molecule in a molecular environment and during the course of chemical reaction is the oxidation number. Unfortunately, no reliable theory is yet available for direct evaluation of the oxidation number and only qualitative quantum chemical approaches based on population analysis[32] or electron density distribution[33-35] are available. Recently Iwata[36] obtained analytical expressions for the number and density of electrons in a sphere centered at an arbitrary point, provided that the wave-functions are of Gaussian type. Using this method Takano *et al.*[37,38] have systematically studied a series of compounds to elucidate the concept of oxidation number but some ambiguities still exist. On the other hand Giambiagi *et al.*[30] have defined oxidation number in terms of bond order indices and found it very useful for neutral species. In our earlier paper[26] we have applied Giambiagi's definition[30] to calculate oxidation numbers for some benzene derivatives at *ab initio* level. Seeing the cost and time factor involved in the above *ab initio* calculations and suitability of MINDO/3 semi-empirical method, it was thought worthwhile to evaluate above parameters using Jug's and Giambiagi's definitions with MINDO/3 method and to see whether or not such calculations could be helpful in electronic structure studies.

The main purpose is therefore, to provide reliable and fairly accurate information on the electronic structures of some amino-benzenes. In the present paper, we have evaluated bond orders, valence indices, exidation numbers, dipole moments and ionization potentials with MINDO/3 method for some amino-benzenes. We have already reported[39] the above parameters with the same technique for some fluoro derivatives of benzene. The results are discussed in the light of available experimental and other theoretical findings.

Computational Details

Gopinathan and Jug[21,22] suggested that the bond order matrix is sub divided into blocks referring to the atoms $A,B,C,\ldots\ldots\ldots\ldots L$ in the molecule as

$$P = \begin{bmatrix} P^{AA} & P^{AB} & P^{AC} \ldots\ldots\ldots P^{AL} \\ P^{BA} & P^{BB} & P^{BC} \ldots\ldots\ldots P^{BL} \\ P^{LA} & P^{LB} & P^{LC} \ldots\ldots\ldots P^{LL} \end{bmatrix} \quad (1)$$

where P^{AA} refers to charge and hybridization on atom A and P^{AB} refers to the bond between atoms A and B.

The diatomic portion of P matrix represented by

$$P^{AB} = \begin{bmatrix} 0 & P^{AB} \\ P^{BA} & 0 \end{bmatrix} \tag{2}$$

is now diagonalised to get the characteristic eigenvalues λ_i corresponding to bond order orbitals (BOOs) and eigenvectors of this matrix. The eigen values are seen to appear in pairs. Gopinathan and Jug[21,22] defined the bond order B_{AB} between the atoms A and B and valence index V_A of atom A in terms of eigenvalues λ_i as

$$B_{AB} = \sum_{i}^{+ve} \lambda_i^2(AB) \tag{3}$$

$$\text{and} \quad V_A = \sum_{B \neq A}^{i} \sum_{i}^{+ve} \lambda_i^2(AB) \tag{4}$$

respectively.

A further diagonalization of the intra-atomic part P^{AA} of the matrix P reproduces the eigenvalues (orbital occupancies) referred to as natural hybrid orbitals (NHOs). These eigenvalues can be used to define the valence index V_A by the equation

$$V_A = \sum_{a} \left(2q_a - q_a^2 \right) \tag{5}$$

a's being number of atomic orbitals centered on A and q's are their respective occupancies.

Lastly the same operation applied on the 'complete' off diagonal sub-matrix defined by equation of Gopinathan and Jug[21] yields the corresponding natural bond orbitals (NBOs) eigenvalues ξ_i and are used to define the valence index of atom A by the equation

$$V_A = \sum_{i}^{+ve} \xi_i^2 \tag{6}$$

These eigenvalues also appear in pairs. The percentage "excess valence" of different atoms in the molecule has also been calculated in MINDO/3 method by the expression

$$E_A = \left(V_A^r - V_A \right) \times 100 / V_A^r \tag{7}$$

where V^r_A is the reference valency of atom A and V_A is its valency in the molecule under consideration. Following Mayer's suggestion[40,41] we use the term "excess valence" instead of Gopinathan and Jug's "free valence" in order to avoid the use of latter in two different meanings. The definition of normal–, hyper– and sub-valence are given in Gopinathan and Jug's papers[21,22].

Giambiagi *et al.*[30] defined the oxidation number Ξ_A of an atom by the relation

$$\Xi_A = \left(|Q_A|/Q_A\right) \sum_{A \neq B} B_{AB} \tag{8}$$

where Q_A is the net charge on A and the sum is carried out over all the atoms with a polarity different from that of A.

The MINDO/3 program is used as such to evaluate net charges, ionization potentials and dipole moments and extended to incorporate Jug's and Giambiagi's suggestions to calculate bond orders, valence numbers and oxidation numbers respectively.

Each one of the molecule under consideration has been treated as planar with all the ring angles of 120°. The successive substituents ground state geometry has been taken from the Landolt-Bornstein[42] table. The C–C, C–H, C–N and N–H bond lengths are 1.397, 1.084, 1.420 and 1.040 A° respectively and $\angle$ C–N–H is 126.5°.

Results and Discussions

Bond orders and valence indices : The calculated bond order and valence indices as defined by Gopinathan and Jug[21,22] for mono and di amino benzenes are shown in Fig. 1 which shows that the magnitudes of the above parameters are very close to the values required classically. It is interesting to note that the eigenvalues λ_i in semi-empirical theory are obtained just by diagonalising the two centre parts of the bond order matrix whereas in *ab initio* SCF theory one has to use the modified density matrix (orthogonalised basis sets) and then diagonalising its two centre parts in order to get the value of λ_i. The modified density matrix with orthogonalised basis sets can be obtained by applying Lowdin's orthogonalisation technique[43] on the coefficient matrix with unorthogonalised basis sets. Eqn. (3) is used to evaluate bond orders from these eigenvalues. These eigenvalues occur in pairs i.e. $\pm \lambda_i$ satisfying the pairing theorem[21,22]. Thus the eigenvectors corresponding to the positive and negative eigenvalues refer to bonding and anti-bonding orbitals. Obviously the smallest positive eigenvalue corresponds to the interaction of two basis functions which remain virtually unaffected during molecular formation.

Similar to our prior studies[39] the magnitude of the bond order of C–C bonds attached to the substituent bond is found to have smallest value than the magnitudes corresponding to other C–C bonds. However, the magnitude of the C_6–C_1 bond in o-diamino benzene differs considerably from the C_1–C_2 bond because of the fact that the C_1–C_2 bond is flanked by substituent –NH_2 and therefore, reducing its magnitude of bond order. Furthermore if we compare the magnitude of bond order of C_1–C_2 bond for aniline and p-diaminobenzene, we find both of them almost equal (a difference of 0.009) which means that the C_1–C_2 bond is least influenced by the presence of another substituent –NH_2 at para position.

Unlike the C–H bonds, the magnitude of bond orders of N–H bonds in all the molecules is the same indicating that they are unaffected with the position of the substituents.

Valence indices computed using bond order matrix from (i) sum of the squares of the positive eigenvalues of the BOOs of the appropriate diatomic blocks (eqn.4), (ii) occupancies

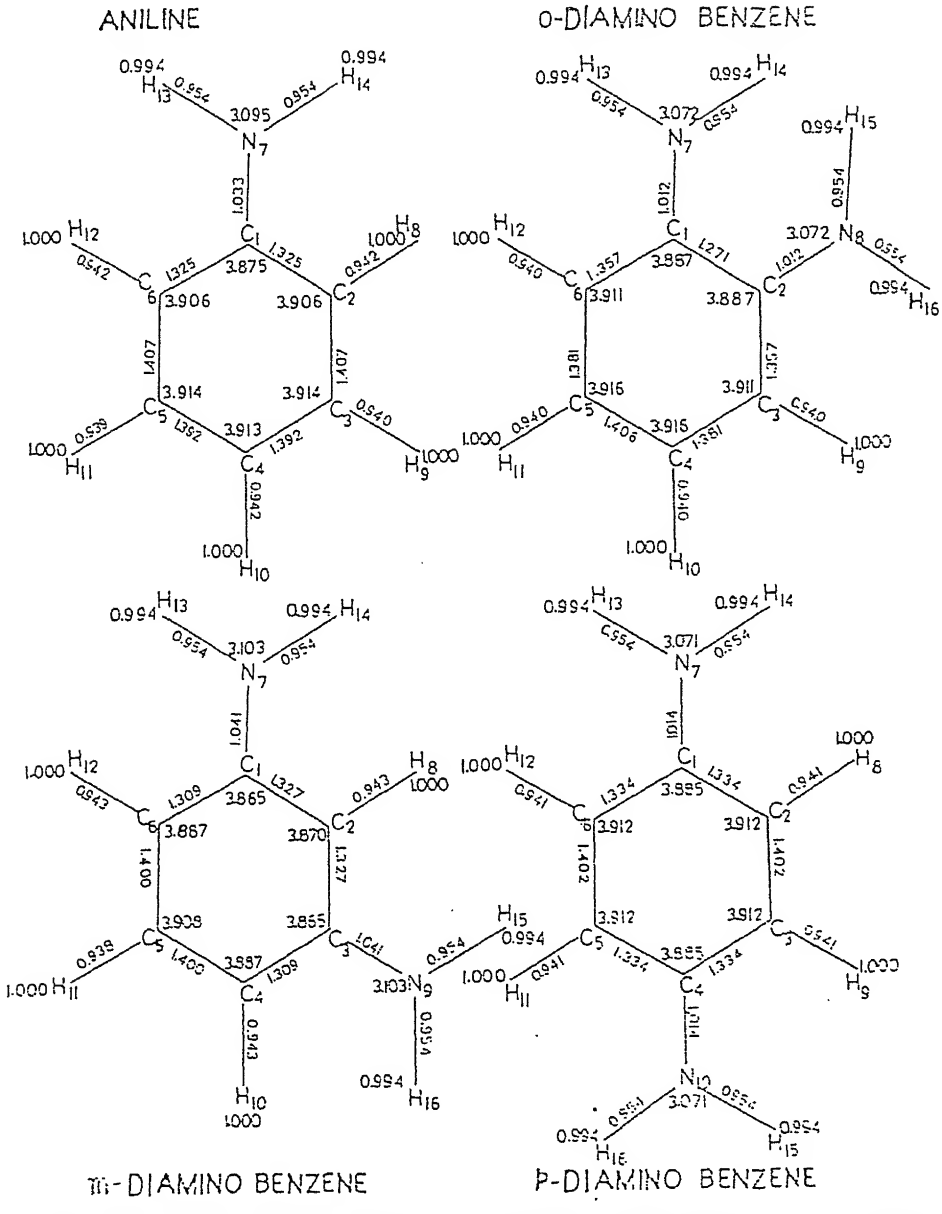

Fig. 1 – Bond order indices of different bonds and valence indices of different atoms shown along the side of bonds and on the site of atoms respectively (NBOs, NHOs and BOOs values of valence indices have been found coincident)

of the NHOs (eqn.5), (iii) sum of the squares of the positive eigenvalues of the NBOs (eqn. 6) lead to the same values as summarised in Fig. 1. It is obvious from Fig. 1 that the calculated valence index values are very close to those coming from classical concepts. It is to be mentioned that σ and π separability is maintained as one of the NHOs remains an unchanged 2ρ orbital as is seen from the fact that diagonalisation does not affect the occupancy of this orbital. Similar results have also been found in earlier studies[9,39].

In an attempt to explore the further possibility of covalent bond formation Mayer[28,29,40,41] proposed an idea of 'excess valence' and 'valence defect'. One can easily see (Table 1) that the "excess valence" for all the hyper valent nitrogen atoms and "valence defect" for rest of the sub-valent atoms are so insignificant that all the atoms of the molecule can be treated as unreactive. The definitions of hyper-, normal and subvalences are given in Gopinathan and Jug's original papers[21,22]. However, the term "free valence" used by them for "excess valence" or "valence defect" is unfortunate because the free valence for closed shell systems should be equal to zero. This difference in the reference and calculated valence indices can be attributed to the delocalization and polarization effects. It should be mentioned that we are dealing with the reactivity as a tendency for covalent bond formation, nucleophilic or electrophilic reactivity is thus excluded.

Table 1–Valency and covalent chemical reactivity of mono and di-substituted amino benzenes

Aniline		o-diamino benzene		m-diamino benzene		p-diamino benzene	
Atoms	Free valence (%)[a]	Atoms	Free valence (%)[a]	Atoms	Free valence (%)[a]	Atoms	Free valence (%)a
C_1	+3.13	C_1	+2.83	C_1	+3.38	C_1	+2.88
C_2	+2.35	C_2	+2.83	C_2	+3.25	C_2	+2.20
C_3	+2.15	C_3	+2.23	C_3	+3.38	C_3	+2.20
C_4	+2.18	C_4	+2.10	C_4	+2.83	C_4	+2.88
C_5	+2.15	C_5	+2.10	C_5	+2.30	C_5	+2.20
C_6	+2.50	C_6	+2.23	C_6	+2.83	C_6	+2.20
N_7	–3.17	N_7	–2.40	N_7	–3.43	N_7	–2.37
		N_8	–2.40	N_9	–3.43	N_{10}	–2.37

*The free valence (%) values of hydrogen atoms in different molecules, not listed in order to reduce the size of the table, are found to have either zero or small free valence values.
A positive and negative signs of free valence values are indicative of sub and hyper valence respectively.

Oxidation numbers and net atomic charges : The calculated MINDO/3 oxidation numbers and net atomic charges for aniline and isomeric diamino benzenes are reported in Table 2. This definition of oxidation numbers[30], appropriate for neutral species, ensures that oxidation numbers in a molecule add up to zero. From the table, it is seen that a small variation in electronic densities may switch the polarities and yield very different oxidation numbers. Thus it clearly means that in covalent bonding situations, assigning oxidation number are best avoided[44]. Since the positive and negative signs of the oxidation numbers are correlated with the signs of the net atomic charges and therefore unable to describe the subtle balance in σ and π effects. The assumption of sp^2 hybridisation on the carbon atoms implies a charge population described as $2s^1$, $2p_x^1$, $2p_y^1$, $2p_x^1$. The present calculation do show a similar distribution of charges except on the carbon atoms attached to the substituent (table not

given). The deficit of electrons in the 2*s* orbital of the carbon atom, in the molecule under study as compared to free carbon representing promotion from 2*s* to a 2*p* orbital is explained as being due to the energy gain in the molecular formation from sp^2 hybridised orbitals.

Table 2 - Oxidation numbers and net atomic charges of the atoms*

Aniline		o-diamine benzene		m-diamino benzene		p-diamino benzene	
Atoms	Oxidation Numbers	Atoms	Oxidation Numbers	Atoms	Oxidation Numbers	Atoms	Oxidation Numbers
C_1	+3.707(+224)	C_1	+2.548(+130)	C_1	+3.786(+271)	C_1	+3.721(+165)
C_2	−3.804(−104)	C_2	+2.548(+130)	C_2	−3.741(−212)	C_2	−2.326(−049)
C_3	+3.830(+061)	C_3	−2.331(−056)	C_3	+3.786(+271)	C_3	−2.326(−049)
C_4	−2.807(−063)	C_4	−0.135(−006)	C_4	−3.773(−168)	C_4	+3.721(+165)
C_5	+3.880(+061)	C_5	−0.132(−006)	C_5	+3.857(+112)	C_5	−2.226(−049)
C_6	+3.804(−104)	C_6	−2.331(−056)	C_6	−3.773(−108)	C_6	−2.331(−049)
N_7	−2.968(−224)	N_7	−2.968(−220)	N_7	−3.065(−223)	N_7	−2.947(−224)
H_8	+0.971(+006)	N_8	−2.968(−220)	H_8	+0.967(+018)	H_8	+0.967(+003)
H_9	−0.966(−010)	H_9	+0.973(+004)	N_9	−2.979(−223)	H_9	+0.967(+003)
H_{10}	−0.032(−000)	H_{10}	−0.018(−004)	H_{10}	+0.968(+011)	N_{10}	−2.947(−224)
H_{11}	−0.966(−010)	H_{11}	−0.018(−004)	H_{11}	−0.967(−014)	H_{11}	+0.967(+003)
H_{12}	+0.971(+006)	H_{12}	+0.973(+004)	H_{12}	+0.968(+011)	H_{12}	+0.967(+003)
H_{13}	+0.970(+078)	H_{13}	+0.958(+077)	H_{13}	+1.056(+080)	H_{13}	+0.977(+075)
H_{14}	+0.970(+078)	H_{14}	+0.973(+040)	H_{14}	+0.970(+078)	H_{14}	+0.972(+075)
		H_{15}	+0.958(+077)	H_{15}	+0.969(+080)	H_{15}	+0.972(+075)
		H_{16}	+0.973(+040)	H_{16}	+0.970(+078)	H_{16}	+0.972(+075)

*Values of net atomic charges are in the parenthesis and are represented in units of 10^{-3} electrons.

Ionization potentials and dipole moments : The values of the above parameters for the molecules under study are reported in Table 3. The ionization potentials calculated from Koopmann"s Theorems[45] are very much consistent with the experiments[46,47] for aniline. The symmetry of the HOMO (highest occupied molecular orbital), an indication of the symmetry

Table 3 - Dipole moments and ionization potentials of mono and di-substituted amino benzenes

Molecules	Dipole moments (Debye)	Ionization potential (in atomic units)
Aniline	0.98	−0.289 π
	(0.94)[a]	(−0.282)[c]
	(0.39)[b]	(−0.295)[d]
	(1.53)[e]	
o-Diamino benzene	1.50	−0.269 π
m-Diamino benzene	1.00	−0.281 π
p-Damino benzene	0.00	−0.263 π

[a] Yadav, J.S. (1973) Ph. D. Thesis, B.H.U., Varanasi, [b] Singh, O.P. & Yadav, J.S. (Unpublished work), [c] Ref. 46, [d] Ref. 47, [e] Ref. 48.

of the ionized species, is found to be of π symmetry. This is in agreement with the usual assumption that the excitation and ionization mechanisms are mainly controlled by electrons in conjugated and aromatic molecules. However, the dipole moments differ considerably from the experimental[48] as well as other theoretical findings (Table 3).

Conclusions

Keeping the cost of calculation and computation time involved, it can be concluded that the MINDO/3 method may be used for elucidating such useful concepts like bond orders, valence indices, and parameters like ionization potentials to other set of molecules. However, the dipole moment could not be reproduced by this method and therefore, it is concluded that the parameterization incorporated for its calculation in MINDO/3 is not appropriate. On the other hand the AM1 (Austin Model 1)[49] model provides satisfactory results of dipole moment which are very close to experimental findings. The evaluation of dipole moments with AM 1 model for such systems is in process and the results will be published in future communications.

Acknowledgements

Two of the authors (A.K. and O.P.S.) thank U.G.C., New Delhi for the award of teacher fellowship and research grant respectively. A.K. also thanks Dr. J.P. Singh, Principal, L.B.S. (P.G.) College, Gonda for granting academic leave and encouragement. The authors thank Professor D.K. Rai, Department of Physics, B.H.U., Varanasi for his fruitful comments and suggestions.

References

1. Dai, Y., Dunn, K. & Boggs, J.E. (1984) *J. Mol. Struct. (Theo. Chem.)* **109** : 127.
2. Dewar, M.J.S. & Storch, D.M. (1985) *J. Am. Chem. Soc.* **107** : 3898.
3. Dewar, M.J.S. & Thiel, W.J. (1977) *J. Am. Chem. Soc.* **99** : 4899.
4. Bingham, R.C., Dewar, M.J.S. & Lo, D.H. (1975) *J. Am. Chem. Soc.* **97** : 1285.
5. Schroder, S. & Thiel, W. (1985) *J. Am. Chem. Soc.* **107** : 4422.
6. Yadav, J.S., Mishra, P.C. & Rai, D.K. (1973) *Mol. Phys.* **26** : 193.
7. Yadav, J. S., Mishra, P.C. & Rai, D.K. (1972) *J. Mol. Struct.* **13** : 253.
8. Yadav, L.S., Singh, O.P. & Yadav, J.S. (1987) *J. Mol. Struct.* **49** : 121.
9. Yadav, L.S., Singh, O.P., Yadav, P.N.S. & Yadav, J.S. (1987) *Ind. Jour. of Pure & Appld. Phys.* **25** : 300.
10. Singh, O.P. & Yadav, J.S. (1986) *Int. J. Quan. Chem.* **29** : 1283.
11. Rudenberg, K. (1961) *J. Chem. Phys.* **34** : 1884.
12. Parr, R.G. & Borkmann, R.F. (1968) *J. Chem. Phys.* **49** : 1055.
13. Politzer, P. (1969) *J. Chem. Phys.* **50** : 2780.
14. Wiberg, K.B. (1968) *Tetrahedron* **24** : 1083.
15. Kaufmann, J.J. (1967) *Int. J. Quantum Chem. Symp.* **1** : 485.
16. Jug, K. (1977) *J. Am. Chem. Soc.* **99** : 7800.
17. Jug, K. (1978) *J. Am. Chem. Soc.* **100** : 6581.
18. Jug, K. (1984) *Croatica Chem. Acta* **57** (5) : 941.
19. Jug, K. (1984) *Jour. Com. Chem.* **5** (6) : 555.

20. Jug, K. (1979) *Theor. Chim. Acta (Berl.)* **51** : 331.
21. Gopinathan, M.S. & Jug, K. (1983) *Theor. Chim. Acta* **63** : 497.
22. Gopinathan, M.S. & Jug, K. (1983) *Theor. Chim. Acta* **65** : 511.
23. Singh, O.P. & Yadav, J.S. (1985) *J. Mol. Struct. (Theo. Chem.)* **124** : 487.
24. Singh, O.P. & Yadav, J.S. (1985) *Proc. Indian Acad. Sci. (Chem. Sci.)* **95** : 427.
25. Singh, O.P. & Yadav, J.S. (1987) *J. Mol. Struct. (Theo. Chem.)* **149** : 91.
26. Singh, O.P., Singh, A.P., Kumar, A., Yadav, L.S. & Yadav, J.S. (1988) *Proc. Ind. Acad. Sci. (Chem. Sci.)* **100** (5) : 441.
27. Yadav, L.S. & Yadav, J.S. (1988), *J. Mol. Struct. (Theo. Chem.)* **165** : 289.
28. Mayer, I. (1983) *Int. J. Quantum Chem. Symp.* 1: 270.
29. Mayer, I. (1983) *Chem. Phys. Lett.* **97** : 270.
30. Giambiagi, M.S., Giambiagi, M. & Jorge, F.E. (1984) *Z. Naturforsch Teil* A **39** : 1259.
31. Dean, S.M. & Richards, W.G. (1975) *Nature* **258** : 133.
32. Mulliken, R.S. (1955) *J. Chem. Phys.* **23** : 1833.
33. Bader, R.W.F. (1980) *J. Chem. Phys.* **73** : 2871.
34. Collians, J.B. & Streitwiser, A. Jr. (1980) *J. Comput. Chem.* 1: 81.
35. Hilal, R. (1980) *J. Comput. Chem.* **1** : 348, 358.
36. Iwata, S. (1980) *Chem. Phys. Lett.* **69** : 305.
37. Takano, K., Hosoya, H. & Iwata, S. (1962) *J. Am. Chem. Soc.* **104** : 3998.
38. Takano, K., Hosoya, H. & Iwata, S. (1984) *J. Am. Chem. Soc.* **106** : 2787.
39. Kumar, A., Yadav, L.S., Yadav, J.S. & Singh, O.P. *Proc. Ind. Acad. Sciences* (communicated)
40. Mayer, I. (1984) *Int. J. Quantum. Chem.* **26** : 151.
41. Mayer, I. (1985) *Theoret. Chem. Acta. (Berl.)* 67 : 315.
42. Landolt & Bornstein's Table (1976) Vol. 2, p. 7, Springer Verlag.
43. Lowdin, P.O. (1950) *J. Chem. Phys.* **18** : 365.
44. Cotton, F.A. & Wilkinson, G. (1979) *Advanced Inorganic Chemistry,* 3rd Ed.,
45. Pople, J.A. & Beveridge, D.I. (1970) *Approximate Molecular Orbital Theory,* Mc Graw Hill, Book Co. Inc., New York, p. 36.
46. Vilesov, F.L. & Terenin, A.N. (1957) *Dokladay Akad. Nauk. USSR* **115** : 744.
47. Watanabe, K. (1957) *J. Chem. Phys.* **26** : 542.
48. Dewar, M.J.S. & Thiel, W.J. (1977) *J. Am. Chem. Soc.* **99** : 4907.
49. Dewar, M.J.S., Goebisch, E.G., Healy, E.F. & Stewart, J.P. (1985) *J. Am. Chem. Soc.* **107** : 3902.

PROC. NAT. ACAD. SCI. INDIA, 61 (A), II, 1991

Spectroscopic characterization of thiostrepton-copper(II) complex

(Key words : I.R. spectroscopy/biological activity/thiostrepton/copper(II))

C. VASANT KUMAR CHARY+, S. RAMBHAV* and V. J. TYAGA RAJU**

+Bhavan's New Science College, Narayanaguda, Hyderabad-500 029, India.
**Department of Biochemistry, University College of Science, Osmania University, Hyderabad-500 007, India.*
***Department of Chemistry, University College of Science, Osmania University, Hyderabad-500 007, India.*
+Author for correspondence.

Received August 13, 1990; Accepted December 20, 1990.

Abstract

The I.R. spectrum of thiostrepton-copper(II) complex (Ths-Cu) of 1 : 4 molar ratio indicated the involvement of some of the –NH, –C=N, –C=O and –C–S groups pertaining to amide, azomethine, ester carbonyl and thiazole rings respectively of the thiostrepton molecule in co-ordination to copper(II). The nature of one metal binding site of the antibiotic molecule was understood by constructing a model. The subnormal Bohr magneton value of the paramagnetic species of Ths-Cu as revealed by magnetic suceptibility measurement suggested an intense metal-metal interactions. Optical absorption study of Ths-Cu in different solvents indicated a distorted octahedral geometry of the complex with the various donor atoms of the ligand molecule occupying the equitorial plane. The structural requirements of the antibiotic for biological activity are discussed.

Introduction

Interaction of antimicrobial agents with metal ions may result in enhancing[1], stabilizing[2], or abolishing[3] their biological activity. Study of metal interactions of antimicrobial agents, therefore, is envisaged to provide valuable information about their structure-activity correlations especially when their metal co-ordinating sites are essential for biological activity.

The molecular structure of thiostrepton (Ths.) (Fig. 1)[4], a peptide antibiotic produced by *Streptomyces azureus*[5] a soil isolate, reveals that it contains sites at which co-ordination to metal ions can occur. During the study of the interaction of Ths. with various bivalent metal cations in relation to biological activity, it was observed that the antibiotic was found to selectively bind to copper(II) in a stoichiometric ratio of 1 : 4 with the loss of its biological activity[6]. The present paper deals with the synthesis and characterization of Ths-Cu complex.

Materials and Methods

The following instruments were used; (a) Pye-Unicam SP3 - 300 ratio recording double beam spectrophotometer for recording the I.R. spectrum. Polystyrene (1601 cm^{-1}) was used for calibration; (b) Beckman DU-50 recording spectrophotometer for electronic absorption spectra; (c) Perkin Elmer atomic absorption spectrophotometer for estimating the metal content in Ths-Cu; (d) EE & G Princeton Applied Research Model 155 vibrating sample magnetometer for measuring the magnetic suceptibility of Ths-Cu at room temperature.

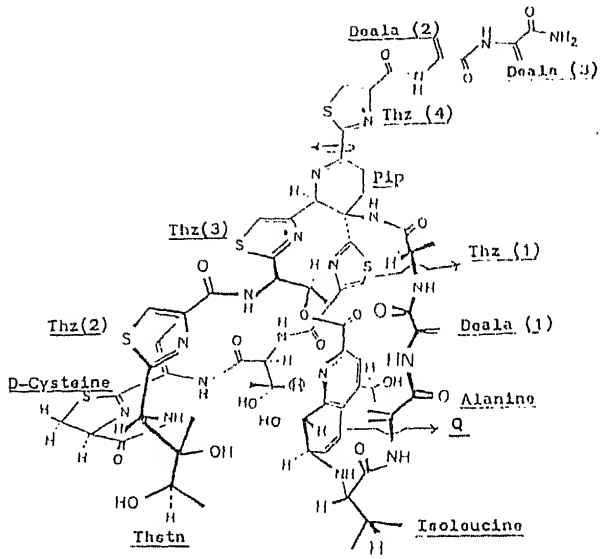

Fig. 1 - A schematic view of the molecular conformation of thiostrepton molecule. Deala - Dehydralanine; Q - Quinaldic acid; Thstn - Thiostreptine; Thz - Thiazole ring; Pip - Piperidine ring.

Nitrogen and chloride analyses were carried out using the standard microanalytical procedures.

Thiostrepton standard (M_r 1650) was a gift sample from the Squibb Institute, New Jersey, USA. All other chemicals were of Analar grade and used directly.

Preparation of thiostrepton-copper(II) complex : The synthesis of Ths-Cu was carried out by mixing to a 4 ml 1,4 dioxane solution of Ths. (1×10^{-4}M), 1 ml of aqueous copper chloride solution containing excess copper(II) (6×10^{-3}M) and incubating the mixture at 37°C for 24 h. Later, to this solution, 200ml dioxane was added and stirred. A light green coloured product was precipitated which was collected by centrifugation. The precipitate was washed successively thrice with dioxane and finally once with ether and dried *in vacuo* over calcium chloride. Yield 78%. The purity of the product was checked by thin layer chromatography using various solvent systems.

Results and Discussion

Some properties of Ths-Cu as compared to that of Ths. are summarized in Table 1. These results indicate that the copper(II) complex of Ths. is an altogether a new molecule differing from native Ths. in many respects. Analytical data shows Ths. to copper (II) and Ths. to chloride molar ratios as 1 : 4 and 1 : 8 respectively. Therefore, the Ths-Cu can be represented with the molecular formula as (Cu_4ThsCl_8). Conductance data (1×10^{-3}M, DMF) showed that Ths-Cu is a non-electrolyte indicating that the eight chloride ions are in the co-ordination sphere.

Table 1 - Comparison of Ths-Cu with the thiostrepton standard.

Property	Thiostrepton	Ths-Cu
Mol. Wt.	1650	2176
Decomp. Temp. (°C)	246-258	170-180
Solubility	Sol. in DMSO, DMF, pyridine, dioxane, $CHCl_3$, acetic acid and higher chain alcohols. Insol. in lower alcohols.	Sol. in DMSO, DMF, pyridine, acetic acid, methanol and in 1mM EDTA (pH 7). Insol in higher alcohols.
Biological activity	Active on Gram +ve bacteria	Ineffective on bacteria
Absorption spectrum		
UV (20% DMSO)	255nm peak and a shoulder at 280nm	260nm peak and shoulders at 280 & 360 nm.
Visible (pyridine)	No absorption	485nm shoulder and 600-800nm peaks.
Specific rotation [α]23°D, (DMSO)	(–) 54°	(–) 16°
Mobility on Tlc	Higher Rf value in non-polar solvent systems & lower Rf value in polar solvent systems	Lower Rf value in non-polar solvent systems & higher Rf value in polar solvent systems
I. R. spectrum	The spectra of both the samples are different and not superimposable	
Elemental analysis		
N	16.1%	Expected - 12.1% Observed - 11.9%
Cu	–	4 atoms/molecule thiostrepton
Cl	–	8 atoms/molecule thiostrepton

Table 2 - Assignments of some of the principal IR absorption bands of thiostrepton.

Wave numbers (cm^{-1})	Approximate frequency description
3300	Amide A band of –NH & –OH & NH_2 str.
3000	Aromatic –C–N str.
1720	Ester carbonyl str.
1680-1600	Amide I of –C=O str. –NH def. –C–N str. and –C–C bending
1575-1480	Amide II of –C–N str. –NH def.
1200	–C–O str. of Sec/Ter. alcohol
800	–NH def.
750	Amide IV of O=C–N def.
587-708	–C–S str.
200	Amide VII tor.

Str. - stretching frequency; def. - deformation/bendng frequency; tor. - torque.

The IR spectrum of Ths. and Ths-Cu were recorded in nujol and in KBr media (Fig. 2). Since nujol has intense absorption signals between 2000-3000 cm^{-1} and also at 1300-1500 cm^{-1} frequencies[7], the spectra of the samples in these regions was read from the KBr media.

The I.R. spectrum of the native Ths. molecule shows intense absorption bands (cm^{-1}) at 3300-3500, 2920-2970, 1720, 1600-1680, 1480-1575, 575-710 (Fig. 2) that can be assigned to –OH, –NH str; –C=N str; ester –C=O str; amide I of –C=O str; and amide II of –C–N str; and –C–S str. respectively (Table 2)[8]. The high intensity of some of these bands is attributed

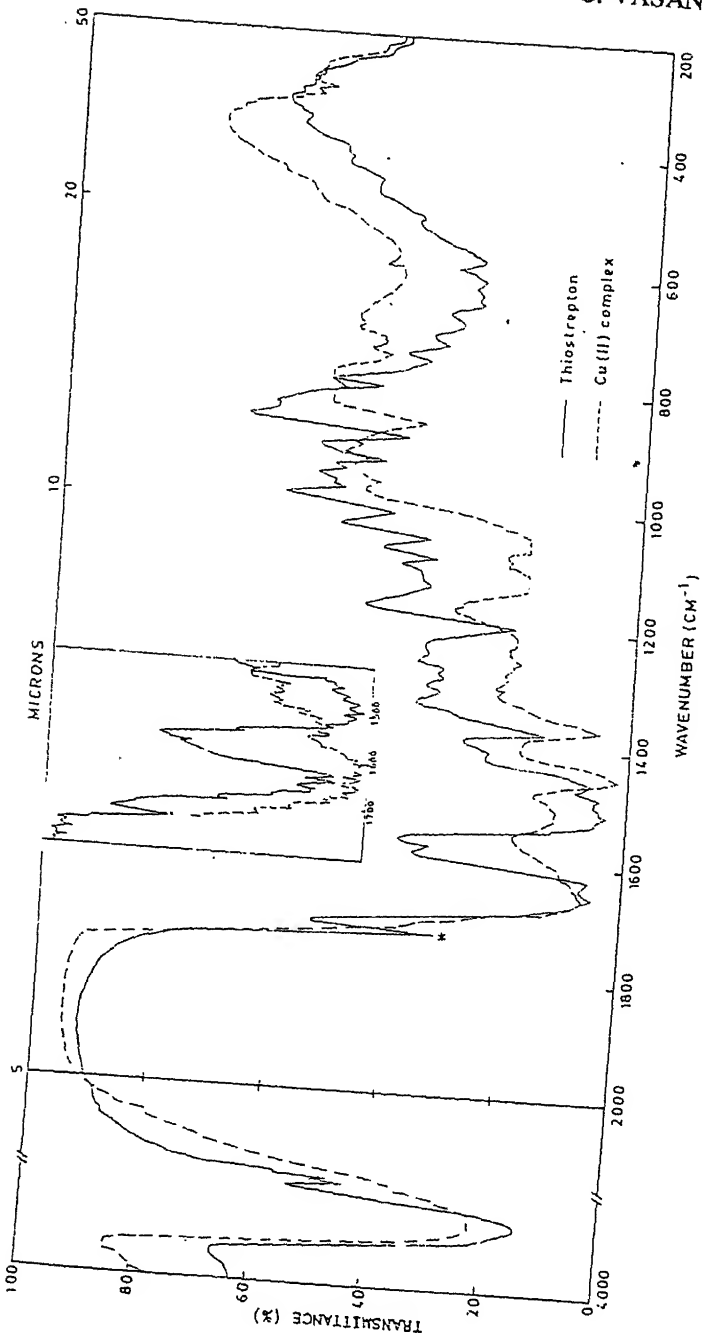

Fig. 2 - I.R. spectra of thiostrepton and its copper(II) complex recorded in nujol. Inset diagram: Portion of the spectrum recorded in KBr.

to multiple number of the corresponding functional groups present in the Ths. molecule.

From the comparison of the I.R. spectrum of metal complex with that of the native molecule (Fig. 2), it is evident that the absorption bands pertaining to amide, azomethine, ester and amide carbonyl and –C–S groupings of the ligand are utilized in co-ordination to copper(II). Since many of these ligand groups are available in the Ths. molecule, the binding of the copper (II) to some of them resulted in broadening or reduced intensity of the corresponding absorption bands. For e.g. broadening of the absorption band at 3300-3500 cm^{-1} in Ths-Cu can be attributed to some metal bound –NH groups and unbound –OH groups[8]. The involvement of peptide nitrogens of Ths. in co-ordinating to copper(II) was also indicated in potentiometric titration study of Ths. in presence of the metal[6]. There is only one ester–C=O group in Ths. molecule (1720 cm^{-1}). Since the I.R. spectrum of Ths–Cu shows a downward shift of this group from 1720 to 1710 cm^{-1}, it indicates the involvement of the ester –C=O group in co-ordination. Similarly, the absorption band of Ths. pertaining to –C–S str. (575 cm^{-1}) is much reduced in intensity in Ths-Cu indicating the involvement of the sulfur atoms of the thiazole ring (Thz) of the antibiotic in co-ordination to the metal ion. The –OH groups of the antibiotic are not expected to interact with the metal since, no stable chelates could be formed involving these groupings.

Some of the absorption frequencies in the region 600-900 cm^{-1} of Ths. are observed to be shifted to lower frequencies in the Ths-Cu, like; 880 cm^{-1} absorption band of Ths. appears to be shifted to 860 cm^{-1} in Ths-Cu. And the 200 cm^{-1} absorption band of Ths. pertaining to amide VII tor. is reduced in intensity in Ths-Cu. Likewise, the region between 200-500 cm^{-1} of Ths-Cu presents a totally different picture as compared to the native Ths. molecule with the appearance of some new structures that can be attributed to $M \rightarrow N$, $M \rightarrow O$ and $M \rightarrow S$ bonding[8,9].

From these data it is hence deduced that the nitrogen atoms of the amide and azomethine groups, some of the oxygen atoms of the amide and ester carbonyl groups, and sulfur atoms of the thiazole ring of Ths. molecule are involved in co-ordinating to the metal ion.

The solution conformation of Ths. molecule (Fig. 1) reveals that there are several –NH groups with the other co-ordinating groups i.e. –C=O, –C=N, –C–S at favourable position to achieve efficient chelation with copper(II). Especially, the involvement of nitrogen atom of piperidine (pip) and sulfur atom of Thz(4), –NH and NH_2 groups of dehydroalganine (deala) (2) and (3) would result in a stable five membered chelate with the possible arrangement shown in Fig. 3. A molecular model of this region of Ths. molecule with the bound copper(II) was constructed. This approach showed that, with the rotation of the single bond between pip and Thz (4) (shows by an arrow mark in Fig. 3), it is also possible to involve the nitrogen atom instead of the sulfur atom of the Thz(4) in co-ordination to the metal ion. Since the entire 'tail' portion of the antibiotic molecule (comprising of the two deala groups, and Thz(4)) are bound to the pip ring), it is possible that, in solution, there could exist a dynamic equillibrium between the nitrogen bound Thz (4) and sulfur bound Thz (4) complexes.

It is interesting to observe from Fig. 1 that, binding of one copper(II) ion at the 'tail' portion of Ths. molecule does not drastically affect the overall conformation of the antibiotic molecule because, the rest of the portion of the molecule is unaffected. In such a case, binding of a metal ion at this region would only slightly affect the biological activity of the antibiotic. Our observations on biological activity of Ths. in presence of copper (II) at 1:1

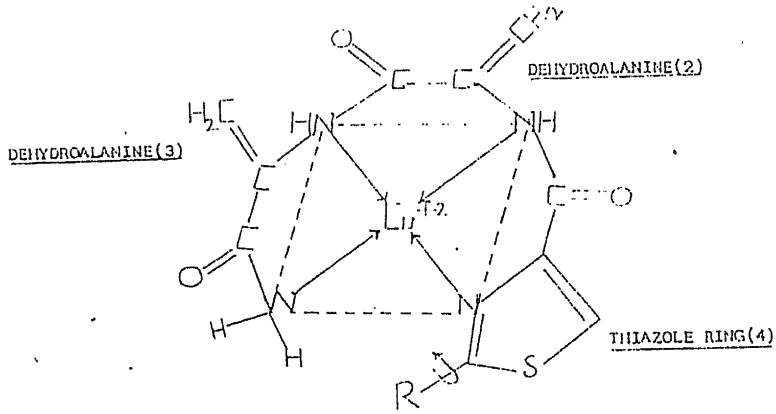

Fig. 3 - Schematic representation of one possible region of thiostrepton molecule with the bound copper(II). R - rest of the portion of the thiostrepton molecule. For purpose of clarity, chlorides in the axial position of the metal ion are not shown in the diagram.

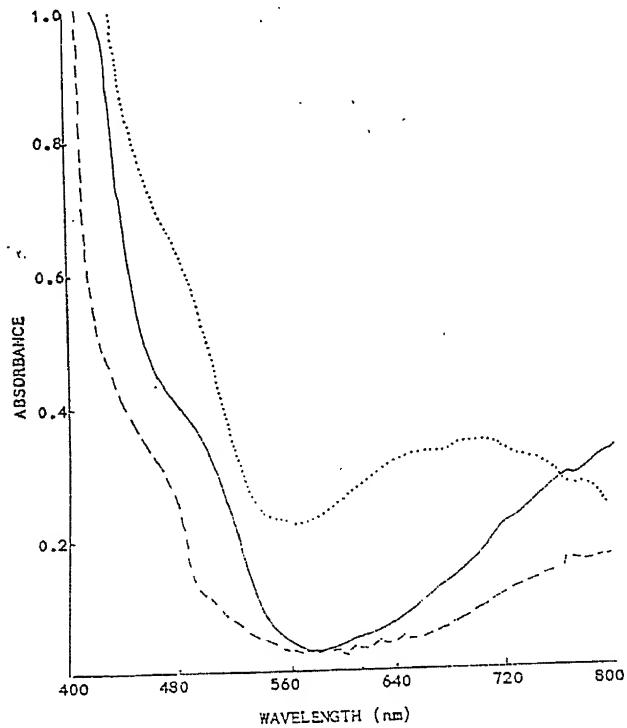

Fig. 4 - Absorption spectra of Ths-Cu in the visible region in DMSO/DMF (—), methanol (-----) and in pyridine (...)

molar ratio showed only 12% loss of activity of the antibiotic[6]. Based on this observation, it is tempting to assume that, at 1:1 molar ratio of Ths. to copper(II), this region may be the site that is initially involved in co-ordinating to the metal thereby forming a stable five membered chelate (Fig. 3). Such stable five membered structures involving the other three copper(II) ions at the other binding sites in the antibotic molecule could also be possible. Therefore, the binding of four copper (II) ions to Ths. molecule is evidently due to the availability of four different sites in the antibiotic where the co-ordinating atoms are present. All the four regions may not be, however, initially accessible for binding to the four copper(II) ions because of unfavourable stereochemical orientations of some of the ligand atoms in these regions. Possibly, the initial binding of one or two metal ions at any of the favoured regions of the molecule would induce electronic perturbations in the entire ring structure of Ths.[10] which would favour the binding by the rest of the copper(II) ions. The binding of all the four copper(II) ions to Ths. molecule would, therefore, greatly affect the overall conformation of the antibiotic molecule rendering it biologically ineffective. Alteration in the I.R. spectrum of Ths-Cu in the fingerprint region (1300-900 cm^{-1}) compared to that of Ths. indicates a change in the conformation of the antibiotic molecule as a result of binding of the four copper(II) ions.

The electronic absorption spectrum of Ths-Cu compared to that of the native Ths. molecule in the U.V. region indicated shifts in both pi $\rightarrow$ pi* and n $\rightarrow$ pi* transitions of the free Ths.[6] Appearance of a new band at 360 nm in the Ths-Cu molecule suggested a bathochromic shift in the transitions that are attributed to metal co-ordination.

The absorption of Ths-Cu in the visible region recorded in different solvents like; methanol, dimethylsulfoxide (DMSO) dimethylformamide (DMF) and pyridine shows that, as the basicity of the solvent increases from methanol to pyridine, the broadening as well as the intensity of the band between 600-800nm increases (Fig. 4). In pyridine, the spectrum shows a broad intense multiple band in the region of 600-800 nm which is resolved into three regions, *viz.* 700, 750 and 780nm being centered at 750nm. These can be attributed to $^2B_{1g} \rightarrow {}^2A_{1g}$, $^2B_{1g} \rightarrow {}^2B_{2g}$, and $^2B_{1g} \rightarrow {}^2E_g$ transitions respectively that are consistent with a distorted octahedral geometry[11].

Magnetic sucptibility measurement of Ths-Cu indicated a sub-normal Bohr magneton value for a single copper(II) ion (0.533). This indicates the existance of a strong metal to metal interaction between the copper(II) ions. The Ths-Cu molecule with the four copper(II) ions can show subnormal magnetic moment due to the two possible antiferromagnetic interactions; (i) the complex molecule can fold in such a way that the four metal ions within the molecule can come close to undergo metal to metal interaction trough chloride bridging; or (ii) if the complex molecules are assumed to stack one above the other, a copper(II) ion in one complex molecule in a distorted octahedral geometry can under spin-spin exchange with similar copper(II) ion in another complex molecule through the chloride bridging[12].

It was due to these interactions between the four copper(II) ions present well within the Ths. molecule that resulted in a single broad unresolved line in the E.S.R. spectrum of Ths-Cu in both DMSO and DMF even at liquid nitrogen temperature though, in pyridine, the spectrum showed good resolution with superhyperfine splittings (results not presented here). A detailed study of E.S.R. investigations are communicated to Current Science, Bangalore.

These results suggest that the four copper(II) ions in the Ths. molecule have a distorted octahedral geometry with the various N/O/S donors of the antibiotic molecule occupying the equitorial square plane, and with the chloride ions at longer distances in the axial plane. However, when the complex was dissolved in pyridine, the chlorides that are weakly interacting with the metal ion are being displaced by the solvent molecules.

In conclusion, it should be emphasized that, it is also possible that the suggested metal co-ordinating groups of the Ths. may not be directly involved in its biological activity. This is because, metal induced changes in the architecture of an antibiotic molecule at groupings other than those involved in metal binding may also render the molecule biologically ineffective[3]. Therefore, it is the changes induced in the overall conformation of the Ths. molecule as a result of binding of the four copper(II) ions that resulted in elimination of its biological activity.

Acknowledgements

The instrumentation facilities provided by the National Chemical Laboratories, Pune and Indian Institute of Technology, Madras for recording I.R. spectra and magnetic suceptibility respectively is gratefully acknowledged.

References

1. Adler, R.H. & Snoke, J.E. (1962) *J. Bacteriol.* **83** : 1315.
2. Garbutt, J.T., Morehouse, A.L. & Hanson, A.H. (1961) *J. Agric. Food Chem.* 9 : 285.
3. Weinberg, E.D. (1957) *Bacteriol. Rev.* **21** : 46.
4. Tori, K., Tokura, K., Yoshimura, Y., Okabe, K., Otsuka, H., Inagaki, F. & Miyazawa, T. (1979) *J. Antibiot.* **32** : 1072.
5. Pagano, J.F., Weinstein, M.J., Stout, H.A. & Donovick, R. (1955-56) *Antibiot. Annu.* 554.
6. Chary, C. Vasant Kumar, Rambhav, S. & Venkateswerlu, G. (1990) *Biol. Metals* (In Press).
7. Dyer, J.R. (1987) *Applications of Absorption Spectroscopy of Organic Compounds*, Prentice Hall of India Pvt. Limited, New Delhi, p. 22.
8. Colthup, N.B., Daly, L.H. & Wibertley, S.E. (1964) *Introduction to Infrared and Raman Scpectroscopy*, 1st Ed., Academic Press, London.
9. Nakamoto, K. (1970) *Spectra of Inorganic and Co-ordination Compounds*, 2nd Ed., Wiley Interscience, New York, p. 219.
10. Chatterjee, D. & Nandi, U.S. (1978) *J. Sci. & Ind. Res.* 37 : 449.
11. Tyaga Raju, V.J., Ranabaore, V., Atre, V. & Ganorkar, M.C. (1982) *J. Indian Chem. Soc.* **59** : 199.
12. Mabbs, F.E. & Machin, D.J. (1973) *Magnetism and Transition Metal Complexes*, Chapman & Hall, London, p. 170.

PROC. NAT. ACAD. SCI. INDIA, 61 (A), II, 1991

Diethazine hydrochloride as a new reagent for rapid spectrophotometric determination of cerium (IV), arsenic (III) and nitrite

(Key words : spectrophotometry/diethazine hydrochloride/cerium(IV)/arsenic(III)/nitrite)

Received November 11, 1989; Revised April 4, 1990; Accepted June 16, 1990.

Abstract

Diethazine hydrochloride is proposed as a new reagent for the rapid spectrophotometric determination of cerium (IV), arsenic (III) and nitrite. The reagent forms red coloured species with cerium (IV) instantaneously at room temperature in phosphoric acid medium. The species has an absorption maximum at 516 nm with a sensitivity of 15 ng cm^{-2}. The method has been used for the analysis of cerium alloys and for the determination of arsenic (III) and nitrite.

The colour reaction of diethazine hydrochloride (DH), 10 [2-(diethylamino)ethyl] phenothiazine hydrochloride with cerium (IV) has been studied for the rapid spectrophotometric determination of cerium (IV), arsenic (III) and nitrite. The proposed method offers the advantages of simplicity, rapidity, sensitivity and stability without the need for heating or extraction.

Stock solutions of cerium (IV) sulphate in 0.5 M sulphuric acid, sodium arsenite (prepared from arsenic trioxide) and sodium nitrite were prepared and standardised by literature method[1]. A 0.3% (wt/vol) solution of DH was prepared in doubly distilled water and stored in an amber bottle in a refrigerator. Solutions of diverse ions of suitable concentrations were prepared using analytical grade reagents. Beckman model DB spectrophotometer with matched 1 cm quartz cell was used for absorbance measurements.

Determination of cerium (IV) : An aliquot of the stock solution containing 12-500 μg of cerium (IV), 15 ml of 10M phosphoric acid and 2 ml of 0.3% DH solution were taken and the solution diluted to 25 ml with doubly distilled water. The solution was mixed well and the absorbance was measured at 516 nm against a corresponding reagent blank prepared in the same manner. The amount of cerium in the sample solution was deduced from the calibration curve.

Determination of arsenic (III) : 1 ml of 5 M sulphuric acid, 0.5 ml of osmium (VIII) (1 μg) and 1 ml of 0.002M cerium (IV) solution were transferred to each of eleven 25 ml volumetric flasks. An aliquot of the stock solution containing 3.8-87.5 μg of arsenic (III) was added only to ten 25 ml flasks and mixed well. An eleventh 25 ml flask was used for a simultaneous blank determination. 15 ml of 10M phosphoric acid and 2 ml of 0.3% DH solution were added to all the flasks, diluted to the mark and shaken well and the absorbances measured at 516 nm against a reagent blank containing no cerium (IV) and arsenic (III). The amount of arsenic (III) in a test solution was then deduced from the calibration graph constructed by plotting the concentration of arsenic (III) *vs.* the difference in the absorbance readings between the blank (in eleventh flask) and the sample.

Determination of nitrite : 1 ml of 0.002M cerium (IV) sulphate and 2 ml of 2M sulphuric acid were taken in each of eleven 25 ml volumetric flasks. 2 ml of sodium nitrite solution containing 2.5-62.5 μg of nitrite was transferred into each of ten volumetric flasks and the eleventh flask was used for blank experiment. The solutions were well mixed, left for 5 min,

the colour was developed by adding phosphoric acid and DH solution, the absorbances measured and the amount of nitrite in the test solution was determined as described in the procedure for the determination of arsenic (III).

Cerium (IV) readily oxidises DH to red coloured species in sulphuric or phosphoric acid medium. The maximum colour development takes place instantaneously at room temperature ($28 \pm 1^{\circ}C$) in 5.5-6.3M phosphoric acid solutions. The red coloured species assumed to be a radical cation[1] shows maximum absorption at 516 nm and the absorbance remains constant for about 45 min. Phosphoric acid (6M) was chosen because in the presence of sulphuric acid the reaction is less sensitive and less stable. The reagent blank and the metal ion under similar conditions do not absorb around this wavelength thus promoting excellent analytical conditions. A 24-fold molar excess of DH is necessary for maximum colour development. The absorbance values are insensitive to temperature range 5-55°C, but beyond 55°C, the absorbance gradually decreases. The red species is cationic in nature as revealed by ion-exchange experiments. There is no appreciable change in the absorbance if the order of addition of reactants is varied. Beer's law is obeyed over the concentration range 0.5-20 ppm of Ce(IV). The optimum concentration range evaluated by Ringbom's method[2] is 1.2-18.0 ppm. The molar absorptivity and Sandell's sensitivity are 9.7×10^3 dm^3 mol^{-1} cm^{-1} and 15 ng cm^{-2} respectively. The standard deviation calculated from six determinations in a solution containing 4 ppm of Ce(IV) is 0.01 and the relative error is less than 2%.

It is seen that many diverse ions especially lanthanides do not interfere in the determination of Ce(IV). The major advantage of this method is that DH can be used as a selective reagent for the determination of Ce(IV) in presence of large quantities of other lanthanides in readily attainable oxidation states without the use of masking agents. The proposed method was successfully applied to the analysis of misch metal containing 50% Ce, 25% La, 15% Nd, 5% Fe and 5% mixtures of Pr, Eu, Gd and Er.

Arsenic (III) and nitrite were indirectly determined. Arsenic (III) was quantitatively oxidised instantaneously to arsenic (V) by a known excess of cerium (IV) sulphate (20-80%) in 0.5M sulphuric acid medium containing 1 μg of Os (VIII) which did not interfere under the experimental conditions. Nitrite was quantitatively oxidised to nitrate in 0.5M sulphuric acid in 5 min, by a known excess of cerium (IV) sulphate (20-80%). The unreacted Ce (IV) was then determined by the proposed method. In the absence of other reducing substances, the reduction in the absorbance of the red colour produced by the fixed amount of cerium (IV) was directly proportional to the amount of arsenic (III) and nitrite present. Ce(III), As(V) and nitrate formed in the reaction were colourless and did not interfere. 0.15-3.5 ppm of As(III) and 0.1-2.5 ppm of nitrite could be determined. This method can be used for the determination of micro-quantities of other substances which are quantitatively oxidised by Ce(IV) in sulphuric acid medium to colourless non-interfering products.

References

1. Dwivedi, P.C., Gurudath Rao, K., Bhat, S.N. & Rao, C.N.R. (1975) *Spectrochim. Acta* **31A** : 129.
2. Ringbom, A. (1939) *Z. Analyt. Chem.* **115** : 332.

K.S. JAGADEESH and H. SANKE GOWDA

Department of Polymer Science and Technology,

S.J. College of Engineering, Mysore-570 006, India.

PROC. NAT. ACAD. SCI. INDIA, 61 (A), II, 1991

An improvement in the spectrophotometric method of determination of cobalt(II) using sodium diethyldithiocarbamate

(Key words : spectrophotometric method/cobalt(II)/diethyldithiocarbamate)

Received August 11, 1989; Accepted June 28, 1990.

Abstract

The spectrophotometric method for determining cobalt(II) using diethyldithiocarbamate has been modified by which even quite small quantities of Co(II) can be determined.

Sodium diethyldithiocarbamate (Na_2L) is used for the determination of various metal ions[1]. Lacoste *et al.*[2] have reported determination of cobalt (II) using sodium diethyldithiocarbamate. A green coloured complex CoL_2 (structure I) is formed which absorbs at 650 nm in $CHCl_3$.

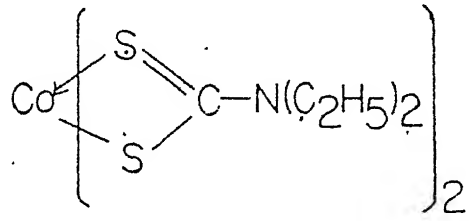

(I)

We have developed a calibration curve in the range 1-6 mg of Co(II) / ml. For developing the colour, 1 ml of a Co(II) solution in the above concentration range was treated with 2 ml of 2% sodium diethyldithiocarbamate and 10 ml of the acetate buffer (CH_3COOH–CH_3COONH_4) of pH 6.3. This aqueous solution was extracted with two lots of 20 ml of $CHCl_3$ and volume was made to 50 ml. It gave λ_{max} at 650 nm on a Beckman spectrophotometer model DU. The same procedure was repeated for other concentrations.

Recently, when we attempted to estimate Co(II) in the concentration range less than 0.3 mg/ml, it did not give any absorption when the above procedure was adopted. However, when instead of 50 ml, a total of 25 ml volume of the solution was made, it gave absorption, thus it was decided to modify the above method.

In the modified method, which is recommended as a graduate level experiment, a calibration curve in the range 0.1 to 1.9 mg Co(II)/ml was made. For this, 1 ml of the standard Co(II) solution containing cobalt (II) in the concentration range 0.1 to 1.9 mg/ml was treated with 10 ml of buffer and the aqueous solution was extracted using 10 ml, lots of $CHCl_3$ instead of 20 ml (Lacoste' procedure) and volume made to 25 instead of 50 ml. The calibration curve is shown in Fig. 1 and one can see that quite small quantities of Co(II) can be determined. The λ_{max} was 640 instead of 650 nm and it may be due to the use of different instruments. In the modified method, Shimdazu-UV-visible-spectrophotometer was used.

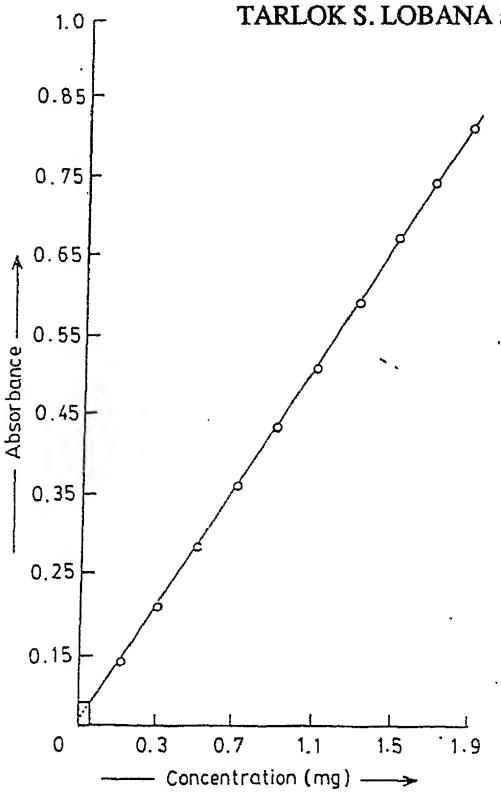

Fig. 1 – N, N-diethyldithiocarbamate method for the estimation of Co(II), concentration range 0.1 - 1.9 mg, λ_{max} = 640 nm.

A standard Co(II) solution was made by EDTA method using xylenol orange as the indicator (end point–pink to yellow)[3].

Financial assitance from C.S.I.R., New Delhi (Scheme No. 1(1095)/87-EMR-II) and research facilities by the Guru Nanak Dev University are gratefully acknowledged.

References

1. Sandell, E.B. & Onishi, H. (1978) *Chemical Analysis*, Vol. 3, 4th Ed., Wiley Interscience,.
2. Lacoste, R.J., Earing, M.H. & Wiberley, S.E. (1951) *Anal. Chem.* **23** : 871.
3. Bassett, J., Denny, R.C., Jeffery, G.H. & Mendham, J. (1978) '*Vogel's Text Book of Quantitative Inorganic Analysis*', E.L.B.S. and Longman, London.

TARLOK S. LOBANA and PUSHVINDER K. BHATIA

Department of Chemistry, Guru Nanak Dev University, Amritsar–143 005, India.

and

$$(2.2)\quad f(x) \doteq \int_0^\infty u\, g(u)\, G_\nu(xu)\, du,$$

then

$$(2.3)\quad 2^{-\sigma} \operatorname{Sin}(\pi\nu)\, y^{\sigma+3/2}\, \phi(y, \mu) =$$

$$= \int_0^\infty u\, g(u) \Big\{ A.\ (u/y)^\nu .\ {}_2F_1\Big[1 + (\mu+\nu+\sigma)/2,\ 1+(\nu-\mu+\sigma)/2;\ \nu+1; -u^2/y \Big] -$$

$$- B.\ (u/y)^{-\nu} .\ {}_2F_1\big[1 + (\mu-\nu+\sigma)/2,\ 1 + (\sigma-\nu-\mu)/2;\ 1-\nu; -u^2/y\big] \Big\}\, du,$$

where

$$A = \operatorname{Sin}\{(a+\nu)\pi\}.\ \Gamma\left(1+\frac{\mu+\nu+\sigma}{2}\right).\ \Gamma\left(1+\frac{\nu-\mu+\sigma}{2}\right) \Big| \Gamma(\nu+1),$$

$$B = \operatorname{Sin}(a\pi)\ \Gamma\left(1+\frac{\mu-\nu+\sigma}{2}\right).\ \Gamma\left(1+\frac{\sigma-\nu-\mu}{2}\right) \Big| \Gamma(1-\nu)\ .$$

provided

(i) $\int_0^\delta |\, t^{1\pm\nu}\, g(t)\,|\, dt$ and $\int_\delta^\infty |\, t^{\frac{1}{2}}\, g(t)\,|\, dt$ are convergent,

(ii) $\min(\sigma \pm \nu) > \mu - 2,\ y > 0.$

Theorem 2. Let

$$(2.4)\quad \phi(y, \mu) = \int_0^\infty (xy)^{\frac{1}{2}}\, k_\mu(xy)\, .x^{\rho-3/2}\, .\, f(1/x)\, dx,$$

and

$$(2.5)\quad f(1/x) = \int_0^\infty u\, g(u)\, G_\nu(u/x)\, du\ ,$$

then

$$(2.6)\quad 2^{2-\rho}\ .\ y^{\rho-\frac{1}{2}}\ .\ \phi(y, \mu) = \int_0^\infty u\, g(u) \left[G^{30}_{04}\left(\frac{u^2y^2}{16} \middle| \frac{\nu}{2}, \frac{\rho+\mu}{2}, \frac{\rho-\mu}{2}, -\frac{\nu}{2} \right) \times \right.$$

$$\left. \times \operatorname{Cos}(a\pi) + (-)^{m+1} \operatorname{Sin}(a\pi)\, G^{40}_{15}\left(\frac{u^2y^2}{16} \middle| \begin{matrix} \frac{1-\nu-2m}{2} \\ \frac{\nu}{2}, -\frac{\nu}{2}, \frac{\rho+\nu}{2}, \frac{\rho-\mu}{2}, \frac{1-\nu-2m}{2} \end{matrix} \right) \right] du,$$

provided

(i) $\int_0^\delta |\, t^{1\pm\nu}\, g(t)\,|\, dt$ and $\int_\delta^\infty |\, t^{\frac{1}{2}}\, g(t)\,|\, dt$ are convergent,

(ii) m is integer, $y > 0$ and $\rho > \mu - 3/2$.

Theorem 3. Let

$$(2.7)\quad \phi(y, k+\tfrac{1}{2}, m) = \int_0^\infty (xy)^{-k-\frac{1}{2}} e^{-xy/2} W_{k+\frac{1}{2}, m}(xy)\, x^{-\rho} f(x^{\frac{1}{2}})\, dx,$$

and

$$(2.8)\quad f(x^{\frac{1}{2}}) = \int_0^\infty u\, g(u)\, G_\nu (x^{\frac{1}{2}} u)\, du,$$

then

$$(2.9)\quad 2^{2\rho-2}\phi(y, k+\tfrac{1}{2}, m) = \int_0^\infty u^{2\rho-1} g(u) \times$$

$$\times \left[\operatorname{Cos}(a\pi)\, G_{32}^{12}\left(\frac{4y}{u^2} \middle| \begin{matrix} \rho - k/2, -2k, \rho + \nu/2 \\ -k+m, -k-m \end{matrix} \right) + \right.$$

$$\left. \times \operatorname{Sin}(a\pi)\, G_{43}^{22}\left(\frac{4y}{u^2} \middle| \begin{matrix} \rho - \nu/2, \rho + \nu/2, -2k, \rho + \frac{1}{2} + \nu/2 \\ -k+m, -k-m, \rho + \nu/2 + \frac{1}{2} \end{matrix} \right) \right] du,$$

provided

(i) $\int_0^\delta |\, t^{1 \pm \nu} g(t)\,|\, dt$ and $\int_\delta^\infty |\, t^{\frac{1}{2}} g(t)\,|\, dt$ are convergent,

(ii) $-3/4 - 2k < \rho < \min(-k \pm m) + \nu/2 + 1, y > 0.$

$G_{mn}^{pq}\left(x \middle| \begin{matrix} \cdots \\ \cdots \end{matrix} \right)$ is the Meijer's G-function.

3. *Proof of theorem* 1. Substituting the value of $f(x)$ from (2.2) in the equation (2.1). we obtain

$$\phi(y, \mu) = \int_0^\infty (xy)^{\frac{1}{2}} k_\mu(xy) x^{\sigma+\frac{1}{2}} dx \int_0^\infty u\, g(u)\, G_\nu(xu)\, du$$

$$= \int_0^\infty u\, g(u)\, du \int_0^\infty (xy)^{\frac{1}{2}} x^{\sigma+\frac{1}{2}} k_\mu(xy)\, G_\nu(xu)\, dx$$

$$= \int_0^\infty u\, g(u)\, du.\ \operatorname{Cosec}(\pi\nu) \int_0^\infty (xy)^{\frac{1}{2}} x^{\sigma+\frac{1}{2}} k_\mu(xy) \times$$

$$\times \{ \operatorname{Sin}\{(a+\nu)\pi\} J_\nu(xu) - \operatorname{Sin}(a\pi) J_{-\nu}(xu) \}\, dx.$$

The change of the order of integration is justified under the conditions given in the theorem. The final result is obtained by using [2, pp. 137].

Proof of theorem 2. Substituting the value of $f(1/x)$ from (2.5) in the equation (2.4), we obtain

$$\phi(y, \mu) = \int_0^\infty (xy)^{\frac{1}{2}} k_\mu(xy)\, x^{\rho-3/2}\, dx \int_0^\infty u\, g(u)\, G_\nu(u/x)\, du$$

$$= \int_0^\infty u\, g(u)\, du \int_0^\infty (xy)^{\frac{1}{2}}\, x^{\rho - 3/2}\, k_\mu(xy)\, G_\nu(u/x)\, dx$$

$$= y^{\frac{1}{2}} \int_0^\infty u\, g(u)\, du \int_0^\infty x^{\rho-1}\, k_\mu(xy) \left\{ \operatorname{Cos}(a\pi)\, J_\nu(u/x) + \operatorname{Sin}(a\pi)\, \gamma_\nu(u/x) \right\} dx.$$

The change of the order of integration is justified under the conditions given in the theorem. The final result is obtained by using [2, pp. 375].

Proof of theorem 3. Substituting the value of $f(x^{\frac{1}{2}})$ from (2.8) in the equation (2.7), we obtain

$$\phi(y, k+\tfrac{1}{2}, m) = \int_0^\infty (xy)^{-k-\frac{1}{2}}\, e^{-xy/2}\, W_{k+\frac{1}{2},m}(xy)\, x^{-\rho}\, dx \times$$

$$\times \int_0^\infty u\, g(u)\, G_\nu(ux^{\frac{1}{2}})\, du$$

$$= \int_0^\infty ug(u)\, du \int_0^\infty (xy)^{-k-\frac{1}{2}}\, e^{-xy/2}\, W_{k+\frac{1}{2},m}(xy)\, x^{-\rho}\, G_\nu(ux^{\frac{1}{2}})\, dx$$

$$= \int_0^\infty 2^{2\rho-2}\, u^{2\rho-1}\, g(u)\, du \int_0^\infty \left(\frac{4ty}{u^2}\right)^{-k-\frac{1}{2}} e^{-4yt/2u^2}\, W_{k+\frac{1}{2},m}(4yt/u^2) \times$$

$$\times t^{-\rho}\, G_\nu(2t^{\frac{1}{2}})\, dt$$

$$= 2^{2\rho-2} \int_0^\infty u^{2\rho-1}\, g(u)\, du \int_0^\infty t^{-\rho}\, G_{12}^{20}\left(\frac{4yt}{u^2}\middle| \begin{matrix} -2k \\ -k+m,\ -k-m \end{matrix}\right) \times$$

$$\times \left\{ \operatorname{Cos}(a\pi)\, J_\nu(2t^{\frac{1}{2}}) + \operatorname{Sin}(a\pi)\, \gamma_\nu(2t^{\frac{1}{2}}) \right\} dt,$$

since $\left(\frac{4ty}{4^2}\right)^{e^{-\frac{4yt}{u^2}}} W_{k+\frac{1}{2},m}(4yt/u^2) = G_{12}^{20}\left(\frac{4yt}{u^2}\middle| \begin{matrix} -2k \\ -k+m,\ -k-m \end{matrix}\right)$.

The change of the order of integration is justified under the conditions given in the theorem. The final result is obtained by using [2, pp. 420].

REFERENCES

1. R. G. Cooke, *Proc. Lond. Math. Soc.*, 24 (1925) 381-420.
2. A. Erdelyi (Editor), Tables of integral transforms, vol. 2 McGraw-Hill (1945).
3. G. H. Hardy, *Proc. Lond. Math. Soc.*, 23 (1925).
4. C. S. Meijer, *Proc. Nederl. Akad. Wetensch*, 43 (1940) 599-608, 702-711.
5. C. S. Meijer, *Proc. Nederl. Akad. Wetensch.*, 44 (1941) 727-737.
6. K. N. Srivastava and B. R. Bhonsle, Math. Student., (to appear).

SOME PROBLEMS ON SYSTEMS OF ORDINARY DIFFERENTIAL EQUATIONS

By

M. RAMA MOHANA RAO

Department of Mathematics, Osmania University, Hyderabad—7, A. P.

[Received on 4th November, 1963]

ABSTRACT

In this note, we shall consider and unify a variety of problems on differential systems. For instance, the results cover global existence, boundedness and stability with respect to its approximate system, uniqueness and existence of harmonic solutions.

§ 1. Consider the differential systems

$$y' = p(y,t) + q(y,t) \qquad y(t_0) = y_0 \ (t_0 \geq 0) \tag{1·1}$$

$$x' = p(x,t) \qquad x(t_0) = x_0 \tag{1·2}$$

where y, x, p, and q are n-dimensional vectors and where p and q are continuous functions on the product space $\triangle = I \times R^n$. Let I be the interval $0 \leq t < \infty$; and R^n be the n-dimensional Euclidean space. Also let $R^+ = [0, +\infty]$. Let $\| y \|$ denote the norm of the element y.

The behaviour of the system of differential equations of the form (1·1) is frequently studied by comparing with those of the system (1·2) particularly when the perturbation term in (1·1) is small, in some cases for sufficiently large t. One of the problems of principle interest that arise in this connection is concerned with the question of whether the boundedness, stability and other properties of the system (1·1) are shared with the system (1·2). The present note takes up this question when the perturbations satisfy certain conditions.

The following definitions are required before proceeding further :—

Let $y(t)$ and $x(t)$ be any two solutions of the systems (1·1) and (1·2) respectively

(d_1) The system (1·1) or (1·2) is said to be equi-norm-bounded with respect to the system (1·2) or (1·1), if for each α greater than zero and $t_0 \geq 0$, there exists a positive function $\beta(t_0,\alpha)$ continuous in t_0 for each α satisfying

$$\| y(t) - x(t) \| < \beta(t_0,\alpha)$$

for all $\| y_0 - x_0 \| \leq \alpha$ and $t \geq t_0$.

(d_2) The system (1·1) or (1·2) is said to be equi-stable with respect to the system (1·2) or (1·1), if for each $\epsilon > 0$ and $t_0 \geq 0$, there exists a positive function $\eta(t_0,\epsilon)$ continuous in t_0 for each ϵ, satisfying

$$\| y(t) - x(t) \| < \epsilon$$

for all $\| y_0 - x_0 \| \leq \eta(t_0,\epsilon)$ and $t \geq t_0$.

Note: If $\beta(t_o,\alpha) = \beta(\alpha)$, $\eta(t_o,\epsilon) = \eta(\epsilon)$ *i. e.* they are independent of t_o, equi- will be replaced by uniformerly—in the above definitions.

§ 2. We require the following theorem proved elsewhere [5]. We shall state in a suitable form whose proof needs a very little modification of the proof given in [5].

Theorem 1.—Let the functions $m(t)$ and $\psi(t)$ be vectors, continuous on $t_o \leqslant t < \infty$ and satisfy the inequality

$$\lim_{h \to 0^+} \operatorname{Sup} \left(\frac{1}{h} \right) \left[m(t+h) - m(t) \right] \not\leqslant \omega\, t,\ m(t) + \| \psi(t) \|)$$

where the function ω is continuous and defined on $1 \times R^+$ Then

$$m(t) \leqslant M(t) \qquad \text{for } t_o \leqslant t < \infty. \tag{2·1}$$

where $M(t)$ is the maximal solution of

$$z' = \omega\,(t,\ z(t) + \psi(t)\,) \qquad M(t_o) = M_o \tag{2·2}$$

Then we have the following theorem

Theorem 2.—Let the function $\omega(t, z + x)$ be continous, non-decreasing in $z+x$ and defined on $1 \times R^+$. Suppose

(i) $\| y - x + h\,[p\,(y,\ t\,) - p\,(x,\ t)] \| \leqslant \| y - x \|$

and

(ii) q satisfy the condition

$$\| q\,(y,\ t) \| \leqslant \omega\,(\,\| y \|\,,\ t) \tag{2·3}$$

Let $M(t)$ be the maximal solution of

$$z' = \omega\,(t,\ z + x) \qquad M(t_o) = M_o \tag{2·4}$$

Then, if $y(t)$ and $x(t)$ are any two solutions of (1·1) and (1·2), we have

$$\| y(t) - x(t) \| \leqslant M(t)$$

Proof:—Let $m(t) = \| y(t) - x(t) \|$

therefore $m(t+h) = \| y(t+h) - x(t+h) \|$

we have

$$\begin{aligned} m(t+h) &\leqslant \| y - x + h\,[p(y,t) - p(x,t)] \\ &\qquad + h\,q(y,t) \| + \| \epsilon_1 h \| + \| \epsilon_2 h \| \\ &\leqslant \| y - x + h\,[p\,(y,\ t) - p\,(x,\ t)] \| + h \| q(y,\ t) \| \\ &\qquad + \| \epsilon_1 h \| + \| \epsilon_2 h \| \end{aligned}$$

Since ϵ_1 and ϵ_2 tend to zero as h tends to zero, and using the conditions (i) and ii), we obtain

$$\lim_{h \to 0^+} \operatorname{Sup} \left(\frac{1}{h} \right) \left[m(t+h) - m(t) \right] \leqslant \omega\,(t,\ \| y \|\,)$$

Since $\| y \| - \| x \| \leqslant \| y - x \|$ and by non-decreasing character of ω in $z + x$, we have

$$\lim_{h \to 0^+} \operatorname{Sup} \left(\frac{1}{h} \right) \left[m(t + h) - m(t) \right] \leqslant \omega \left(t, m(t) + \| x(t) \| \right)$$

The application of the theorem 1, yields

$$\| y(t) - x(t) \| \leqslant M(t) \tag{2·5}$$

Remark :—Suppose $x(t) = 0$, theorem 2 includes theorems 1, 2, 4 in [3] if the solutions of (2·4) are assumed to be bounded as $t \to \infty$. Also the global existence of the solutions of (1·1) followed immediately by use of the results of Wintner [10] if we assume that all the solutions of (2·4) exist for all t.

Now we are in a position to prove the following :

Theorem 3:—Suppose that the assumptions of theorem 2 hold. Suppose further that (*a*) the differential equation (2·4) is equi-bounded, then the systems (1·1) and (1·2) satisfy the definition (d_1).

(*b*) the identically zero solution of (2·4) is equi-stable, then the systems (1·1) and (1·2) satisfy the definition (d_2).

The proof of this theorem is an immediate consequence of theorem 2 and the assumptions in view of the definitions.

Note : The equi-will be replaced by uniformly—in the above theorem if the functions involved are independent of t_0.

Remarks :—If $p(x,t) \equiv 0$, we get the same concepts relative to an arbitrary solutions of $y' = q(y,t)$.

§ 3. In this section we shall consider the existence of harmonic solution of (1·1). Suppose that the functions p, q and ω are smooth enough to ensure the uniqueness of solutions. Let $p(y,t)$, $q(y,t)$ and $\omega(t, z + x)$ be periodic in t with a period unity. We are interested in the solutions of (1·1) whose period is also unity are called harmonic solutions. We have the following :

Theorem 4 :—Let the function $\omega(t, z + x)$ be continuous, non-decreasing in $z + x$ and defined in $I \times R^+$. Suppose

(i) $\| y - x + h [p(y, t) - p(x, t)] \| \leqslant \| y - x \|$

(ii) q satisfy the condition

$$\| q(y, t) \| \leqslant \omega (\| y \|, t)$$

Suppose that the differential equation (2·4) has a harmonic solution. Then, if the system (1·2) has a bounded, non-decreasing solution, the system (1·1) has a harmonic solution.

We require the following lemma :

Lemma: Let E be an inductively ordered set and let F be a transformation from E into E such that for any X belonging to E we have $FX \geqslant X$. Then there is atleast one point belonging to E such that $F(X) = X$.

This lemma is due to Zorn. cf [1]

Proof of theorem 4:—The proof of this theorem is similar to the proof of the theorem 4 given in [4].

Remarks : If, further $p(x,t)$ is periodic in t with a period unity, the existence of a harmonic solution of (1·2) is assured by the result of [7] and it is also sufficient to prove the theorem.

§ 4. In this section, we shall consider a more general uniqueness theorem. Let us consider the systems (1·1) and (1·2) again. Suppose $t_0 = y_0 = x_0 = 0$ and restrict the interval of t to $0 \leqslant t < a$.

Theorem 5 :—Let the function $\omega(t, z + x)$ be continuous, non-decreasing in $z + x$ and defined for $0 < t < a$, $z + x \geqslant 0$. Suppose

(i) $\| y - x + h[p(y, t) - p(x, t)] \| \leqslant \| y - x \|$

(ii) q satify the condition

$$\| q(y, t) \| \leqslant \omega(\| y \|, t)$$

Suppose the only solution $M(t)$ of $z' = \omega(t, z + x)$ on $0 < t < a$ such that

$$M(0^+) = M'(0^+) = 0$$

is the tri-vial solution. Then there is at most one solution and the same solution for both the system (1·1) and (1·2) on $0 \leqslant t < a$.

It is clear that the uniqueness result in [6] can also be defined accordingly.

Note ; Similar theorems contained in [4] for two different systems. But we have considered here the original system and its approximate system. Moreover theorem 1 is a more generalisation of a lemma used in [4] as pointed out in [5].

REFERENCES

1. D. W. Hall and G. L. Spencer II : Elementary Topology INC., New York P. 277-280 (1955).
2. Coddington, E. A. and N. Levinson : Theory of Ordinary differential equations, New York McGraw-Hill (1955).
3. Lakshmikantham V. : On the boundedness of solutions of non-linear differential equations, *Proc. of Amer. Math. Soc.* 8, pp. 1044-1048 (1957).
4. Lakshmikantham V. : Notes on a variety of problems of differential systems, *Arch. Rat. Mech. Anal.*, Vol. 10, 2, 119-126 (1962).
5. M. Rama Mohana Rao : A note on an integral inequality, *Jr. Ind. Math. Soc.* (To appear).
6. M. Rama Mohana Rao : Some Problems on General Uniqueness and successive approximations, *Proc. Nat. Acad. Scs. India*, Vol. 33, Sec. A, Part II, P. 205-212 (1963).
7. B. Vishwanatham : The Existence of harmonic vibrations, *Proc. Amer. Math. Soc.*, **4**, Pp. 371-372 (1953).
8. Yoshizawa, T : Stability and boundedness of systems, *Arch. Rat. Mech. Anal.* **6**, 609-621 (1960).
9. Yoshizawa, T., Funkcialaj Ekvacioj, 2, 95-142 (1959).
10. Wintner, A. : The infinities in the non-local existence problem of ordinary differential equations, *Amer. J. of Math.* **68**, 173-178 (1946).

STABILITY CONSTANTS OF PALLADIUM, COPPER, NICKEL, ZINC, AND MANGANESE COMPLEXES OF 3-HYDROXY-3-PHENYL-1-p-ACETAMIDO PHENYLTRIAZENE

By

D. N. PUROHIT, S. M. DUGAR *and* N. C. SOGANI

Chemistry Department, University of Rajasthan, Jaipur,

[Received on 2nd December, 1963]

ABSTRACT

Stabilities of palladium, copper, nickel, zinc, and manganese chelates of 3-hydroxy-3-phenyl-1-p-acetami dophenyl triazene have been determined in 70% v/v dioxan-water mixture by employing Bjerrum-Calvin pH titration technique. The titration medium was maintained at a constant ionic strength (0·1M, KCl) and at a temperature, 25 ± 0·5°. Log *K*, palladium 23·204, copper 22 485, nickel 17·883, zinc 15·736, and manganese 12·673.

In recent years Sogani *et al.*[1–5] have reported hydroxy-triazenes as a very useful class of chelating reagents. They possess common functional grouping – N (OH) – N = N –. The parent compound of the series, 3-hydroxy-1, 3-diphenyl-triazene, is a higbly selective reagent for palladium[1] and copper[2]. Substitution of different groups at different positions of the aryl nuclei of the parent compound influenced the stabilities of resulting metal chelates. The present investigation deals with the determination of stabilities of bivalent metal chelates of para acetamido substituted hydroxytriazene, namely, 3-hydroxy-3-phenyl-1-p acetamido-phenyltriazene, in 70% v/v dioxan-water mixture, by employing Calvin and Melchior's method[6] commonly referred as Bjerrum-Calvin pH titration technique[6]. Titrations were carried out in duplicate using 40:1 ratio of ligand to metal ion concentration.

EXPERIMENTAL

Ligand Solution.—3-Hydroxy-3-phenyl-1-p-acetamidophenyltriazene was prepared by employing the method given by Sogani *et al*[4] Weighed amount of this compound was dissolved in 70% v/v dioxan-water mixture and diluted to give 0·04M solution.

Standard palladium, copper, nickel, zinc, and manganese solutions.—Analytical grades of palladium chloride, copper chloride, nickel sulphate, zinc oxide, and manganese sulphate were used for preparing standard solutions. After standardising these solutions by usual methods, these were diluted to give 0·002M solution.

Sodium hydroxide.—Approximately 0·1N carbonate free sodium hydroxide was prepared and standardised with analytical grade potassium hydrogen phthalate. It was diluted to give 0·02M solution.

Dioxan.—The B. D. H. dioxan was purified by Weissberger's method[7].

Potentiometric titrations.—The pH-titrations of the ligands with standard alkali solution in absence and in the presence of different metal ions were carried out by using Cambridge bench-type pH-meter which gave values accurate to 0·01 pH unit.

The pH-meter was standardised before, and checked after, each titration with buffer solutions of pH 4·0 and 9·2 Electrode system consisted of glass electrode (pH range 1 – 13) and reference as saturated calomel-electrode.

10 ml. of 0·04M ligand solution in 70% v/v dioxan-water mixture were pipetted in a titration vessel. Sufficient amount of 0·02M nitric acid was added to it, to lower the pH to about 2. Final ionic concentration was maintained at 0·1M by adding 2·5 ml. of 2M KCl. When titrating in presence of metal ions, 5 ml. of 2×10^{-3}M metal solution were added at this stage. The total valume of the contents was made to 50 ml. by adding varying amounts of dioxan and water in such proportions that it finally became 70% v/v dioxan-water mixture. It was titrated against 0·02M sodium hydroxide. The temperature of the solution throughout the titration was maintained at 25 ± 0·5°. The pH-meter readings obtained at a given alkali addition in duplicate titrations were reproducible with a maximum variation of ± 0·01 pH unit. The titration curves are given in Figs. 1 and 2.

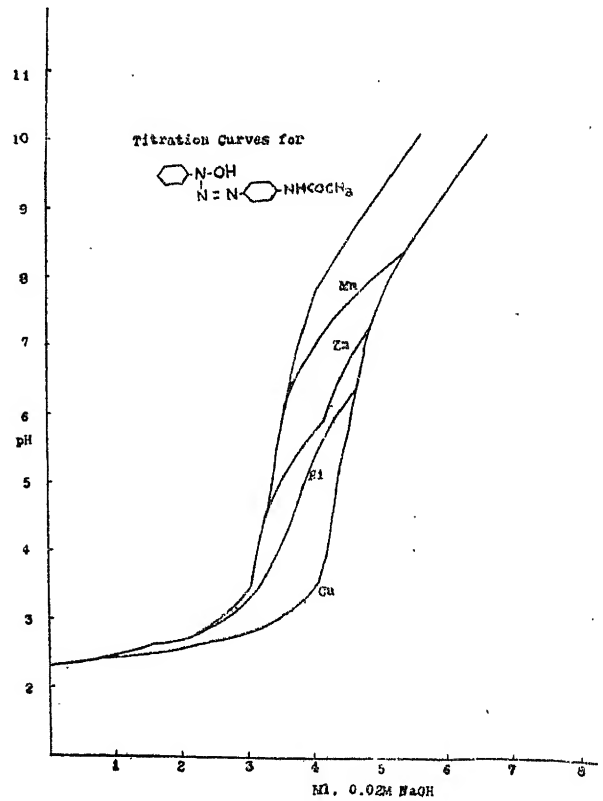

Fig. 1

Calculations.—The horizontal distance between the reference titration curve and the curve obtained in presence of a metal ion gives the amount of metal bound ligand. This value divided by the total metal ion concentration gives the value for $\bar{n}$. In this way the values of $\bar{n}$ at different pH values were calculated,

At any pH, the value of free ligand ion concentration, [T], was calculated from the total ligand concentration, [HT], and its dissociation quotient. This is based on the assumption that the amount of chelating agent over metal ion is so great that the removal of HT by chelation does not cause any significant change in the equilibrium : $HT \rightleftarrows H^+ + T^-$. The pK value of 3-hydroxy-3-phenyl-1-p-acetamidophenyltriazene has been determined spectrophotometrically[8] as 11·663.

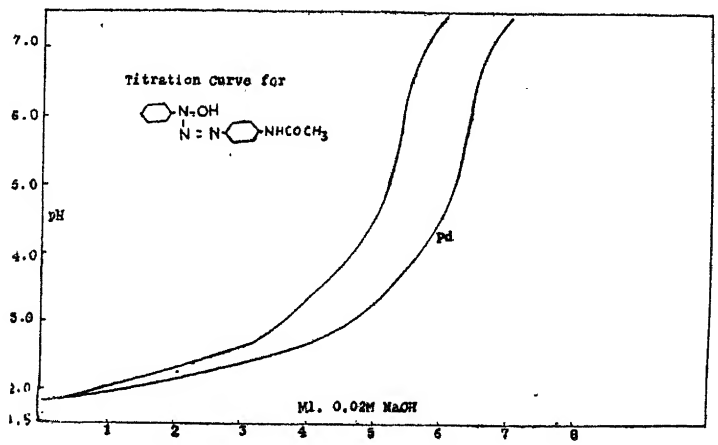

Fig. 2

In calculating the values for $\bar{n}$ and [T], the concentrations were corrected for changes in volume, produced by addition of alkali during titrations. In this way, a service of values for $\bar{n}$ and [T], corresponding to different pH values, was obtained. The results are given in Table Nos. 1 to 3. The formation curves for metal chelates of 3-hydroxy-3-phenyl-1-p-acetamido-phenyltriazene are shown in Fig. 3. The

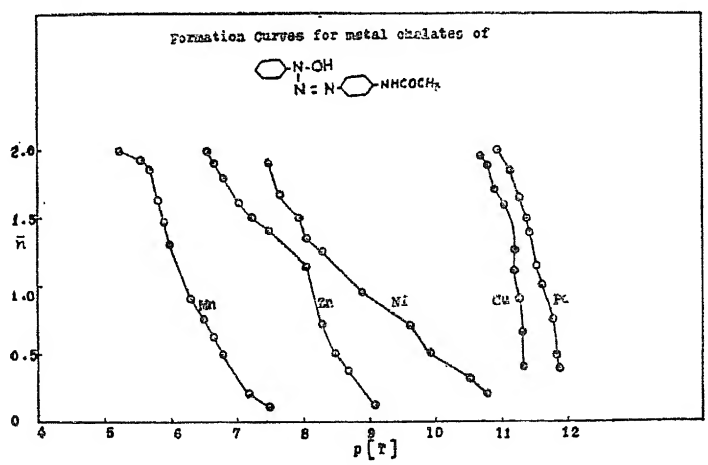

Fig. 3

values for log k_1, log k_2, and log K_{av} ($\frac{1}{2}$ log K) for different metal chelates were read directly from the formation curves and are given in Table 4.

TABLE 1

Formation curve data for metal chelates of 3-hydroxy-3-phenyl-1-p-acetamidophenyltriazene

Palladium			Copper		
pH	$\bar{n}$	p [T]	pH	$\bar{n}$	p [T]
1·90	0·40	11·866	2·42	0·40	11·349
1·95	0·50	11·818	2·45	0·65	11·321
2·00	0·75	11·770	2·48	0·90	11·293
2·15	1·00	11·627	2·60	1·10	11·181
2·25	1·15	11·531	2·75	1·60	11·036
2·35	1·40	11·435	2·90	1·70	10·888
2·40	1·50	11·386	3·00	1·90	10·789
2·50	1·65	11·289	3·10	1·95	10·690
2·65	1·85	11·146			
2·85	2·00	10·947			

TABLE 2

Formation curve data for metal chelates of 3-hydroxy-3-phenyl-1-p-acetamido phenyltriazene

Nickel			Zinc		
pH	$\bar{n}$	p [T]	pH	$\bar{n}$	p [T]
2·90	0·20	10·881	4·70	0·11	9·088
3·25	0·32	10·535	5·12	0·36	8·669
3·85	0·50	9·938	5·30	0·50	8·490
4·15	0·70	9·639	5·50	0·72	8·291
4·90	0·95	8·891	5·75	1·14	8·043
5·50	1·25	8·293	6·30	1·42	7·495
5·75	1·35	8·044	6·55	1·50	7·246
5·85	1·50	7·945	6·75	1·62	7·047
6·15	1·68	7·646	7·00	1·80	6·798
6·30	1·92	7·497	7·15	1·92	6·649
			7·25	2·00	6·549

TABLE 3

Formation curve data for metal chelates of 3-hydroxy-3-phenyl-1-p-acetamido phenyltriazene

Manganese		
pH	$\bar{n}$	p [T]
6·31	0·10	7·480
6·60	0·20	7·191
7·00	0·50	6·793
7·15	0·61	6·644
7·30	0·75	6·495
7·50	0·93	6·296
7·80	1·30	5·998
7·95	1·48	5·850
8·00	1·62	5·801
8·15	1·88	5·652
8·25	1·93	5·553
8·65	2·00	5·184

TABLE 4

Stability constants of metal chelates of 3-hydroxy-3-phenyl-1-p-acetamido-phenyltriazene

Metal ion	log k_1	log k_2	log K_{av}	log k_1 k_2
Palladium	11·818	11·386	11·531	23·204
Copper	11·335	11·150	11·225	22·485
Nickel	9 938	7·945	8·770	17·883
Zinc	8·490	7·246	8·120	15·736
Manganese	6·793	5·880	6·200	12·673

DISCUSSION

The consumption of alkali during the course of titration can be due to the ligand, the hydrolysis of metal ion, and the ligand protons liberated in complex formation.

The ligand under study is a very weak acid ($pK = 11{\cdot}663$). Thus, the ligand proton as such is not in a titrable form. Hydrolyses of these metal ions has been studied in 70% v/v dioxan-water mixture[8]. The pH for $\bar{n} = 1{\cdot}5$ in all the cases is lower than the pH at which the hydrolysis of these metal ions start. Hence, hydrolyses of these metal ions do not interfere in the stability measurements. Moreover, there was no precipitation during chelation titrations, clearly ruling out the possibility of hydrolyses of these metal ions in the presence of large excess of the ligand.

Thus, the consumption of an excess of alkali in chelation titration over the simple ligand titration is due to ligand protons liberated during the complex formation. This may be represented as:

$$M^{2+} + HT + OH^- \rightleftharpoons MT^+ + H_2O \quad (1)$$

$$MT^+ + HT + OH^- \rightleftharpoons MT_2 + H_2O \quad (2)$$

The order of stability of hydroxytriazene metal chelates has been found as palladium > copper > nickel > zinc > manganese.

The authors express their gratitude to Prof. R. C. Mehrotra for providing facilities in the department.

REFERENCES

1. N. C. Sogani and S. C. Bhattacharya, *Anal. Chem.*, **28**, 81 (1956).
2. N. C. Sogani and S. C. Bhattacharya, *Anal. Chem.*, **28**, 1616 (1956).
3. N. C. Sogani and S. C. Bhattacharya, *J. Indian Chem. Soc.*, **36**, 563 (1959).
4. T. C. Jain, H. K. L. Gupta, and N. C. Sogani, *ibid.*, 37, 531 (1960).
5. H. K. L. Gupta and N. C. Sogani, *ibid.*, 38, 771 (1961).
6. M. Calvin and N. C. Melchior, *J. Amer. Chem. Soc.*, 70, 3270 (1948).
7. A. Weissberger and E. S. Proskauer, Organic Solvents, Oxford, 1935, p. 139.
8. D. N. Purohit, Ph.D. Thesis, University of Rajasthan (1963).

CHEMICAL EXAMINATION OF SESBANIA GRANDIFLORA (LINN.) PERS. LEAVES : PART II. ISOLATION AND STUDY OF A SAPONIN

By

R. D. TIWARI *and* R. K. BAJPAI*

Department of Chemistry, University of Allahabad, Allahabad

[Received on 7th December, 1963]

ABSTRACT

The ethanolic extract of the leaves of Sesbania grandiflora (Linn). Pers. yields a saponin m. p. 235-240°C which on acid hydrolysis furnished an acid sapogenin, m. p. 300-302° and galactose, rhamnose and glucuronic acid. The sapogenin has been identified as oleanolic acid (3β hydroxy -$\triangle^{12}$ oleanene-28 oic acid).

The isolation and chemical examination of an aliphatic alcohol (grandiflorol) from the leaves of Sesbania grandiflora (Linn.) Pers., has been described in an earlier communication[1].

The ethanolic extract of the dried leaves of Sesbania grandiflora after the removal of grandiflorol[1], on concentration and subsequent treatment with an excess of chloroform, gave a precipitate of crude saponin which was extracted with ether, benzene and acetone successively and dissolved in methanol and precipitated by addition of ether, thus affording a light yellow coloured, amorphous and hygroscopic compound, sintering at 140° and melting between 180-200°. This was crystallised several times from ethanol when a cream coloured amorphous hygroscopic compound, melting at 225-230° was obtained which gave all the characteristic tests for saponin[2].

Further purification was achieved by acetylation followed by deacetylation[3] and deionisation[4] using Amberlite IR 120 (H) resin. After recrystallisation from ethanol a cream coloured amorphous powder melting at 235-240° was obtained. Although still hygroscopic, it was pure as only one spot was observed during its paper chromatography and paper electrophoresis.

The saponin was hydrolysed using 4N sulphuric acid whereby an acid sapogenin separated out. The liquid part of the hydrolysate after the removal of sulphuric acid with barium carbonate and passing over IRA-400 ion exchange

**Present Address*: Government Degree College, Panna (M. P.)

resin was concentrated and on paper chromatography it was found to contain galactose, rhamnose and glucuronic acid. This was also confirmed by paper electrophoresis using borate buffer.

The acid sapogenin after crystallisation from ethanol was treated with 10% sodium hydroxide to give a sodium salt which on subsequent decomposition with hydrochloric acid gave the product which on crystallisation from methanol was obtained in the form of fine needles, m. p. 300-302°.

On analysis the sapogenin has been found to be $C_{30}H_{48}O_3$. It gave yellow colour with tetranitromethane and also colour reactions of triterpenes[5]. The acidic character of the compound and formation of monoacetate showed that it is a hydroxy triterpenoidal acid. The preparation and study of its acetate, methyl ester and the methyl ester of the acetate and also its infra-red spectrum have confirmed its identity with oleanolic acid (3 β-hydroxy -$\triangle^{12}$ -oleanene -28-oic acid).

The leguminosae family is a rich source of triterpenoidal sapogenins[4,7,8]. The plant Sesbania grandiflora (Linn.) Pers. from the leaves of which oleanolic acid has been isolated, belongs to the Papilionaceae sub-group of the Leguminosae family. From the two more species of the same genus i. e. from Sesbania aculeata[8] and Sesbania aegyptiaa[9] seeds, oleanolic acid has been isolated as a sapogenin by the hydrolysis of the saponin occuring in them.

EXPERIMENTAL

Extraction of the Saponin:

Ethanolic extract of the dry leaves of Sesbania grandiflora after removal of grandiflorol was further concentrated to a syrupy consistency. To this a very large excess of chloroform was gradually added while stirring the solution well with the help of a magnetic stirrer; a brown gummy mass floating on the surface of the solution thus obtained was washed well with cold chloroform and then exhaustively extracted with ether and benzene in succession. The light grey coloured residue left now was dissolved in a minimum amount of warm methanol and ether was added to it. The saponin was obtained as a flocculent yellow coloured powder. The process of dissolving in methanol and precipitating with ether was repeated several times, when a light yellow coloured, amorphous, hygroscopic compound sintering at 140° and melting at 180-200° was obtained. It was recrystallised several times from absolute ethanol and obtained in the form of a cream yellow coloured compound m. p. 225-230°. It was still hygroscopic and retained moisture tenaciously. It gave all the tests for saponin[2].

Purification of Saponin by acetylation and deacetylation :

Acetylation of the Saponin: The saponin was warmed with dry pyridine and acetic anhydride was added to it. The contents were shaken well, the flask was stoppered and left for twenty four hours at room temperature and then added to crushed ice. The water insoluble acetate got deposited which was filtered at the pump, washed well with water, dissolved in minimum amount of chloroform and precipitated with ether. The saponin acetate was cream coloured amorphous powder m. p. 160 65°.

Deacetylation of the saponin acetate:

The saponin acetate was treated with 2% aqueous solution of sodium hydroxide, the contents were shaken well for two hours and then warmed for few minutes on a water bath. The mixture was allowed to stand at room temperature for twenty hours, the saponin acetate was gradually deacetylated to saponin and a clear solution was obtained. The saponin solution was passed through a column of Amberlite I-R 120 (H) ion exchange resin, after which it was concentrated and dissolved in ethanol. Acetone was gradually added to it while stirring the solution well; the cream coloured saponin so obtained was crystallised from ethanol. The saponin was still hygroscopic m. p. 235-240°, yield = 0·1% of the airdried leaves.

Paper chromatography of the saponin:

The aqueous solution of the saponin was applied on a strip of Whatman No. 1 filter paper. The chromatogram was developed for four hours in *n*-butanol-acetic acid-water (4:1:5) using ascending technique[10]. The chromatogram was dried in air and sprayed with 25% tri-chloroacetic acid in ether and dried at 120° for 5 minutes when a single spot was observed.

Paper electrophoresis of the saponin:

The aqueous solution of the saponin was applied to a strip of whatman No. 3 filter paper and was subjected to horizontal clectrophoresis at 300 volts for six hours, using borate buffer (pH 9.4). The paper was dried at room temperature and then sprayed with 25% tri-chlor-acetic acid in ether and dried for five minutes at 120° when a single spot was revealed.

Hydrolysis of the saponin:

The saponin was dissolved in water and to this excess of 4N sulphuric acid was added; the mixture was heated on water bath for twenty hours. Frothing was reduced by occasionally adding a little amount of ethanol to the reaction mixture. The genin obtained as a white precipitate was separated from the hydrolysate by filtration under suction.

Identification of Sugars in the saponin hydrolysate:

The saponin hydrolysate after separation of the genin was shaken with barium carbonate, the precipitated barium sulphate and excess barium carbonate were filtered off and washed with hot water. The combined filtrate and the washings were concentrated under reduced pressure. The hydrolysate was also neutralised by allowing it to pass through Amberlite IRA-400 ion exchange resin and the neutralised solution was concentrated under vacuum.

Paper chromatography of Sugars:

The saponin hydrolysate was chromatographed on whatman No. 1 filterpaper, in two different solvents using (a) *n*-butanol-acetic acid-water (4:1:5) and (b) *n*-butanol-ethanol-ammonia-water (45:5:1:49) using descending technique. After development, the chromatograms were sprayed with aniline-hydrogenphthalate. Three spots were shown by each chromatogram. The Rf values of these revealed the presence of galactose, rhamnose and glucuronic acid.

This was also confirmed by running a chromatogram of saponin hydrolysate spot along side with authentic galactose, rhamnose and glucuronic acid, the sugar spots of the saponin hydrolysate compared well with those of authentic sugars. Since glucose and galactose show nearly the same rate of migration there was little doubt regarding the identity of galactose. The benzylamine derivatives of glucose and galactose exhibit a marked difference in their movement[12]. A chromatogram of benzylamine derivative of saponin hydrolysate alongside with benzyl amine derivatives of authentic glucose and galactose was developed in *n*-butanol-ethanol-ammonia-water (45:5:1:49). The chromatogram was sprayed with 0·01% solution of ninhydrin in butanol. The saponin hydrolysate showed a spot corresponding to the benzyl-amine derivative of galactose and not of glucose. Absence of ketoses was confirmed, by spraying one of the chromatograms of saponin hydrolysate, with naphthoresorcinol-trichloro acetic acid when no spot was revealed.

Paper electrophoresis of saponin hydrolysate:

A spot of the saponin hydrolysate was applied on a strip of whatman No. 3 filter paper, along side with this, spots of authentic sugars, galactose, rhamnose and glucuronic acid were also applied. The paper was subjected to horizontal electrophoresis at 300 volts for six hours using borate buffer. The paper was then sprayed with aniline-hydrogen-phthalate reagent and the presence of galactose, rhamnose and glucuronic acid was confirmed.

Isolation of the genin:

The genin was crystallised from ethanol when it gave fine needles m. p. 290-292°. The genin was taken in ethanol and treated with 10% aqueous sodium hydroxide, the mixture warmed on the water bath and kept for few minutes at room temperature. Alcohol was distilled off under reduced pressure. The deposited crystalline sodium salt was extracted with ether, but on distilling off ether no residue could be obtained. The sodium salt left after extraction with ether was dissolved in ethanol and acidified with an excess of dilute hydrochloric acid. The precipitated genin was washed well with water and crystallised from ethanol giving needles melting at 300-302°.

It gave yellow colour with tetranitromethane, a red violet colour with acetic anhydride and concentrated sulphuric acid (Liebermann-Burchard reaction), a purple colour with commercial thionyl chloride (Noller's reaction) and purple colour with chlorosulfonic acid (Brieskorn test)[5].

Found : C, 79·09% ; H, 10·53% ; Mol. wt. 458 (neutralisation) ; calculated for $C_{30}H_{48}O_3$, C, 78·94%, H, 10·52%, Mol. wt. 456.

$$[\alpha]_D^{30} = + 78^\circ \text{ (c, 1·00 in chloroform) ;}$$

Infra-red spectra:

The peaks at 3420 cm^{-1} (-OH), 2933 cm^{-1} ($-CH_3$, $-CH_2$), 1701 cm^{-1} (-COOH), 1464 cm^{-1} ($C-CH_3$) and 1389 cm^{-1}, 1366 cm^{-1}, 1347 cm^{-1}, 1325 cm^{-1},

1305 cm^{-1}, 1269 cm^{-1} (oleanolic acid type)[6] were obtained in the I-R spectrum of the compound in KCl.

Acetylation of the genin:

The acid genin (800 mg) was mixed with acetic anhydride (4ml) and freshly dried pyridine (2 ml). The mixture after being heated for three hours on a water bath was allowed to stand overnight at room temperature. The genin acetate was crystallised from methanol-chloroform as feathery white needles m. p. 260-262°. Found: C, 77·31% H, 10·19%, acetyl group, 8·22%; calculated for $C_{30}H_{47}O_3$-$COCH_3$ C, 77·11%, H, 10·04%, acetyl group 8·64% (for one-acetyl group.

Hydrolysis of the genin acetate.

The acid genin acetate (200 mg) was refluxed with 10% methanolic potassium hydroxide, for three hours, methanol was distilled off and contents treated with water, the sparingly soluble salt was filtered, dissolved in little amount of ethanol and ethanolic solution was neutralised with dilute hydrochloric acid. The precipitate obtained was crystallised from methanol to fine needles m. p. 300-302°. No depression in the melting point was observed when mixed with the original acid genin.

Methyl ester of the acid genin:

The genin (200 mg) in ether-methanol solution was treated with an excess of the ethereal solution of diazomethane. The solvent was evaporated off and the residue was crystallised from dilute ethanol yielding fine silky needles m. p. 195-97°. When treated with stannic chloride in thionyl chloride it gave a light pink colour, becoming deep red on standing. Found, C, 79·02%; H, 10·57%; calculated for $C_{31}H_{50}O_3$; C, 79·14%, H, 10·64%.

Acetyl methyl ester of the genin:

Acetyl methyl ester of the genin was obtained by the diazomethane treatment of the acid genin acetate in the usual way. After crystallisation from chloroform-methanol it was found to melt at 216-219°. It developed a light yellow colour with stannic chloride in thio nyl chloride.

Found; C, 77·59% H, 10·27%; calculated for $C_{33}H_{52}O_4$; C, 77·34%; H, 10·16%

The melting point of the acid genin was not depressed when mixed with an authentic sample of oleanolic acid.

ACKNOWLEDGEMENTS

Authors are thankful to Dr. I. P. Varshney, Chemistry Department, Muslim University, Aligarh for a sample of oleanolic acid for comparison and to the Kanta Prasad Research Endowment Trust for a research scholarship to one of them (R. K. B.).

REFERENCES

1. Tiwari, R. D., Bajpai, R. K. and Khanna, S. S., *Arch. der Pharm.*, **297**, 310 (1964).
2. Sannie, C., H., *Anal. Biochim. Med*,, **9**, 175, (1948).
3. Farmer, R. H. and Laidlaw, R. A., *J. Chem. Soc.*, 4201 (1955).
4. Varshney, I. P. and Khan, Mohd. S. Y., *J. Sci. industr. Res. India*, **21B**, 30, (1962).
5. Paech, K. and Tracey, M. V., Modern Methoden Der Pflanzenanalyse, Springer Verlag, Berlin, Volume 3, p. 64 (1955).
6. Shatzke, G , Lampert F. and Tschesche, R., *Tetrahedron*, **18**, 1417 (1962).
7. Varshney, I. P. and Khan, Mohd. S. Y., *J. Pharm, sci.*, **50**, 923 (1961).
8. Varshney, I. P. and Khan, Mohd. S. Y., *J. Sci. industr. Res., India*, **21B**, 401 (1962).
9. Farooq, M. O., Varshney, I. P. and Khan, Mohd. S. Y., *J Amer. Pharm. Assn. Sci. Edn.*, **48**, 466 (1955).
10. Sarkar, B. and Rastogi, R. P., *J. Sci. industr. Res. India*, **19B**, 106 (1960).
11. Jensen, K. B. and Tennoe, K., *J. Pharm. Pharmacol.*, **7**, 334 (1955).
12. Barker, S. A., Bourne, E. J., Grant, P. N. and Stacey, M., *Nature*, **177**, 1125 (1956).

FINITE STRAIN IN A ROTATING SHAFT

By

Md. MAHFOOZ ALI SIDDIQUI

Dept. of Mathematics, Osmania University, Hyderabad

[Received on 13th November, 1963.]

ABSTRACT

Using non-liner strain components :

$$2\varepsilon_{ij} = u_{i,j} + u_{j,i} - u_{k,i}\, u_{k,j}$$

and the non-liner stress strain relations :

$$T_{ij} = \lambda I_1 (1 - I_1) S_{ij} + 2 [\mu - (\lambda + \mu) I_1] \varepsilon_{ij} - 4\mu \varepsilon_{ai}\, \varepsilon_{aj}$$

and a perturbation constant, K, the problem of an isotropic circular shaft rotating with angular velocity ω, is solved completely, with the radial and longitudinal displacements calculated.

We consider a solid shaft of circular cross-section of radius a, rotating with an angular velocity ω. The shaft is taken to be of an isotropic material, and the symmetrical manner in which it is strained leads us to assume a radial displacement and a longitudinal extension only, given by

$$\begin{aligned} u &= K\, u(r) \\ W &= K\, w(\chi) \end{aligned} \qquad (1.1)$$

where $u(r)$ is a function purely of r and $w(z)$ a function purely of z, and K is a perturbation constant, whose squares and higher powers we propose to neglect in the linear theory, where as second order terms in K are retained when applying the non-linear theory.

For the linear theory the components of strain are

$$e_{rr} = K u'(r)\,;\ e_{r\theta} = e_{\theta\chi} = e_{\chi r} = 0$$

$$e_{\theta\theta} = K \frac{u(r)}{r} \qquad (1.2)$$

$$e_{zz} = K \omega'(z)$$

The components of stress are

$$\widehat{rr} = \lambda K \left(u' + \frac{u}{r} + W' \right) + 2 K \mu u'$$

$$\widehat{\theta\theta} = \lambda K \left(u' + \frac{u}{r} + W' \right) + 2 K \mu \frac{u}{r}$$

$$\widehat{\chi\chi} = \lambda K\left(u' + \frac{u}{r} + W' \right) + 2 K \mu \omega' \qquad (1.3)$$

$$\widehat{r\theta} = \widehat{\theta\chi} = \widehat{\chi r} = 0$$

These stresses must satisfy the body-stress equations

$$\left(\frac{\partial}{\partial r}\widehat{rr} + \frac{1}{r}\widehat{rr} - \widehat{\theta\theta}\right) + \rho r\omega^2 = 0 \; ; \; \frac{\partial}{\partial \chi}\widehat{\chi} = 0$$

which give

$$K\left(u'' + \frac{u'}{r} - \frac{u}{r^2} \right) + \frac{\rho}{\lambda - 2\mu} r\omega^2 = 0 \qquad (1.4)$$

and $W'' = o$

Thus $u = A r - \rho \frac{\omega^2}{8 k (\lambda + 2\mu)} r^3$ (1.5)

$W = B \chi$

where A and B are constants and the particular solution $u = \frac{1}{r}$ of (1.4) is not admissible, since u has to be bounded at $r = 0$, the shaft being complete up to the centre. The boundary conditions to be satisfied are

$$\widehat{rr} = 0 \text{ for } r = a \qquad (1.6)$$

the outer surface being stress-free.

Also, for the resultant longitudial tension to vanish over the plane ends it is necessary that

$$\int_0^a r \widehat{\chi\chi} \, dr = 0 \qquad (1.7)$$

The conditions (1.6) and (1.7) give

$$2 (\lambda + \mu) A + \lambda B - \frac{2\lambda + 3\mu}{4 k (\lambda + 2\mu)} \rho \omega^2 a^2 = 0 \qquad (1.8)$$

$$2 \lambda A + (\lambda + 2\mu) B - \frac{\lambda \rho \omega^2 a^2}{4 k (\lambda + 2\mu)} = 0 \qquad (1.9)$$

which immediately yield

$$A K = \frac{\rho \omega^2 a^3 (\lambda + \mu)(\lambda + 6\mu)}{8 \mu (\lambda + 2\mu)(3\lambda + 2\mu)} \qquad (1.10)$$

$$B\,K = -\frac{\lambda\,\rho\,\omega^2 a^2\,(2\lambda+11\mu)}{8\,\mu\,(\lambda+2\mu)} = \qquad (1\cdot11)$$

Therefore the radial displacement as given by the linear theory is

$$u = K\,u\,(r)$$

$$= \frac{\rho\,\omega^2\,a^2\,(\lambda+\mu)\,(\lambda+6\,\mu)r}{8\mu\,(\lambda+2\,\mu)\,(3\lambda+2\mu)} - \frac{\rho\omega^2}{8\,(\lambda+2\mu)}\,r^3 \qquad (1.12)$$

and the displacement in the z-direction is

$$W = K\,W\,(\chi)$$

$$= -\,\rho\,\omega^2\,a^2\,\lambda\,\frac{(2\lambda+11\mu)}{8\mu\,(\lambda+2\mu)}\,\chi \qquad (1.13)$$

When applying the non-linear theory of elasticity, *i.e.* when we take the non-linear strain components (1.10) and the non-linear stress-strain relations given by

$$T_{ij} = [\lambda I_1\,(1-I_1)]\;S_{ij} + 2\,[\mu - (\lambda+\mu)\,I_1]\;G_{ij} - 4\mu\,\varepsilon_{\alpha i}\;\varepsilon_{\alpha j}\,;$$

we assume

$$u = u_1 + Kv\,(r) \qquad (1.14)$$

$$W = w_1 + Ks\,(\chi)$$

where u_1, and w_1 are the linear theory solutions, (1.12) and (1.13)

The strain domponents corresponding to (1.14) will be

$$\varepsilon_{rr} = Ku_1' + K^2\,(v' - \tfrac{1}{2}\,u_1'^2)$$

$$\varepsilon_{\theta\theta} = K\,\frac{u_1}{r} + K^2\left(\frac{v}{r} - \tfrac{1}{2}\,\frac{u_1^2}{r^2}\right) \qquad (1.15)$$

$$\varepsilon_{zz} = K\,W_1' + K^2\,(s' - \tfrac{1}{2}\,W_1'^2)$$

$$\varepsilon_{r\theta} = \varepsilon_{\theta\chi} = \varepsilon_{\chi r} = 0$$

The stresses will be

$$\widehat{rr} = \lambda\Big[K\left(u_1' + \frac{u_1}{r} + W_1'\right) + K^2$$

$$\left\{\left(v' + \frac{v}{r} + s'\right) - \tfrac{1}{2}\left(u_1'^2 + \frac{u_1^2}{r^2} + W_1'^2\right)\right\}\Big]$$

$$- \lambda K^2\left(u_1' + \frac{u_1}{r} + W_1'\right)^2 + 2\mu\,[K\,u_1' + K^2\,(v' - \tfrac{1}{2}\,u_1'^2)]$$

$$- 2(\lambda + \mu) K^2 \left[u' \left(u_1' + \frac{u_1}{r} + W_1' \right) \right]$$

$$- 4\mu k^2 u_1'^2 \qquad (1.16)$$

$$\widehat{\theta\theta} = \lambda \left[K \left(u_1' + \frac{u_1}{r} + W_1' \right) + K^2 \left\{ \left(v' + \frac{v}{r} + s' \right) - \tfrac{1}{2} \left(u_1'^2 + \frac{u_1^2}{r^2} + W_1'^2 \right) \right\} \right]$$

$$- \lambda K^2 \left(u_1' + \frac{u_1}{r} + W_1' \right)^2 + 2\mu \left[K \frac{u_1}{r} + K^2 \left(\frac{v}{r} - \frac{u_1^2}{2r^2} \right) \right]$$

$$- 2(\lambda + \mu) K^2 \left[\frac{u'}{r} \left(u_1' + \frac{u_1}{r} + W_1' \right) \right]$$

$$- 4\mu K^2 \frac{u_1^2}{r^2} \qquad (1.17)$$

$$\widehat{zz} = \lambda \left[K \left(u_1' + \frac{u_1}{r} + W_1' \right) + K^2 \left\{ \left(v' + \frac{v}{r} + s' \right) - \tfrac{1}{2} \left(u_1'^2 + \frac{u_1^2}{r^2} + W_1'^2 \right) \right\} \right]$$

$$- \lambda K^2 \left(u_1' + \frac{u_1}{r} + W_1' \right)^2 + 2\mu \left[K W_1' + k^2 \left(s' - \tfrac{1}{2} W_1'^2 \right) \right]$$

$$- 2(\lambda + \mu) K^2 \left[W_1' \left(u_1' + \frac{u_1}{r} + W_1' \right) \right] \qquad (1.18)$$

$$- 4\mu K^2 W_1'^2$$

The equations of equilibrium are

$$\frac{\partial}{\partial r} \widehat{rr} + \frac{1}{r} (\widehat{rr} - \widehat{\theta\theta}) + \rho_1 \omega^2 = 0$$

and $$\frac{\partial}{\partial \chi} \widehat{\chi\chi} = 0$$

which reduce to

$$v'' + \frac{v'}{r} - \frac{v}{r} = -(10\lambda A + 4\lambda B + 16\mu A + 2\mu B)\frac{\rho\omega^2}{K(\lambda + 2\mu)^2} r + \frac{49\lambda + 83\mu}{16K^2(\lambda + 2\mu)^3}\rho^2\omega^4 r^3 \tag{1.19}$$

and $S'' = 0$

Therefore

$$v = Cr - (10\lambda A + 4\lambda B + 16\mu A + 2\mu B)\frac{\rho\omega^2}{8(\lambda + 2\mu)^2K} r^3 + \frac{49\lambda + 83\mu}{24 \times 16K^2(\lambda + 2\mu)^3}\rho^2\omega^4 r^5 \tag{1.20}$$

and $S = D\chi$

where C and D are constants.

If we write

$$A_1 = AK = \rho\omega^2 a^2 \frac{(\lambda + \mu)(\lambda + 6\mu)}{8\mu(\lambda + 2\mu)(3\lambda + 2\mu)}$$

$$B_1 = BK = -\lambda\frac{\rho\omega^2 a^2(2\lambda + 11\mu)}{8\mu(\lambda + 2\mu)}$$

$$L_1 = \frac{10\lambda A_1 + 4\lambda B_1 + 16\mu A_1 + 2\mu B_1}{8(\lambda + 2\mu)^2}\rho\omega^2 \tag{1.21}$$

$$M_1 = \frac{49\lambda + 83\mu}{24\lambda\ 16(\lambda + 2\mu)^3}\rho^2\omega^4$$

the boundary conditions over the curved surface and the plane ends, given by

$\widehat{rr} = 0$ for $r = a$ and $\int_0^a r\,\widehat{\chi\chi}\,dr = 0$ become

$$2(\lambda + \mu)CK^2 + \lambda DK^2 = 9(\lambda + \mu)A_1^2 + \frac{3\lambda}{2}B_1^2 + 2(3\lambda + 2\mu)A_1B_1 - \frac{\rho W^2 a^2}{4(\lambda + 2\mu)}\left\{5(4\lambda + 5\mu)A_1 + (7\lambda + 3\mu)B_1\right\} + \frac{3\rho^2\omega^4 a^4}{64(\lambda + 2\mu)^2}(14\lambda + 23\mu) + 2(2\lambda + 3\mu)L_1 a^2 + 2(3\lambda + 5\mu)M_1 a^4 \tag{1.22}$$

and

$$2\lambda CK^2 + (\lambda + 2\mu)DK^2 = 5\lambda A_1^2 + 7/2(\lambda + 2\mu)B_1^2 + 4(\lambda + 2\mu)A_1B_1 - \frac{\rho\omega^2 a^2}{4(\lambda + 2\mu)}(5\lambda A_1 - 2\mu B_1) + \frac{7\lambda\rho^2\omega^4 a^4}{64} + 2\lambda L_1 a^2 - 2\lambda M_1 a^4 \tag{1.23}$$

From (1.22) and (1.23)

$$CK^2 = \frac{4\lambda^2 + 25\lambda\mu + 18\mu^2}{2\mu(3\lambda + 2\mu)} A_1^2 - \frac{\lambda + \mu}{3\lambda + 2\mu} B_1^2 + \frac{(\lambda + \mu)(\lambda + 2\mu)}{\mu(3\lambda + 2\mu)} A_1 B_1$$

$$+ \frac{\rho W^2 a^2}{8\mu(\lambda+2\mu)(3\lambda+2\mu)} \left\{ (15A_1+7B_1)\lambda^2 - 3(5A_1+3B_1)\lambda\mu - 2(25A_1+3B_1)\mu^2 \right\}$$

$$+ \frac{\rho^2 \omega^4 a^4}{128\mu(\lambda+2\mu)^2(3\lambda+2\mu)} \left\{ 35\lambda^2 + 153\lambda\mu + 138\mu^2 \right\} \qquad (1.24)$$

$$+ \frac{(\lambda+\mu)(\lambda+6\mu)}{2\mu(3\lambda+2\mu)} a^2 L_1$$

$$+ \frac{(\lambda+2\mu)(3\lambda+5\mu)}{2\mu(3\lambda+2\mu)} a^4 M_1$$

and

$$DK^2 = \frac{6\lambda^2 + 23\lambda\mu + 12\mu^2}{2\mu(3\lambda + 2\mu)} B_1^2 - \frac{2\lambda(4\lambda + 5\mu)}{\mu(3\lambda + 2\mu)} A_1^2$$

$$+ \frac{2(4\mu^2 + 5\lambda\mu - \lambda^2)}{\mu(3\lambda + 2\mu)} A_1 B_1$$

$$+ \frac{\rho\omega^2 a^2}{8\mu(\lambda + 2\mu)(3\lambda + 2\mu)} \left\{ 4(15A_1+7B_1)\lambda^2 + 2(60A_1+19B_1)\lambda\mu + 5(5A_1+2B_1)\mu^2 \right\}$$

$$- \frac{\rho^2\omega^4 a^4 \lambda(35\lambda+62\mu)}{64(\lambda+2\mu)^2(3\lambda+2\mu)} - \frac{5\lambda^2 + 15\lambda\mu + 6\mu 2}{\mu(3\lambda + 2\mu)} a^2 L_1$$

$$+ \frac{(3\lambda + 5\mu)(5\lambda + 2\mu)}{\mu(3\lambda + 2\mu)} a^4 M_1 \qquad (1.25)$$

Therefore the radial displacement is

$$u = \left(\frac{\rho\omega^2 a^2 (\lambda + \mu)(\lambda + 6\mu)}{8\mu(\lambda + 2\mu)(3\lambda + 2\mu)} + CK^2 \right) r - \left(\frac{\rho\omega^2}{8(\lambda + 2\mu)} + L_1 \right) r^3$$

$$+ \frac{(49\lambda + 83\mu)\rho^2\omega^4}{24 \times 16(\lambda + 2\mu)^3} r^5$$

where the value of CK^2 is given by (1.24)

The longitudinal extension is given by

$$W = \left[DK^2 - \rho\omega^2 a^2 \frac{\lambda(2\lambda + 11\mu)}{8\mu(\lambda + \mu)} \right] \chi$$

where the value of DK^2 is given by (1.25)

REFERENCES

1. B. R. Seth, Finite Strain in a rotating shaft. *Proc. Indian Acad. Sc.* (A) **14** (1944).
2. E. D. Murnaghan, The foundations of the theory of elasticity—(1947) "Non-linear problems in the Mechanics of continua." New-York, 1949.
3. F, D. Murnaghan, "Finite deformation of an elastic solid". John Wiley and Sons, 1951.

STUDIES ON THE EFFECT OF SOIL MOISTURE CONDITIONS AND POTASSIUM APPLICATION ON THE NUTRITIVE VALUE OF RICE

By

SANT SINGH *and* KRISHNA KANT SINGH

College of Agriculture, Banaras Hindu University, Varanasi

[Received on 26th December, 1963]

ABSTRACT

An examination of the data presented shows that more nutritive grain can be produced in a short duration variety of paddy, if the plant is subjected to progressively depleted soil moisture conditions during the ripening period. Protein accumulation is greatly increased if plant is treated with potassium in two split doses. With regard to its composition (amino acid), it is not practically affected by any treatment.

INTRODUCTION

During the last three decades or so, considerable amount of work touching the various aspects of the nutritional quality of rice has been carried out in this country. Soil moisture plays the most dominating role in plant's life and is largely responsible for the accumulation of various nutrients in the grain. But unfortunately very little information is available which can throw light on this important subject. It is also a matter of considerable significance to find out the effect of some specific salt upon the aecumulation of various nutrients in the grain when it is applied in different soil moisture conditions.

The authors (1963) have found that in a short duration variety of paddy, stoppage of irrigation a few days earlier than harvesting and application of potassium in instalments cause greater production of grain per unit area. The chief objective of undertaking this study was to see the extent to which these treatments affect the nutritive value of the grain. So far as is known no such work has been reported which can throw light on this important aspect and the present study is an attempt to fill up the gap to some extent.

EXPERIMENTAL METHOD

Pre-harvest Operations.

An early maturing variety of paddy *viz.*, N_{22} was selected for the purpose. Other details regarding filling of pots with soil, raising of seedlings in the nursery, transplanting, weeding, inter-culturing etc., remained the same as in the previous paper (Authors, 1963).

Plants growing in the pots received liberal but equal and measured amount of water till the commencement of the grain maturation period *i. e.*, upto 60 days after transplanting. At the beginning of the period, all the pots were brought inside the glass-house so as to avoid the interference due to rain, dew etc., during the course of the experimentation.

Pots were now divided in two sets. The first one received liberal but equal and measured volume of water and the level of standing water was maintained 2″ above the soil surface till the end of the harvest, and was denoted as I_n. In case of the other, after keeping 2″ of standing water at the commencement of the

period, no further supply of irrigation was provided and the plants were then forced to grow under progressively depleted soil moisture condition. This set was denoted as I_1.

Plants of each set received potassium in the form of potassium sulphate at the rate of 40 lb K_2 per acre in the following manner:

(1) K_o—Control, *i. e.*, no application of potassium.

(2) K_1—The whole amount was applied just after one week of transplantation in a single dose.

(3) K_2—The whole lot was split in two equal doses, the first one was applied one week after transplanting and the other one month later.

(4) K_3—In this case the amount was divided in three equal doses and each one was applied at an interval of one month starting from one week after transplanting.

Pots under the following 8 treatment combinations were arranged in a factorial experimental design with three replications:

(1) $I_n K_o$, (2) $I_n K_1$ (3) $I_n K_2$, (4) $I_n K_3$, (5) $I_1 K_o$, (6) $I_1 K_1$, (7) $I_1 K_2$ and (8) $I_1 K_3$.

Harvesting and Preparation of Grain Sample:

Harvesting of the crop was done when the grains were fully ripened. It was noted that moisture depleted plants took about 5 days more than the normally irrigated ones. After the harvest, grains were separated from the straw and their husks were removed very carefully. The hulled rice was then ground to a fine powder in an electrically operated micro-grinding mill and the sample was then dried in an electric oven, bottled and sealed.

Chemical Analyses:

Help of Loomis and Shull (1937) was taken for the determination of total carbohydrate and crude protein in the sample. The value of crude protein was obtained by multiplying the total nitrogen with the factor 6·25. Soxhlet apparatus was used to obtain ether solubles. The period of extraction was 8 hours and the condensation rate was maintained at 4-5 drops per second. The extract was then dried for 30 minutes at 100°C, cooled and weighed.

For the detection of various amino acids in the sample, paper chromatographic method as suggested by Block and Weiss (1956) was used. The chromatogram developed from each of the hydrolysates was compared with the standard which was prepared under similar conditions. The help of R_F values as given by Brimley and Barrett (1956) was also taken to recognise them.

EXPERIMENTAL FINDINGS

Data of nutritive value of the rice as presented in the accompanying Table clearly show that stopping of irrigation in an early maturing variety a few days earlier than harvesting causes more accumulation of total carbohydrate, ether soluble and protein than providing continuous irrigation. Higher concentration carbohydrate in both the sets was also favoured when potassium was applied in a single dose, but this method of application was not found useful for the synthesis of ether solubles and protein.

Table Showing the Effect of Soil Moisture Conditions and Potassium Application on the Average Chemical Composition (percentage of dry matter) of Rice

Treatment	Total carbohydrate	Ether solubles	Crude protein	Amino acids detected
(1) I_1K_o	70·76	3·71	7·35	Alanine (Al), aspartic acid (Asp), cystine (C), glycine (Gl), histidine (H), isoleucine (Isol), lysine (Ly), methionine (M), proline (Pr) and serine (Se).
(2) I_nK_1	79·00	3·42	6·04	Al, arginine (A), Asp, C, Gl, H, Isol, Ly, M, Pr, and Se.
(3) I_nK_2	73·53	3·43	8·01	Al, A, Asp, C, Gl, H, Isol, Ly, M, Pr, and Se.
(4) I_nK_3	74·26	2·95	7·31	Same as treatment (2).
(5) I_1K_o	84·30	3·73	7·22	Do.
(6) I_1K_1	83·33	3·57	7·70	Do.
(7) I_1K_2	81·52	3·68	8·44	Do.
(8) I_1K_3	72·82	3·32	7·96	Do.

Further examination of the Table reveals that application of potassium in two instalments encouraged greatly to produce grains containing higher content of protein. It is also clear from the Table that nearly the same amino acids are detected in each treatment and it may be concluded that protein constituents are not affected either by moisture conditions or potassium application.

DISCUSSION

One of the remarkable findings of the study is that stoppage of fresh supply of irrigation water a few days earlier than harvesting of a short duration variety of paddy causes more accumulation of total carbohydrate, ether solubles and protein in the grain. As has been stated earlier, moisture depleted plants took about 5 days more in completing their life-cycle than the normally irrigated ones, and therefore, during the extra 5 days the former might have accumulated more nutrients than the latter. Low level of soil moisture generally causes better aeration and thereby more extension of root system in the direction of available moisture and nutrients. This extension of root system might have helped the plant in overcoming not only the severe drought injury but also in greater absorption of nutrients from untackled area, and thus the nutritive value of the grain might have ultimately been increased. Miller and Duley (1925) obtained in maize, and also Kido and Yanatori (1961) in rice, more nutritive grains in plants grown on well aerated soil.

The grains of normally irrigated plants ripened earlier and this might be due to better supply of nitrogen to the plant (Russell, 1961). This increased

supply of nitrogen might have encouraged new vegetative growth, and the nutrients which should have gone for the enrichment of the grain, might have been diverted towards the new developing regions thus lowering the nutritive value.

Application of potassium, except in few cases, failed to increase the content of either carbohydrate or ether soluble compounds, but its application, particularly in split doses, definitely encouraged more accumulation of protein in both the conditions of soil moisture. As during the later period of growth, potassium is secreted from the plant body to the soil (Sayre, 1948), it is likely that split application might have met the deficiency at any time and thus reduced the rate of protiolysis to amino acids and amides (Wall, 1940 and Richards and Berner, 1954). This might account for the greater amount of protein in the grain.

Paddy grains as affected by various treatments have practically the same amino acids and it appears that protein constituents are genetically controlled.

SUMMARY AND CONCLUSIONS

The present investigation was undertaken to see the extent to which soil moisture conditions during the grain maturation period and potassium application affect the nutritive value of the grain of a short duration variety of rice. The main findings and conclusions may be stated as below:

(1) Progressively depleted soil moisture is beneficial for the production of more nutritive grain.

(2) More proteinacious grain can be produced by the application of split doses of potassium. Application in two instalments have been found to be most useful.

(3) Grains as affected by different treatments practically have the same amino acids and it appears that the protein constituents are genetically controlled.

ACKNOWLEDGEMENTS

The authors express their sincere thanks to the University Grants Commission for awarding a scholarship to the junior author. Thanks are also due to the Principal, College of Agriculture, Banaras Hindu University for providing necessary facilities for carrying out the experiment.

REFERENCES

1. Block, R. J and Weiss, K. W., "Amino Acid Handbook; Methods and Results of Protein Analysis." Springfield, Thomas Co., U. S. A Publication (1956).
2. Brimley, R. C. and Barrett, F. C., "Practical Chromatography." Chapmen and Hall Ltd., London (1956).
3. Kido, M. and Yanatori, S., *Proc. Crop Sci. Soc. Japan*, **30** (1), 5 (1961); *Biol. Abst.* **38**, 11297.
4. Loomis, W. E. and Shull, C. A., "Methods in Plant Physiology", McGraw Hill Book Co. Inc. U. S. A. Publication (1937).
5. Miller, M. F. and Duley, F. L., *Mo. Agri. Expt. Stat. Res. Bull.*, **76**, 1 (1925).
6. Richards, F. J. and Berner, E., *Ann. Bot.*, 18, 15 (1954).
7. Russell, E. W., "Soil Conditions and Plant Growth" Longmans (London) Publication, 9th edition, (1961).
8. Sayre, J. D., Plant Phys., 23, 267 (1948).
9. Singh, S. and Singh, K. K., *Proc. Nat. Acad. Sci.*, 33, 437 (1963).
10. Wall, M. E., *Soil Sci.*, **49**, 393 (1940).